The *In Vitro* Effects of Pure and Street Methamphetamine on the Proliferation and Cell Cycle of Mouse Brain Endothelial (bEnd5) cells

By

Patrick Siyambulela Mafunda (2325175)

Submitted in Fulfillment of the Requirements for the Degree of

Master of Science (MSc)

Department of Medical Biosciences

Faculty of Natural Sciences

University of the Western Cape

Supervisor: Professor D Fisher

Co-Supervisor: Dr K Gamieldien

November 2012

DECLARATION

I, Patrick Siyambulela Mafunda (2325175), declare that "**The *In Vitro* Effects of Pure and Street Methamphetamine on the Proliferation and Cell Cycle of Mouse Brain Endothelial (bEnd5) cells**" is my own work, that has not been submitted before for any degree or assessment at any other university, and that all the sources I have used or quoted have been indicated and acknowledged by means of complete references.

Patrick Siyambulela Mafunda: November 2012

Date Signed :

ACKNOWLEDGEMENTS

First and foremost, I want to thank God for giving me the opportunity to gain more knowledge "Hosea 4: 6".

To my parents for all their sacrifices and giving me this level of education. Without your encouragement, I would not have succeeded. Your support was very important all the time.

To my supervisor Prof. David Fisher, I sincerely thank you for the opportunity you granted me, to learn the first steps in research in order to be among the best one day. Your expertise, time and motivation were much appreciated.

My utmost thanks to Dr. Kareemah Gamieldien for always being there for me. You became a mother, motivator and leader throughout my MSc. Your lab expertise and skills have meant a lot to me and they will always be beneficial. I wouldn't have made it without your support (*thank you*).

Ernest Maboza, thanks for your fantastic support.

To the Neurobiology Group (NBG) members (2011-2012) who created an environment that made the research lab a pleasure to work in.

Department of Medical Biosciences for the opportunity to perform my MSc research and the support needed for this study to succeed.

The National Research Foundation (NRF) for the financial support.

Lastly, to all my friends who supported me through it all.

ABSTRACT

The blood-brain barrier (BBB) is an interface between the brain parenchyma and the circulating system. This barrier plays a vital role in protecting the CNS by restricting free paracellular diffusion of molecules from the systemic circulation. Methamphetamine (MA) is a highly addictive psychostimulant and has demonstrated neurotoxic properties as well as the ability to compromise the BBB. MA exposure is strongly linked with increased oxidative stress which can result in a decrease in the integrity of the BBB.

The aim of this study was to investigate *in vitro* effects of pure and street MA "tik" on DNA proliferation and cell cycles in mouse brain endothelial (bEnd5) cells.

Trypan blue was used to determine effects of MA (0.0001M-1mM) on cell viability and % cell growth. The Cell Titer Glo® luminescent assay and nonradioactive analogue, 5-bromo-2'-deoxyuridine (BrdU) was used to detect ATP and DNA levels, respectively. Cell cycles (propidium iodide incorporation) were analysed using flow cytometry. Statistical analysis was performed using Wilcoxin Rank Sum Test in which $P<0.05$ was denoted as significant.

Results of this study showed that:

1. Viability of bEnd5 cells exposed to all selected concentrations of MA were unaffected when compared to controls ($P>0.05$)

2. % Cell growth was suppressed by MA exposure at 96hrs in comparison to that of controls (P≤0.03).

3. Cells exposed to MA had significant higher ATP concentrations than control cells at 96hrs (P ≤.0.03)

4. DNA synthesis was markedly suppressed in cells exposed to pure MA and street MA sample 4 (P≤0.03), while was similar and higher in cells exposed to street MA sample 1 (P=0.39), and street MA sample 2 and 3 (P≤0.04), respectively at 96hrs.

5. bEnd5 cell were arrested between 72 and 96hrs at the G1-S phase.

In conclusion, this study demonstrated pure and illicit samples of MA obtained from forensic police did not affect the viability of bEnd5 cells, however resulted in the significant suppression of their cell numbers. This growth inhibition may be due to MA-induced cell cycle arrest at the G1-S phase. The study also showed that compounds found in the samples of street MA produced results significantly different to that of pure MA.

Key words: Blood brain barrier, methamphetamine, viability, ATP, DNA proliferation, cell cycle.

LIST OF ABBREVATIONS

ABCN1	P-glycoprotein
AMPK	5' AMP-activated protein kinase
ATP	Adenosine triphosphatase
BBB	Blood Brain Barrier
bEnd5	Immortalized mouse brain endothelial cells
BMEC	Brain microvascular endothelial
BrdU	Bromodeoxyuridine
Ca^{2+}	Calcium ion
CNS	Central nervous system
DA	Dopamine
DAT	Dopamine transporter
DEA	Drug Enforcement Administration
DNA	Deoxyribonucleic acid
EDTA	Ethylenediaminetetraacetic acid
ER	Endoplasmic reticulum
ESAM	Endothelial cell-selective adhesion molecule

ETC	Electron transport chain
EtOH	Ethanol
GC-MS	Gas chromatography–mass spectrometry
GLUT-1	Glucose transporter 1
HI	Hydriodic acid
JAM	Junctional adhesion molecule
K^+	Potassium ion
KO	Knockout
MA	Methamphetamine
MRCSA	Medical Research Council of South Africa
Na^+	Sodium ion
NADP	Nicotinamide adenine dinucleotide phosphate
NADPH	Nicotinamide adenine dinucleotide phosphate-oxidase
NE	Norepinephrine
NET	Noradrenalin transporter
PI	Propidium Iodide
PIPES	Piperazine-N,N′-bis (2-ethanesulfonic acid)
PPP	Pentose phosphate pathway

Red P	Red phosphorus
ROS	Reactive oxygen species
RT	Room Temperature
SA	South Africa
SACENDA	South African Community Epidemiology Network on Drug Use
SERT	Serotonin transporter
TEM	Electron microscopy
TJs	Tight junctions
VEGF	Vascular endothelial growth factor
VMAT	Vesicular monoamine transporter
%	Percentage
<	Less than
>	Greater than
≤	Less than or equal to
≥	Greater than or equal to

TABLE OF CONTENTS

LIST OF FIGURES

LIST OF TABLES

APPENDIX

CHAPTER 1

Introduction

Methamphetamine (MA) is a highly psychostimulant street drug that is addictive and toxic to the animal and their neural tissue (Krasnova *et al.,* 2009). The use of MA poses a significant health problem as it has become a worldwide challenge with an estimated 15 to 16 million users (Krasnova *et al*., 2009). According to the Medical Research Council of South Africa (MRCSA), by 2007, the number of patients admitted for treatment reporting MA as their primary or secondary substance of abuse had increased by 49% between 2002 to 2006 December. MA was reported as a primary drug of abuse and its prevalence was the highest in the Western Cape Province (35%) when compared to other provinces in South Africa (SA).

MA causes neuromophological and psychological effects in the brain and also causes changes in the morphology of the vascular circulation of the brain; it also affects the blood brain barrier (BBB). The BBB is present at the interface between the brain and the circulating system (Shinsuke *et al.*, 2009). The anatomical and structural location of the BBB is at the brain microvascular endothelial cells (BMEC) of the capillaries, of the brain, and epithelial cell surface of the choroid plexus (Dixon *et al.*, 2006). Studies showed that MA changes the BBB function by altering the tight junction (TJ) proteins between endothelial cells in the central nervous system that restrict the passage of solutes (Martins *et al.*, 2011), Yuan *et al* (2011) study focused on the effects of MA have on its neurophysiological effects. Not much has been reported on the *in vitro* effects of MA on the BBB and its components.

MA bought at the street for illegal consumption is manufactured in clandestine labs and it is not 100% pure. Samples obtained on the street are normally called "tik" in the Western Cape province of South Africa. The aim of this study was to investigate the *in vitro* effects of pure and street MA ("tik") on the physiological and functionality of the immortalized mouse brain endothelial (bEnd5) cells as a model of the BBB.

1.1 Anatomy of the Blood Brain Barrier

The BBB is present at the interface between the brain parenchyma and the intravascular compartment (Shinsuke *et al.*, 2009). This interface between the blood and the brain tissue is formed by the brain BMEC of brain capillaries which display a unique structure characterized by low permeability and the presence of intercellular tight junctions (TJs) and the polarized morphology of BMEC (Kwang., 2006). TJs constitute the primary anatomic substrate of the BBB. The BBB exists because the endothelial cells that line the capillaries of the CNS are extensively interconnected by TJs at their lateral surface. When compared to other tissues the blood barrier in the brain is unique (Nicolas *et al.*, 2007). The endothelium of BBB differ from the peripheral endothelium capillaries by having tight intercellular junctions, minimal pinocytotic activity and the absence of fenestrations (Winfried *et al.*, 2006). In addition the BBB endothelium differs from that of other capillaries because of the presence of pericytes within the capillary basement membrane and the astrocyte foot processes that ensheath the capillaries (Fig.1.1). Furthermore, the endothelial cells comprises of an extremely low quantity of transcytotic vesicles. The endothelial cells lining the brain capillaries and the astrocytic endfeet play an essential role in maintaining the BBB structure (Nicolas *et al.*, 2007).

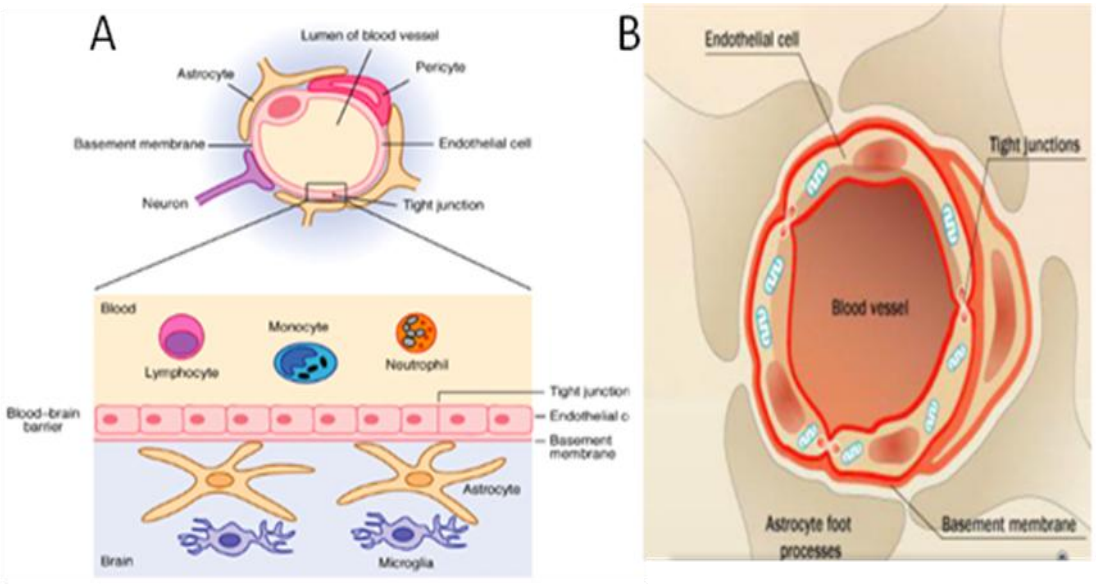

Figure 1.1. A. The brain blood barrier. B Cross section of a cerebral capillary (http://www.docstoc.com/docs/91914042/Blood-brain-barrier).

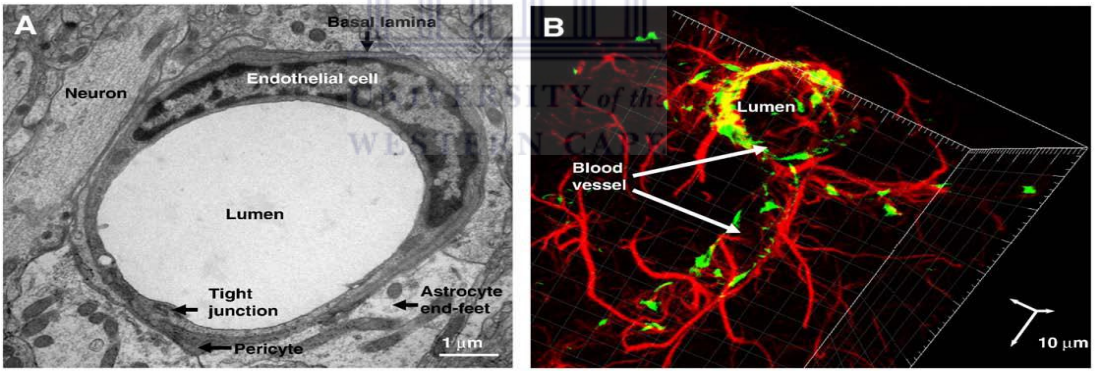

Figure 1.2. The neurovascular unit. A. Electron microscopy (TEM) of rat brain section showing a neurovascular unit. B. Confocal microscopy 3D-reconstruction of rat brain section showing part of cerebral vascular tree: endothelial cells (green) are surrounding with astrocytes (red), which are visualized with von-Willebrand factor and glial fibrillary acidic protein staining respectively (Nicolas et al., 2009).

1.1.2 Tight junctions

Tight junctions (TJs) in the endothelial cell act as a physical barrier forcing most molecules to take a transcellular route across the BBB, rather than moving

paracellularly through junctions, as in most endothelia (Imola *et al.*, 2011). This allows for a greater measure of regulation across the BBB. TJs have been largely implicated in both paracellular permeability and in the generation and maintenance of the physiological polarity of BMEC (Diamond., 1977). TJs form the morphological and functional boundary between the apical and basolateral cell surface domains, particularly in the endothelium of brain capillaries. The presence of an uninterrupted line of TJs at the cell-cell borders is one of the most important elements of BBB phenotype of BMEC. TJs are responsible for the separation of the apical and the basoletaral compartments leading to the functional polarization of the cell, and for the restriction of the paracellular pathway. The molecular components of TJs can be separated into two: transmembrane and cytoplasmic plaque proteins. Transmembrane proteins of endothelial TJs include occludin, junctional adhesion molecules and members of the claudin family (Imola *et al.*, 2011). On the surface, the molecular structure of tight junctions generally appears to be similar in all barrier systems, however, there are differences between epithelial and endothelial TJs (Fig.1.2). For example, BBB endothelial cells differ from epithelial cells by the intercalation of components of adhesion and tight junctions and reveal cadherins along the entire intercellular cleft (Schulze *et al.*, 1993). The BBB TJs of mammalian species are described as having the highest complexity found in the vasculature of the body. TJs are made up of integral proteins (claudins 1 and 5, occludin) and plaque proteins (ZO-1, ZO-2/3, 7H6 and cingulin) that link the integral TJs proteins to the actin cytoskeleton (Fig.1.3), (Imola *et al.*, 2011).

1.1.2.1 Occludin and Claudins

TJs proteins form domains of occluded intercellular clefts, which in freeze-fracture studies can be seen to form an intramembrane network of molecular strands. These strands appeared as a chain of fusion points; using freeze-fracture histological techniques as molecules of TJs transmembrane molecule, occludin (60- kDa protein) was discovered first (Imola *et al.*, 2011). The claudins (20- to 27-kDa) TJ molecules, which together with occludins seem to complete the task of establishing paracellular barrier properties. Both occlidin and claudins are integral membrane proteins that share the four transmembrane domains. The claudins are not randomly distributed throughout the organs, instead are regulated anatomically and inserted into the membrane by mechanisms not completely understood (Wolburg *et al.,* 2002). These proteins are now believed to be primarily responsible for permeability restriction.

1.1.2.2 Adhesion molecule structures between BMEC

Adhesion molecules such as the junctional adhesion molecule family (JAM) and the newly discovered molecule endothelial cell-selective adhesion molecule (ESAM) are localized at lateral walls of the BMECs as well (Wolburg *et al.,* 2002) (Fig. 1.3). JAM at the basal to the TJ strands form desmosomes that provide more solid structural support and join the cytoskeletons of two adjacent cells. JAM-1 (formerly JAM) is expressed in endothelial and epithelial cells, whereas JAM-2 and JAM-3 (formerly VE-JAM) are expressed in most vascular endothelial cells (Wolburg *et al.,* 2002). JAMs function as a mediator of leukocyte-endothelial cell interactions and are regulators of the cell physiological polarity. TJs form unbroken intercellular contacts

that control solute movement through the paracellular pathway across epithelia (Fig. 1.3).

1.1.3 Components of the BBB

The concept that BMEC make up a functional neurovascular unit comes from the observation of their interaction in the normal state and their coordinated response to injury (Maxime *et al.*, 2008). The highly specialized cerebral BMEC of the BBB regulate the entry of circulating substances across the paracellular pathways between adjacent cells into the brain by the TJs. In addition, specialized transcellular transport is regulated by inherent cellular molecules mechanism (Boveri *et al.*, 2006). There, pericytes plays an important role in the regulation of endothelial proliferation. Dysfunction of these cells, results in an abnormal vasculogenesis, endothelial hyperplasia and increased permeability across the BBB (Imola *et al.*, 2011), as can be seen in certain different forms the "end feet" of astrocytes encircle the outside of capillary endothelial cells. This endothelial-glial allegiance has an important influence on the formation and maintenance of the BBB. Astrocytes (Fig1.2) as the third important component of the BBB, covers a crucial part of the endothelial surface. These cells are sources of important regulatory factors (Imola *et al.*, 2011).

1.1.4 Development of the Blood-Brain Barrier

The development of the BBB begins to form during early embryonic development (Shadi *et al.*, 2012). The BMEC develop in the embryo from mesodermal cells at about 18 days gestation. During embryogenesis, the BBB barrier tightness gradually increases throughout development (Shadi *et al.*, 2012). Functionality of the BBB start

early in gestation as seen in rodents. During the embryonic development, the brain capillaries lose their fenestrae and become smaller and thinner in shape (Engelhard., 2003), inter-endothelial cell junctions become more widespread and interconnected (Imola *et al.*, 2011).

TJs proteins which form the structural basis of BBB and restricts the paracellular diffusion of hydrophilic molecules are expressed very early in fetal development, at 18 weeks of gestation (Virgintino *et a*l., 2004). Therefore, studies aimed at measuring the permeability throughout gestation revealed a significant degree of functional tightness developing during early to midgestation (Fig1.4) (Shadi *et al.*, 2012). Studies by Butt *et al*, (1990) showed that vessels demonstrated resistances in the range of 1100-1500 $\Omega.cm^{-2}$ after birth.

Central hemangioblasts form hematopoietic stem cells and peripheral hemangioblasts form angioblasts. Angioblasts are precursors of mature endothelial cells that migrate along with newly formed endothelial cells, after stimulation by the vascular endothelial growth factor (VEGF) to form the first primitive vascular plexus. The tubules continue to enlarge and grow through a process called vasculogenesis. Vasculogenesis is essential for maintaining homeostasis and is tightly regulated by pro- and anti-angiogenic agents (Lamalice *et al.*, 2007). Endothelial cells lining blood vessels do not complete vasculogenesis on their own, but along with periendothelial smooth muscle cells. The vascular smooth muscle cells not only contract, stabilize and protect delicate vessels, but also provide homeostasis of the BBB (Gerecht-Nir *et al*., 2004). Migration of capillary endothelial cells is essential in cascade of events that are involved in vasculogenesis (Lamalice *et al*., 2007).

1.1.5 Transport across the BBB

In the BBB, the BMEC transport nutrients to neurons and clear potentially toxic substances from the brain. These TJs prevent the diffusion of materials between adjacent endothelial cells, allowing only certain small molecules to pass and are a crucial component of the BBB.

In addition to the barrier function of the BBB it has an important carrier function. The transcellular carrier function, of the BMEC is responsible for the transport of nutrients to the brain and removal of metabolites (Maxime *et al.,* 2008). P-glycoprotein (ABCN1) is one of the important carrier transporters, which are able to transport different liphophilic drugs out of the BMEC. Certain small lipid-soluble molecules and blood gases like oxygen and carbon dioxide diffuse passively across the BBB. All the essential polar nutrients like glucose and amino acids require specific transport proteins in order to reach the brain (Imola *et al*, 2011). Glucose is the primary energy substrate of the brain, it enters the brain through the help of glucose transporter 1 (GLUT-1). At the BBB functional specific transporters such as GLUT-1 and organic anion transporting polypeptides (OATPs) are highly expressed (Maxime *et al.*, 2008). GLUT-1 is highly enriched in BMEC.

The essential amino acids cannot be synthesized by the brain and, therefore, must be supplied in the blood vascular system. They enter the brain as fast as glucose. Amino acids are transported into the brain by the leucine-preferring or the L-type transport proteins (Maxime *et al.*, 2008).

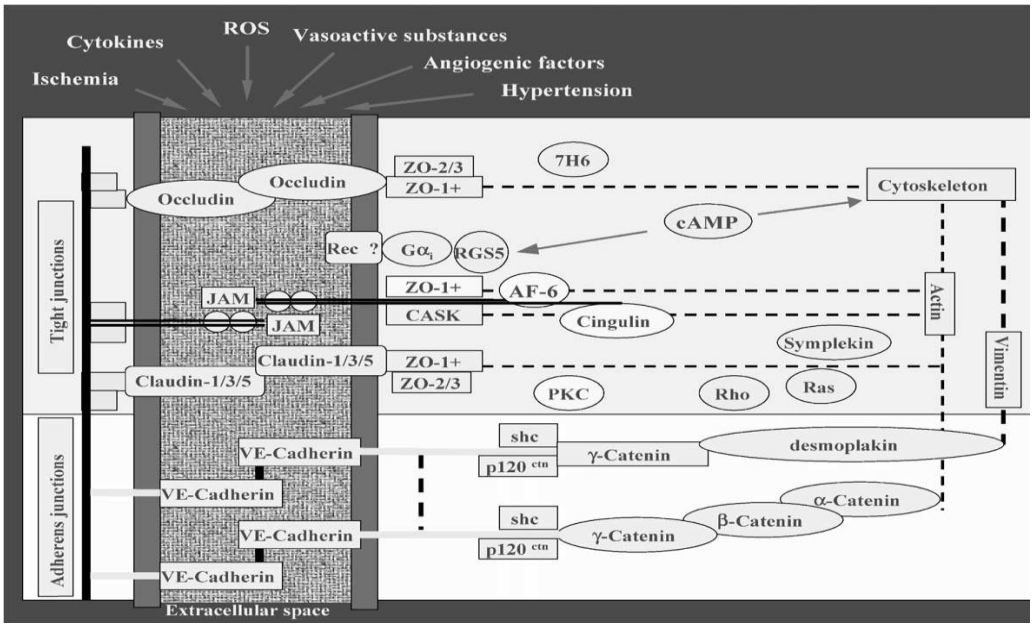

Figure 1.3: Molecular composition of tight and adherens junctions (Wolburg *et. al*., 2002).

1.1.6 Physiological function of the BBB

The BBB strictly regulates the exchanges between the blood and brain compartments, by preventing the paracellular diffusion of hydrophilic solutes, mediating the active transport of nutrients to the brain, flux of hydrophobic molecules and drugs between the brain to the blood and regulates the trans-endothelial migration of circulating blood cells and pathogens (Kwang., 2006). An intact BBB is of key importance since it functions as a selective barrier between the brain and the blood and maintains the homeostasis of the brain parenchymal microenvironment (Janigro *et al*., 1998). Understanding the BBB makes it possible to predict whether a compound's interaction with it is likely to compromise its functionality or whether a compound will reach the CNS compartment in significant amounts and is likely to have a direct effect on brain cells (Maxime *et al.*, 2008). The permeability of the BBB in physiological situations is regulated mainly by astrocyte-derived factors that control

both the transport properties of the endothelium and the organizational tightness of the TJs in the membrane (Hawkins *et al.,* 2005).

1.1.7 Role of the BBB in maintaining the homeostasis in the CNS

It is essential that homeostasis in the BBB is maintained for normal function of the CNS. The BBB lets essential metabolites pass from the blood to the CNS but blocks most molecules that are greater than 500 daltons, such as hormones, neurotransmitters, viruses and bacteria which are consequently prevented from crossing the BBB. It also implies that many drugs, which could be used as potential treatment for disorders of the CNS, cannot be used (e.g Dopamine cannot pass the BBB then L-dopa is utilized, L-dopa for dopamine). The establishment of TJs maintain cell polarity, results in a specific distribution pattern of distinct transporters, non-selective drug export pumps and receptors on the apical and basolateral plasma membranes (Cereijido *et al.,* 1998).

Transporting of large molecules such as, glucose and amino acid across the BBB, both *in vivo* and *in vitro,* including single-pass indicator diffusion and cultured endothelial cells methods have been studied. Compromised permeability and transport properties at the BBB may lead to alterations in cerebrovascular regulatory mechanisms of blood flow resulting in disrupted signalling between the BMEC and associated cells such as neurons and glial cells (Maxime *et al.*, 2008). The BBB, with regard to metabolites has been viewed as a passive system (Maxime *et al.*, 2008).

1.1.7.1 Ion homeostasis and BBB

Proper neuronal function necessitates a highly regulated extracellular environment, in which the concentrations of ions such as Na^+, K^+, and Ca^{2+} must be maintained within a very narrow range. Control of extracellular K^+ concentration is of particular importantance for the functioning of the brain (Schielik *et al*., 1990). The active uptake of K^+ into brain cells by the Na^+/K^+ exchange pump, which is a membrane-bound enzyme Na^+/K^+-transporting ATPase, is responsible for the maintenance of membrane potentials. BMEC with their TJs strictly regulate entry of K^+ from the blood to the extracellular compartment of the brain via the transcellular BMEC pathways, despite a definite concentration gradient favoring such movement. Sodium ion transporters on the luminal membrane and Na, K-ATPase on the anti-luminal membrane account for movement of sodium from the circulation to the brain. Little is known about the direct effects of MA on the permeability of bEnd5 cells and how it may lead to compromises in regulation of CNS ionic homeostasis.

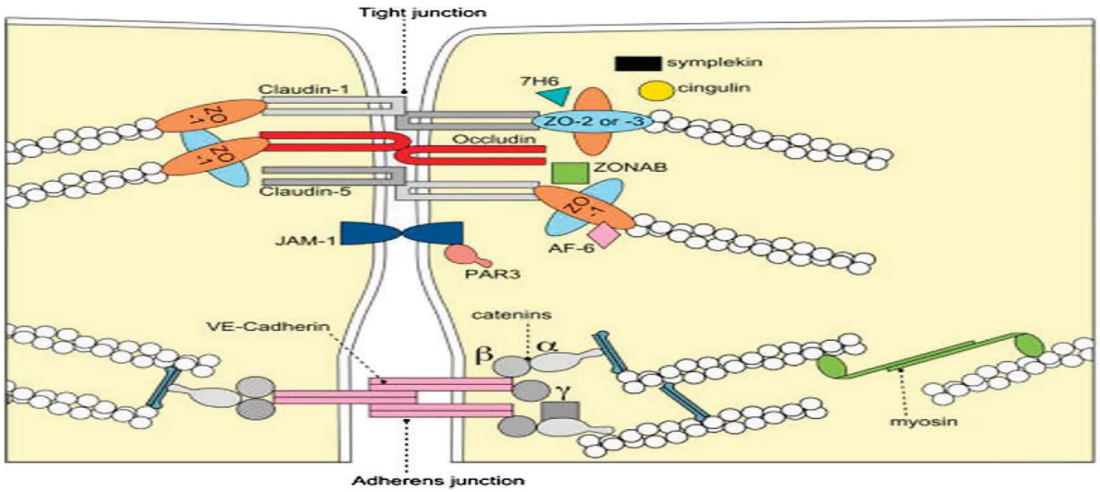

Figure 1.4. TJ protein complex at the apical side of two adjacent cerebral vascular endothelial cells. Intergral proteins such as occludin, claudin, and JAM come together to seal the intercellular gap and limit the diffusion of molecules across the endothelium (Shadi *et al*., 2012).

1.2 Cell Cycle

New endothelial cells necessary to replace cells that die, for tissue growth and repair are produced by cell division. Cell growth and division is determined by a successful cell cycle which is carefully regulated. The most basic function of the cell cycle is to duplicate accurately the vast amount of deoxyribonucleic acid (DNA) in the chromosomes and then segregate the copies precisely into two genetically identical daughter cells (Bruce *et al.*, 2002). There are two major processes which define phases of the cell cycle namely S phase and M phase. DNA duplication occurs during S phase, which requires 10–12 hours and occupies about half of the cell-cycle time in a typical mammalian cell. S phase of the cell cycle is the most preserved and least sensitive to modifications (Clara *et al.*, 2011). After the S phase, chromosome segregation and cell division occur in mitosis (M phase), which requires less time (±2hr) (Bruce *et al.*, 2002). M phase begins with chromosome condensation, followed by the duplication of the DNA strands and the resultant strands are packaged into elongated chromosomes. This phase ends with the strands condensing into more compact chromosomes required for their segregation (Bruce *et al.*, 2002). Mitosis and cytokinesis together define the M phase of the cell cycle, in which the latter refers to the division of the mother cell into two daughter cells. These daughter cells are genetically identical to each other and to their parent cell. M phase only lasts for about 10% of the cell cycle. Most cells require more time to grow and double their mass proteins and organelles than they require to replicate their DNA and divide. Large quantities of energy are required during the S phase. An extra gap phase is inserted in most cell cycles to allow more time for growth, G1 phase between M phase and S phase and a G2 phase between S phase and mitosis. These two gap phases serve (G1 and G2) as more than simple time delays to allow cell growth and to build up energy

for the next phase. They also provide time for the cell to monitor the internal and external environment to ensure that conditions are suitable for division (Bruce *et al.*, 2007). The preparations are completed before the cell commits itself to the major S phase and mitosis. The G1 phase is especially important in this respect. Its length can vary greatly depending on external conditions and extracellular signals from other cells. If extracellular conditions are unfavorable, cells delay progress through G1 and may even enter a specialized resting state known as G0 (G zero), in which they can remain for days, weeks, or even years before resuming proliferation. Indeed, many cells remain permanently in G0 until they or the organism dies (e.g. neural and muscle cells) (Bruce *et al.*, 2007). If extracellular conditions are favorable and signals to grow and divide are present, cells in early G1 or G0 progress through a commitment point near the end of G1. After passing this point, cells are committed to DNA replication, even if the extracellular signals that stimulate cell growth and division are removed. Therefore, the eukaryotic cell cycle is usually divided into four sequential phases: G1, S, G2, and M where G1, S, and G2 are referred as interphase. In a typical human cell proliferating in culture, interphase might occupy 23 hours of a 24 hour cycle, with ±1 hour for M phase (fig. 1.5).

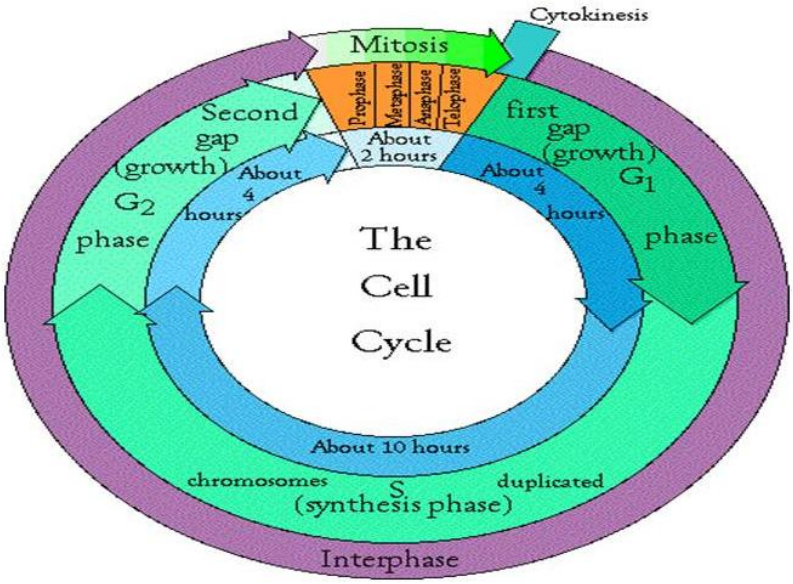

Figure 1.5. The division of the cell cycle (*http://home.earthlink.net*)

1.2.1 Cell cycle proliferation and Apoptosis

Regulation of cell numbers are determined by a complex balance of cell death and cell proliferation. Apoptosis is a genetically controlled response by which eukaryotic cells undergo programmed cell death (Vermeulen *et al.*, 2003). This phenomenon plays a major role in developmental pathway and provides a homeostatic balance of cell populations. Apoptosis and proliferation act in tandem. Cell cycle or apoptosis is likely to be controlled by more than one signal. These signals are necessary to ensure a proper cellular response (Vermeulen *et al.*, 2003). For a tissue to maintain homeostasis, it is dependent on the perfect balance between cell proliferation and apoptosis. A link between cell cycle and apoptosis may be supposed from the fact that a number of similar morphological features exist between mitosis and apoptosis, including substrate detachment, cell rounding, cell shrinkage and chromatin condensation (Vermeulen *et al.*, 2003). Eukaryotic cells have a complex network of regulatory proteins, which controls and that governs progression through the cell

cycle (Bruce *et al.*, 2007). Some of proteins involved in cell cycle and apoptotic pathways include: c-Myc and p53 (Vermeulen *et al.*, 2003). c-Myc is a nuclear phosphoprotein that functions as a transcription factor stimulating both cell cycle progression and apoptosis. c-Myc has a critical role in normal cell cycle progression, especially during transition from G1 to S phase (Vermeulen *et al.*, 2003). p53 is widely recognized as a protein functioning during the cell cycle and apoptosis. p53 regulates these processes by transactivating genes involved in different cellular functions, but p53 also activates transcription-independent mechanisms of apoptosis. Different components (c-Myc and p53) common to cell death and the cell proliferation have been identified and provide a rationale for linking cell cycle and apoptosis.

1.2.2 ATP and Cell Cycle

Energy source of a cell is equal connected to the ATP concentration. Mitochondrial function and its energy source are intimately connected to the cell cycle. Division of a cell is dependent on the relationship between the structures needed to duplicate and energy required for these process. Therefore, the role of energy production during the cell cycle is dependent on the understanding of its regulation. Mitochondria is defined as the power house of a cell, its function involves generating ATP required to power different complex cellular processes such as growth and differentiation (Wallace., 2005). When a cell is given the energy necessary to replicate the entire content, including DNA as well as organelle and membrane components, cells must be able to check if there are nutrients to complete these processes (Wallace., 2005). The cell division is unidirectional and DNA is replicated only once per cycle. Mitochondrial

energy production presents the dividing cell with a challenge in reducing ROS product formation normally via the Krebs cycle in the mitochondria (Wallace., 2005).

Dividing cells can generate energy via pentose phosphate pathway (PPP), with the intermediate products of the NADP molecule. NADPH is the primary co-enzyme involved in innate cellular antioxidant mechanisms that which prevents oxidative damage, as well as an essential cofactor in the reductive biosynthesis of fatty acids, nucleotides and amino acids (Wallace., 2005).

If available nutrients do not meet the metabolic energy requirements, then instead of a cell expending energy on division, cell division is arrested. A mitochondrial checkpoint exists in late G1, where low ATP concentration prompt the activation of an AMPK–p53–cyclin E-dependent pathway that presumably arrests energetically impaired cells instead of committing to cell division (Finke *et al.*, 2009).

1.3 What is Methamphetamine?

MA and related analogs of neuroamphetamines known as ‘speed’, ‘ice’, ‘eve’, or ‘ecstasy’ have become popular as recreational drugs of abuse (Imam *et al,* 2001). The use of the illicit psychostimulant MA, has become a worldwide health problem with an estimated 15 to 16 million users in the world (Granado *at el*, 2011). Between 1992 and 2001 it was reported in the United States (in over 33 states) about a 100% increase in admissions to treatment centers for abuse of MA (Masato *et al.*, 2002). This exceeds the number of heroine and cocaine abusers, making MA the second most widely abused drug after cannabis (Krasnova *et al.*, 2009). MA is one of the most addictive street drugs with a variety of forms and street names. A study performed by the Medical Research Council (MRC) in South Africa (S.A.) showed that the use of

MA was escalating (Plüddemann *et al.*, 2007). By 2007, the number of patients admitted for treatment reporting MA as their primary or secondary substance of abuse had increased by 49% (Plüddemann *et al.*, 2007). Data from South African Community Epidemiology Network on Drug Use (SACENDU) indicated that, use of MA as a primary drug of abuse was the highest in the Western Cape Province (35%) when compared to other S.A. provinces. It has been suggested that MA is far more dangerous than any other drug in S.A. because it makes the user more prone to violence (Plüddemann *et al.*, 2007). Krasnova and coworkers (2009) hypothesised that the inexpensive production of this drug, its low cost and long duration of action added to its wide spread prevalence and appeal.

1.3.1 History of Methamphetamine

MA was first produced by Dr. Nagayoshi Nagiai of Tokyo Imperial University in 1888 by reducing ephedrine with hydriodic acid & Red Phosphorus ((HI/red P), (Fig1.6) (Ogata., 1919). The term “methamphetamine” was derived from the groups in its chemical structure; methyl alpha-methylphenylethylamine. In the early 1900s western civilization discovered the benefits of ephedrine and pseuodephedrine as brochodilators and nasal decongestants. The "*ma huang*" plant was used as the only source of MA. There was a fear that the "*ma huang"* plant, which is a source for the herb ephedra, would be depleted due to the rate at which ephedrine was being consumed (Ogata., 1919). In 1927, a USA researcher Gordon Alles discovered that amphetamine worked as a substitute for ephedrine. Amphetamine then started being synthesized as a substitute for ma huang (a local name for MA in Japan) (Emad., 1929). It was marketed in 1932 as “benzedrine” as an over-the-counter inhaler to treat

nasal congestion. The stimulant effect of amphetamine was first recognized in 1935 and was used to treat narcolepsy. The first published report of amphetamine addiction and psychosis was in 1938 (Person *et al.*, 2005). In the 1940s, the Food and Drug Administration (FDA) approved MA for medicinal purposes, (Person *et al.*, 2005). Amphetamine and MA were categorized as Schedule II drugs in 1971. In Canada ,it became illegal to produce MA for personal and most medical purposes in the mid 1980s, with legislation following in just a few years later, and within a decade there were five specific laws that dealt with MA use, production, or distribution within the United States alone (Person *et al.*, 2005). The first illegal HI/Red Phosphorus lab seized by the Drug Enforcement Administration (DEA) in California was in 1987. A common method of illicit MA manufacture utilizes an alkali metal, typically lithium, and liquid ammonia to chemically reduce ephedrine or pseudoephedrine to form methamphetamine (Person *et al.*, 2005). MA was synthesized from methylamine and phenyl-2-propoanone by another Japanese researcher, A. Ogata in 1919 (Person *et al.*, 2005).

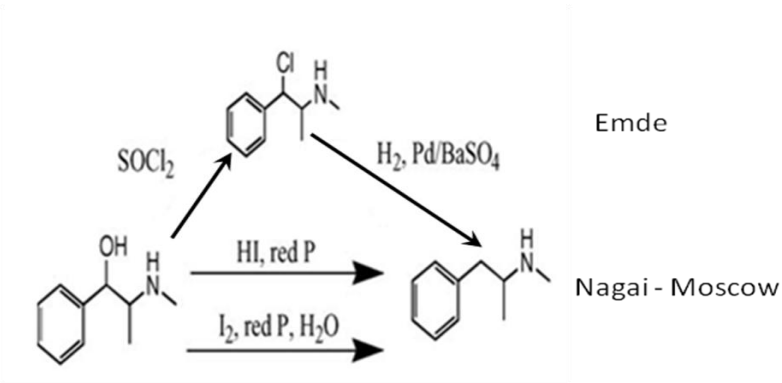

Figure 1.6 . Synthesis of methamphetamine by Emde and Nagai -Moscow method (Jae *et al.*, 2006).

1.3.2 Chemistry and Methods of Manufacturing MA

MA production requires very basic laboratory apparatus and it is for this reason that it can easily be synthesised (Syed *et al.*, 2001). MA is an amphetamine derivative. Amphetamine is an shorten nomenclature from Masato, the drug's older name‘α-methylphenethylamine’ which is an older description of the prototypical compound of which methamphetamine (methylamphetamine, metamfetamine, N-methyl-1-phenylpropan-2-amine) is the N-methyl derivative (Syed *et al.*, 2001).

There are different methods used in the illegal synthesis of MA from ephedrine compounds. The two-step reduction via chloroephedrine (‘‘Emde’’ method) and the direct reduction with hydriodic acid and red phosphorus (‘‘Nagai’’ method) are the most commonly used techniques (Jae *et al.*, 2006). In addition, to these methods reduction of ephedrine with iodine, red phosphorus and water (‘‘Moscow’’ method) is another method that is used for the illicit manufacturing of psychostimulants like MA (Fig.1.6) (Jae *et al.*, 2006).

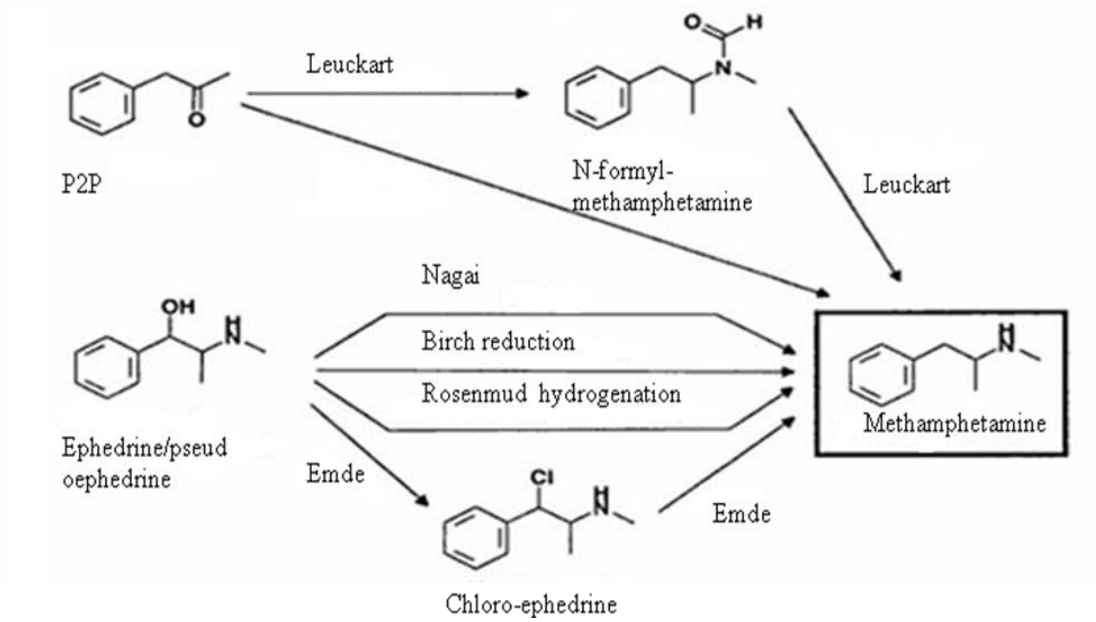

Figure 1.7. Most common synthesis routes of clandestinely manufactured methamphetamine (Remberg *et al.*, 1999).

Current methods known as Iodine/Red P or Lithium/Ammonia methods use pseudoephedrine and became popular as other chemicals became illegal (Fig. 1.7). The hydroxyl group when using the Iodine/Red P of ephedrine is more reactive than the aromatic ring, while excess alkali metal and the presence of a proton source allow the formation of a cyclohexadiene byproduct not found in samples of MA produced from other manufacturing methods (Person *et al.,* 2005). Illegal manufacturing mainly produces MA from pseudoephedrine 2, extracted from commercial cold and flu medications (Matthew *et al.,* 2009). MA is commonly synthesized from either ephedrine/ pseudoephedrine or phenyl-2-propanone (Fig.1.8) (Gabrielle *et al.,* 2010). Hypophosphorous acid method is also one of the commonly used methods to convert ephedrine 3 or pseudoephedrine 2 and subsequence to MA (Matthew *et al.,* 2009). When MA is manufactured from ephedrine/pseudoephedrine, the carbon and nitrogen structure of the product is the same as that of the precursor. The only atom change is the replacement of the ephedrine hydroxyl group with a hydrogen atom (Matthew, *et al.,* 2009). The actions of ephedrine and pseudoephedrine, and in particular their hydrochloride salts, with iodine and hypophosphorous acid result in the formation of MA (fig. 1.9) (Matthew *et al.,* 2009).

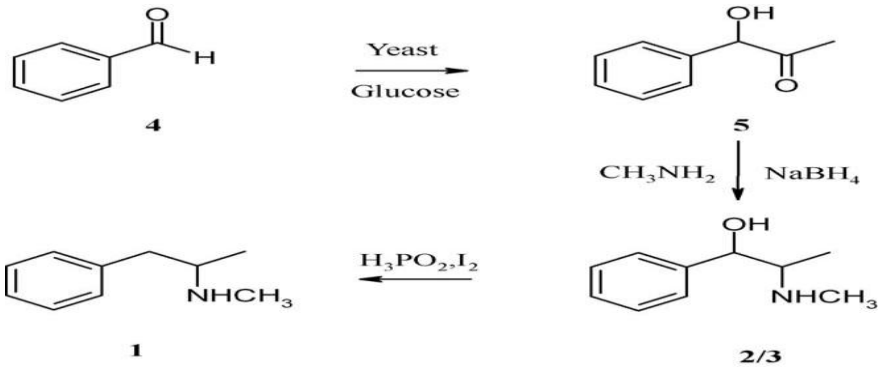

Figure 1.8. Biotransformation of benzaldehyde to l-PAC leading to methamphetamine (Gabrielle *et al*., 2010).

1.3.3 Illegal synthesis of MA

The main supply of illegal MA is from back yard laboratories (Matthew *et al.*, 2009). In the subsequent twenty years, the ephedrine as new form of MA was discovered, such as crystal MA (Fig1.9). The final product of illegal MA manufactured typically contains impurities. Analysis of the impurities provides valuable information about the conditions and the chemicals used in the production of the illicit MA (Jae *et al.*, 2006). Gas chromatography–mass spectrometry (GC–MS) is a method commonly used in forensics for detecting these impurities. This particular method is used because it can separate the complex mixtures and detect trace amounts of compounds. The mass spectrum provides a highly specific'fingerprint' of the compounds detected that can be used to help identify them by MS library database matching (Matthew *et al.*, 2009). GC–MS was instrumental in understanding the production of MA fermentation 'broth' in which benzaldehyde 4 and more interestingly, l-PAC 5, a known precursor of ephedrine 3 and pseudoephedrine 2 were precursors of MA (Matthew *et al.*, 2009). It is easy to see that the existence of these three compounds in a sample of MA during forensic analysis would be indicative that MA manufacture started with the biotransformation of benzaldehyde (Matthew *et al.*, 2009). Other key components in MA production, such as anhydrous ammonia (AA), widely available in agriculture, is also used forensically for identification of the MA source by illicit production (Bloom *et al.*, 2008).

Figure 1.9. Crystal structure of MA (http://www.rehabclinic.org.uk/facts-about-crystal-meth)

1.3.4 Route of administration of MA

Various methods of MA administration are used of which the most common methods are inhalation via smoking, snorting, injection, or taken orally. Intravenous (iv) injection or smoking of the active form of MA are the preferred routes of administration by many drug abusers. This is because the onset of pharmacologic effects is much more rapid and intense than when MA is taken orally or by other nonparenteral routes of administration (Hall *et al.*, 1996). However, smoking MA, which leads to very fast uptake of the drug in the brain, has become more common in recent years, amplifying MA's addiction potential and adverse health consequences. MA most often is used in a "binge and crash" pattern. MA can produce psychosis if used at a higher dose by typically illicit users (≥50mg) (Howard *et al.*, 2008). MA has a much longer duration of action than cocaine and a larger percentage of the drug remains unmetabolized in the body, which prolongs the stimulant effects (Howard *et al.*, 2008). MA also increases the release of dopamine, leading to much higher

concentrations in the synapse, which can be toxic if they are left in high content (Hall *et al.*, 1996).

1.3.5 Metabolism of MA

The liver is the major organ of metabolism in the body. It prepares substances for excretion. Most substances that enter the body need to be metabolized in order to decrease their toxicity to the body, because if they are left in high concentration they can be toxic. The common chemical reactions in the liver such as aromatic hydroxylation, aliphatic hydroxylation, oxidative *N*-dealkylation, S-oxidation, reduction and hydrolysis are the mechanisms that metabolize drugs, thus facilitating their elimination through the kidneys. It is important to understand the metabolic fate of a drug in order to analyze metabolites in biological samples such as blood, urine and feces (Kanamoria *et al.*, 2005).

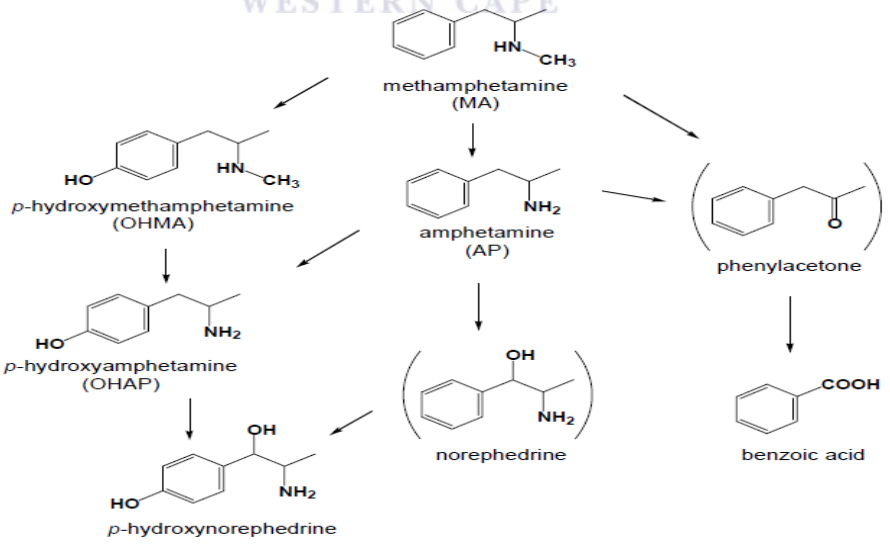

Figure 1.10. Summary of the metabolic pathway of methamphetamine (MA) in the rat liver (Caldwell *et al.*, 1972).

Caldwell *et al.* (1972), reported that human subjects receiving 20mg of the drug orally resulted in about 90% of the metabolised and non-metabolised MA being excreted in the urine within 4 days. During the first day of examination for metabolites, the main metabolites were the unchanged drug (22% of the dose) and 4-hydroxymethamphetamine (15%). Minor metabolites were hippuric acid, norephedrine, 4-hydroxyamphetamine, 4-hydroxynorephedrine and an acid-labile precursor of benzyl methyl ketone (Caldwell *et a.l,* 1972). At day 2 the main metabolites in the urine were 4-hydroxymethamphetamine (31% of dose), 4-hydroxynorephedrine (16%) and unchanged drug (11%). Minor metabolites were amphetamine, 4-hydroxyamphetamine and benzoic acid. Generally, in humans the main metabolite in urine is the unchanged drug, amounting to between 18 and 27% of the dose. In addition seven other metabolites were also found: 4-hydroxymethamphetamine (15%), hippuric acid (5%), amphetamine (2-3%) norephedrine (2%), 4-hydroxynorephedrine (1-2%), 4-hydroxyamphetamine (1 %) and a precursor of benzyl methyl ketone (about 1% of the dose in 24h). In addition to these, an unknown amine (about 1-2 %) and acid (1-3 %) were also detected. MA metabolism in the body could be expected to undergo at least three initial metabolic reactions, namely N-demethylation, aromatic hydroxylation and aliphatic hydroxylation at the methylene group next to the benzene ring (Caldwell *et al*, 1972) . It appears that the primary metabolic reactions are aromatic hydroxylation and N-demethylation and that 'p-hydroxylation' may only occur as a secondary reaction, since only norephedrine (2- amino-1-phenylpropan-1-ol; VII), but not ephedrine (2-methylamino-1-phenylpropan-1-ol), derivatives were found (Caldwell *et al.*, 1972).

There are marked differences in the metabolism of MA in different species. The main reaction in the rat was aromatic hydroxylation, in the guinea pig demethylation and deamination, whereas in man much of the drug, possibly one-half, was excreted unchanged. In rats, about one-tenth of the dose is excreted unchanged and some 3% appears as amphetamine. The main metabolites are the phenols, 4-hydroxymethamphetamine (31%), 4-hydroxynorephedrine (16%) and 4-hydroxyamphetamine (6%). MA is mainly metabolized through p-hydroxylation, β-hydroxylation, *N*-demethylation and deamination in rats (Fig. 1.10) (Caldwell *et al.*, 1972).

The analysis and interpretation of illegal MA derivatives in the blood is a challenging process made difficult by a number of factors. One of the complications comes from determination of the origin of MA in a sample because of possible impurities (Cody, 1993). There are fourteen different metabolite precursors of MA. The main precursors are amphetaminil, benzphatamine, clobenzorex, mefenorex, mesocarb and prenlymine. Prescription MA is available only as the *d*-enatiomer, therefore the presence of both origins could not come from use of prescription MA. knowing origin of the MA used, may therefore indicate illicit or legitimate medicinal use (Cody, 1993).

1.3.6 Psychosomatic effects of MA

The illicit use of MA has had harmful social and public health consequences (Masato *et al.*, 2002). MA effects include sensorial arousal, reduced fatigue, euphoria, positive mood, accelerated heart rate, elevated blood pressure, pupil dilation, increased

temperature, reduced appetite, and short-term improvement in cognitive domains, including sustained attention. Its abuse is associated with a number of negative consequences in humans, particularly anxiety. Cardiovascular and subjective effects appear to increase dose-dependently. It has been reported that MA-associated fatalities arise most commonly from multiple vascular congestion, pulmonary oedema, pulmonary heart congestion, cerebrovascular haemorrhage, ventricular fibrillation, acute cardiac failure or hyperpyrexia (Howard *et al.*, 2008). Its hypertensive effects can produce a number of acute and chronic cardiovascular complications. Continual use may induce neurotoxicity, associated with prolonged psychiatric symptoms, cognitive impairment and an increased risk of developing Parkinson's disease (Howard *et al.*, 2008). It was observed that this neurotoxic drug causes cell death both *in vitro* and *in vivo* at certain concentrations (Deng *et al.*, 2002). Its inconspicuously high abuse potential is owed primarily to its strong euphoric properties. Although the acute effects of recreational drugs are known, mechanisms resulting in the long-term consequences and possible neurotoxicities remain unclear (Yamamoto *et al.*, 2010).

1.3.7 Morphological effects of MA in the brain

MA may cause long-term neural damage in humans, with concomitant deleterious effects on cognitive processes such as memory and attention (Syed *et al.*, 2001). A neuropsychological consequence of MA abuse is cognitive impairment, with working memory deficits remaining long after withdrawal (Asanumaa *et al.*, 2002). It is reported that MA may compromise the CNS because of its ability to alter the permeability of the BBB as a results of it being structurally similar to amphetamine and the neurotransmitter dopamine (Asanumaa *et al.*, 2002). This drug produces

damage to monoaminergic systems in the brain (Asanumaa *et al.*, 2002, Deng *et al,* 2002). Functional imaging studies (Genca *et al*., 2003) in chronic MA users suggested that this agent may affect the white matter. It is also known to cause neuropsychiatric complications including psychosis, strokes, coma and death (Zhoua *et al.,* 2004). The degenerative processes in the central nervous system are thought to occur through either necrosis or apoptosis (Zhoua *et al.,* 2004).

1.4 Mechanism of action of Methamphetamine

MA is an indirect agonist at DA, NE and serotonin receptors, due to their structural similarity. The MA substitutes for these monoamines at membrane-bound transporters, namely the dopamine transporter (DAT), noradrenaline transporter (NET), serotonin transporter (SERT) and vesicular monoamine transporter-2 (VMAT-2) (Hall *et al.*, 1996). *In vitro* studies indicate that MA is twice as potent at releasing noradrenaline when compared to dopamine, and its effect is 60-fold greater with respect to noradrenaline release than serotonin release. MA entering the brain parenchyma causes the release of the neurotransmitters DA, NE and serotonin in the central nervous systems (Fig.1.11). MA causes the release of monoamines that result in long-lasting neurotoxic damage to monoaminergic systems (Thiriet., 2001). Although the mechanisms of MA neurotoxicity at cellular and molecular levels remains to be fully clarified, the accumulated evidence indicates that excessive dopamine and glutamate release as well as the participation of oxygen-based radicals of nitric oxide may play a crucial role (Asanumaa *et al.,* 2002**)**. Because MA-induced toxicity appears to involve interaction of reactive substances and since these compounds can cause neuronal death via apoptotic processes, it is possible that

apoptosis may occur after administration of MA doses via damage to monoaminergic systems (Deng *et al.,* 2000). The accumulated evidence indicates that reactive oxygen species (ROS) are important mediators of the MA-induced neurotoxicity especially in dopamine (DA) systems (Asanumaa *et al.*, 2002). Asanumaa *et al.* (2002) reported that MA induced dopaminergic neurotoxicity which was attenuated in p53-knockout (KO) mice, demonstrating that p53 plays an important role in MA-induced neurotoxicity. Further research data suggest that MA might cause its neurotoxic effects via the production of free radicals and secondary effects in the expression of genes known to be involved in apoptosis (Imam, *et al*, 2001). It is reported that MA-induced release of DA from vesicles to cytosolic and extracellular space, result in free radical formation (Deng *et al*, 2002). Other reports indicate that MA cytotoxicity involves the "mitochondrial death pathway" in a dopamine independent manner in both *in vivo* and *in vitro* models (Genca *et al.*, 2003). MA induces both acute and chronic neurotoxic changes in dopaminergic and serotonergic neurons (Chang *et al.*, 2007). It has also been observed clinically, that chronic MA abuse is associated with persistent neurotoxicity and in some individuals the MA development causes changes to neural system of the CNS even years after stopping the use of a drug (Chang *et al.*, 2007).

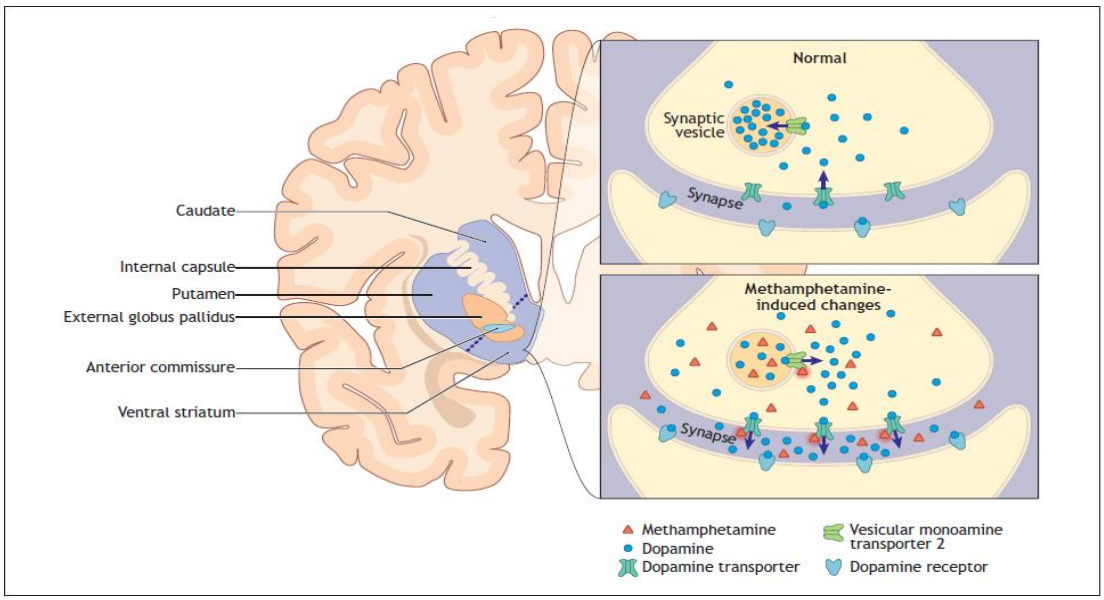

Figure 1.11. Release of dopamine neurotransmitters in the presence of methamphetamine. MA is taken up by the plasma membrane dopamine active transports (DAT) in a manner inhibited by the uptake blocker nomifensine. Once inside the neuron, MA promotes DA release from synaptic vesicles. MA inhibits monoamine oxidase resulting in additional increases in cytosolic DA (Chang *et al*., 2007).

MA contributes to CNS inflammation by stimulating increased release or activation of matrix degrading proteinases, which would lead to the breakdown of the BBB and the influx of inflammatory cytokines, chemokines and macrophages into the brain (Chang *et al.*, 2007). Syed *et al.*, (2001) performed an *In vivo* study in rodents and non-human primates which demonstrated significant activation of astroglia, microglia and mediators of inflammation including prostaglandins, cytokines, interleukin, neurotrophic factors and ROS in response to MA administration. These changes may be responsible for cellular damage of the BBB leading to increased metabolic demands on these vulnerable regions. Cognitive impairment or deficits have been reported in individuals actively using MA, as well as during early and prolonged periods of abstinence. MA has higher lipid solubility than the unsubstituted amphetamine, and thus larger amounts of the drug can rapidly and efficiently cross

the BBB (Syed *et al.*, 2001). The methyl group makes the drug even more effective by facilitating its penetration into the central nervous system (Bloom *et al.*, 2008).

1.4.1 Methamphetamine and the Cell Cycle

With evidence clearly showing that MA causes neuron cell death in monoaminergic terminals and nonmonoaminergic cells and that MA treatment results in oxidative damage to lipids, proteins, and DNA in various regions of the brains, administration of antioxidants, such as ascorbic acid, vitamin E, or baicalein alleviates MA-induced damage (Wu *et al.*, 2007). Studies revealed increasing evidence that MA-induced neurodegeneration to be associated with mitochondria-dependent apoptosis (Wu *et al.*, 2007). MA is a cationic lipophilic molecule that can diffuse into mitochondria and be retained by these organelles (Davidson *et al.*, 2001). An accumulation of positively charged molecules in the mitochondria would in due course result in dissipation of the electrochemical gradient established by oxidative phosphorylation, and inhibit ATP synthesis (Wilson *et a*l., 1996). In addition, administration of MA to mice has been shown to cause an increase in pro-death proteins (BAX, BAD, and BID) but a decrease in anti-apoptotic Bcl-2-related proteins (Bcl-2 and Bcl-XL) (Jayanthi *et al.*, 2001). These proteins are known to interact in the mitochondrial membrane, and therefore, the MA-induced alterations in these protein contents have been suggested to form channels which result a in potential loss across mitochondrial membrane, and additionally allows cytochrome c release. This suggests that mitochondrial damage may contribute to MA-induced neurotoxicity (Chi-Wei Wu *et al.*, 2007). MA induces neurodegeneration through damage and apoptosis of dopaminergic nerve terminals and striatal cells, presumably via cross-talk between the

endoplasmic reticulum (ER) and mitochondria-dependent death cascades (Tian *et al.*, 2009).

In rodents it has been suggested that MA induced apoptosis of striatal glutamic acid decarboxylase-containing neurons by causing ER stress and activate mitochondrial death pathways (Tian *et al.*, 2009). Many studies have shown that the process of cell death induced by MA involve multiple processes including mitochondrial dysfunction. MA-induced apoptosis is a relatively recent discovery (Tian *et al.*, 2009). MA significantly increase apoptosis in animals after long access to MA for self-administration (Clara *et al.*, 2011).

Scrutiny of the literature indicate that most research that has been done in the BBB has focused on the neurons but not much has been reported on the *in vitro* effects of MA on the endothelial cell of the BBB components. This study will provide insight on how MA affects the BBB.

The next chapter (2) describes the methods that were used in this study, while chapter 3 reports on the results of this study. Chapter 4 is dedicated to the discussion of the results and conclusion with the main outcomes of this study.

CHAPTER 2

2. Materials and Methods

2.1 Reagents

Methamphetamine (MA) (Cas No: 51-57-0) was purchased from Sigma-Aldrich, South Africa (S.A). Street MA samples were obtained from the South African Police Department (SAPD) Forensics Laboratory (Kuils River, Western Cape). The street MA samples were shown to have 98% purity according to HPLC analysis. For cell cycle analysis propidium iodide (PI), (Cas No: 255535-16-4) and RNASE (Cat. No: 12091-039) purchased from Sigma-Aldrich, S.A. were used. The Cell Titer-Glo Luminescent Cell Viability Assay (Cat. No. G-7580) for ATP concentration determination was purchased from Anatech (Promega), S.A. DNA synthesis, cell proliferation ELISA (chemiluminescent) (Cat. No. 11669915001) was purchased from Roche, S.A. The sample number for all the assays performed was in duplicate. MA which is water soluble, was added to media after weighing the appropriate amount and added to other cell culture media.

2.2 Analysis of street MA samples using Gas Chromatography

A coupled gas chromatography is an analytical comparative technique where compounds in the gas phase are separated and their characteristic pattern profile (mass spectrum) of the separated compounds are obtained. Gas chromatographic analysis

was carried out on the Agilent 7890A coupled with Agilent 5975C VL MSD (mass selective detector) with triple axis detector. Using an Agilent 7693 Autosampler, 1µl samples was injected under splitless mode through a capillary column (30m X 0.25mm X 0.25µm film thickness). Helium was used as a carrier gas at a flow rate of 1ml/min; and inlet temperature was set at 250ºC. The oven temperature was programmed to run the samples: initial temperature 50ºC/min; followed by an increase of 10ºC/min to 300ºC, and held for ten minutes. The injector and detector temperature was set at 240ºC and 300ºC respectively. For every sample tested a standard sample containing pure MA was also analysed (Fig 2.1-2.4).

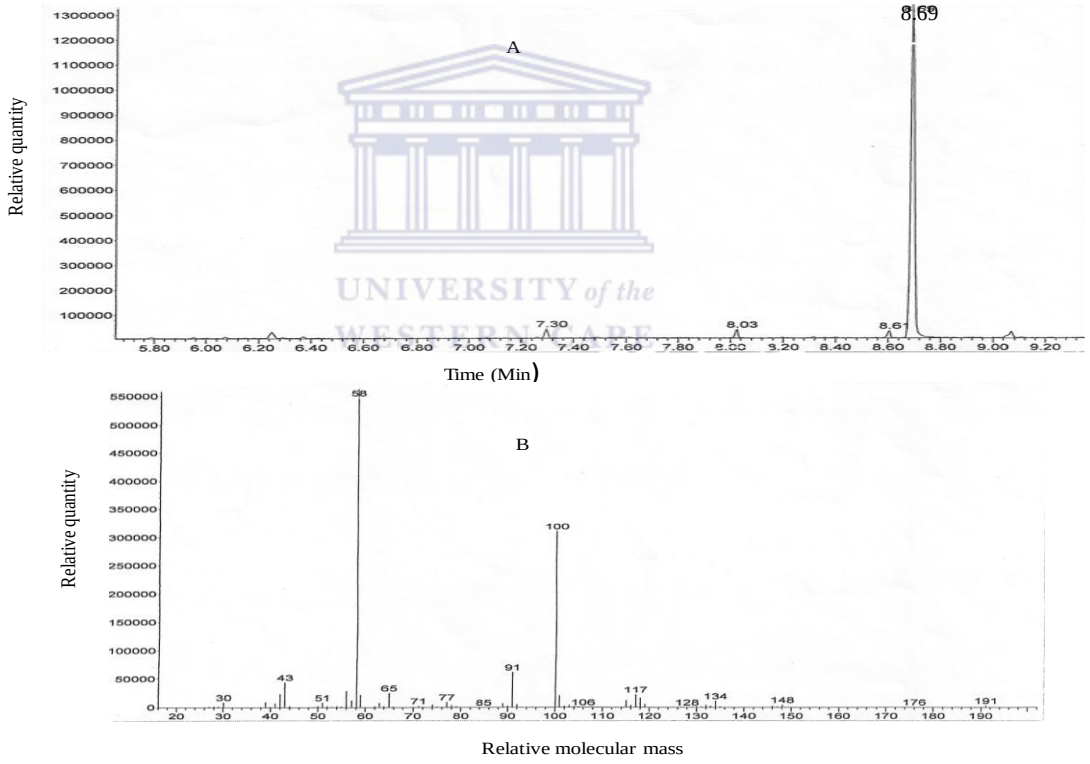

Figure 2.1. The above figure illustrates: A) methamphetamine analysed using GC elucidated at 8.69 min. B) total ion chromatogram of methamphetamine analysed standard using MS for street MA sample 1.

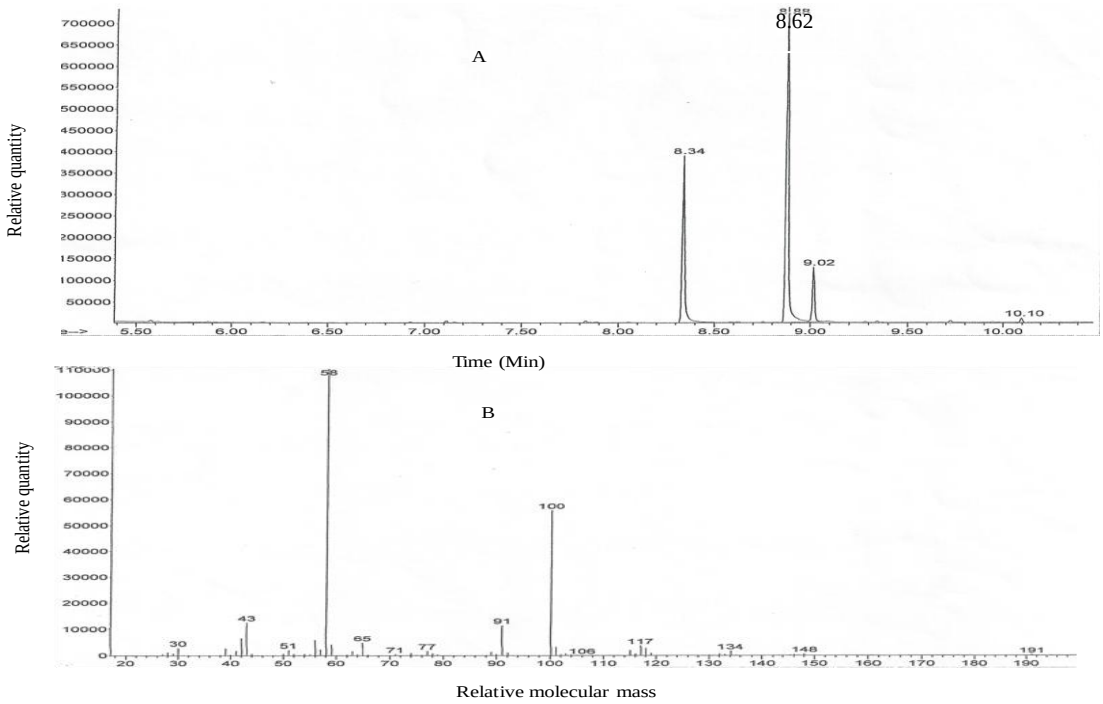

Figure 2.2. The above figure illustrates: A) methamphetamine analysed using GC elucidated at 8.62min. B) total ion chromatogram of methamphetamine analysed standard using MS for street MA sample 2.

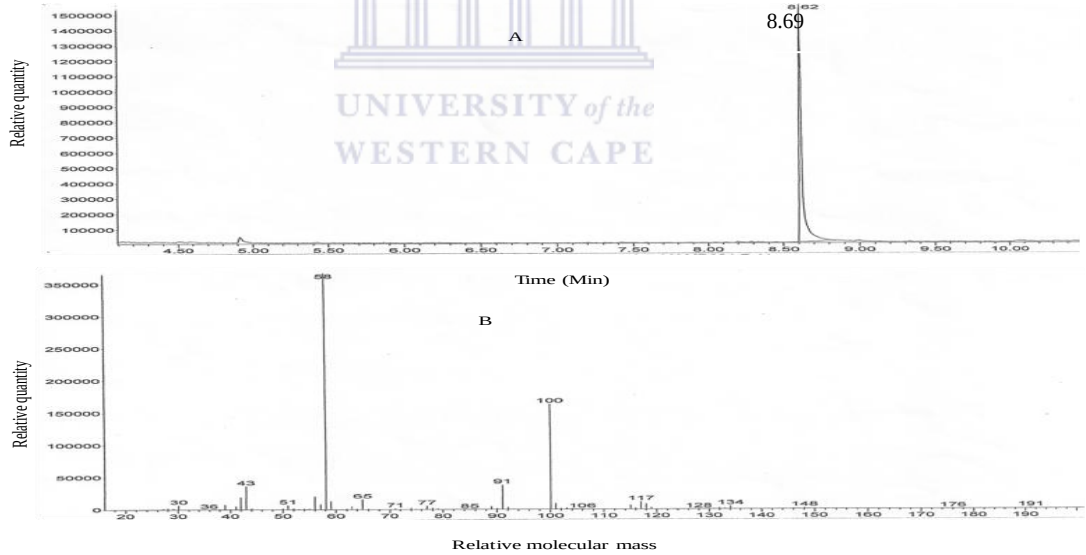

Figure 2.3. The above figure illustrates: A) methamphetamine analysed using GC elucidated at 8.65min. B) total ion chromatogram of methamphetamine analysed standard using MS for street MA sample 3.

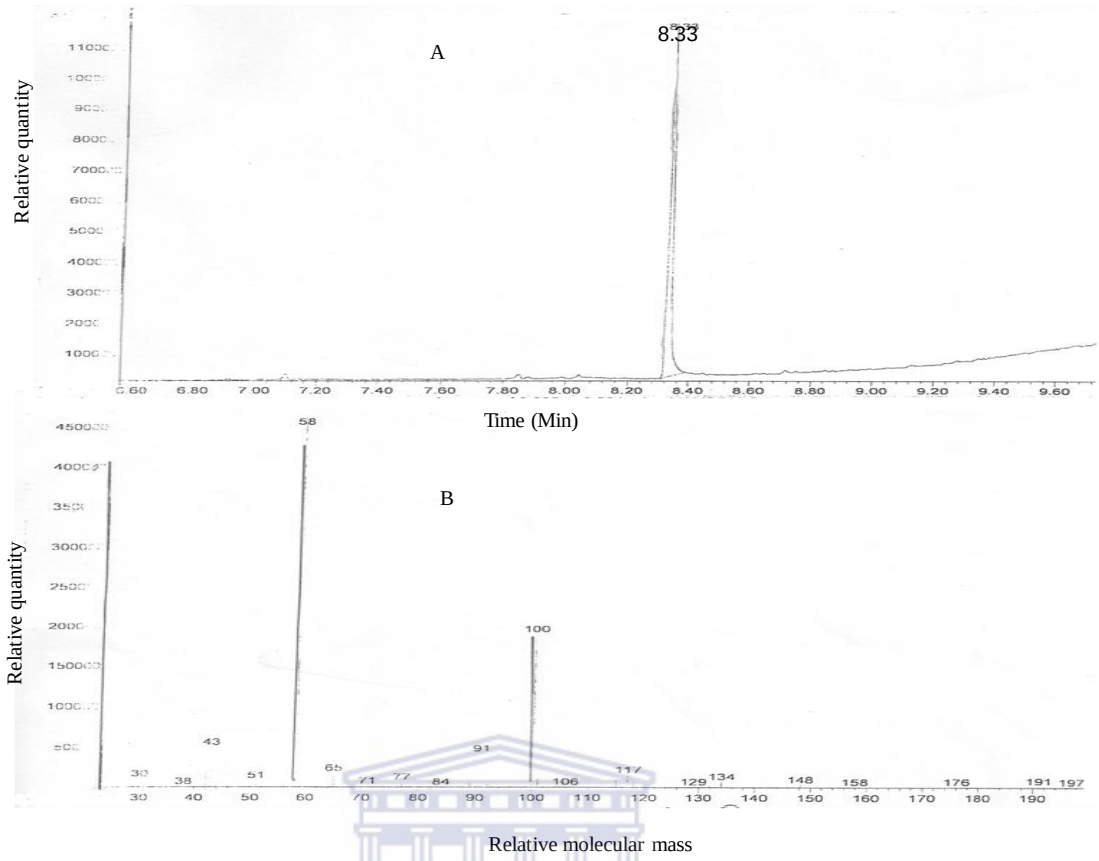

Figure 2.4. The above figure illustrates: A) methamphetamine analysed using GC elucidated at 8.33min. B) total ion chromatogram of methamphetamine analysed standard using MS for street MA sample 4.

2.3 Cell Culture

Immortalised mouse brain endothelial (bEnd5) cells, (Cat. No. 96091930) purchased from Highveld Biologicals was cultured in Delbecco's modified eagle medium (DMEM), (Lonza S.A.), supplemented with 10% Fetal bovine serum (FBS), (Gibco S.A.), and 1% penicillin/streptomycin (Sigma S.A.), 1% l-pyruvate, (Gibco S.A.), 1% non-essential amino acids, (Lonza S.A.). Cells were maintained and incubated in a humidified cell culture incubator at 37°C, with 5% CO_2. Cell passages used for all analysis ranged between P18 and P40.

2.4 Trypan Blue Viability Assays

Trypan blue is taken up by damaged or dead cells due to cell membrane disruption. When cells are viewed under the light microscope, they will appear blue if compromised. Undamaged will be clear when viewed under microscope. bEnd5 cells were seeded at $2x10^4$ cells per 35mm petri-dish in supplemented DMEM. After 24 hours, the media was removed and cells were incubated with selected concentrations of 0.0001mM, 0.001mM, 0.01mM, 0.1mM and 1mM pure MA and street MA samples. Controls cells were exposed to supplemented media only. Cells were trypsinated at the selected time intervals of 24, 48, 72 and 96hrs. Media aspirated prior to the addition of trypsin- Ethylenediaminetetraacetic acid (EDTA), (White Sci, S.A.) was also collected and transferred to designated tubes. Cell viability was determined using the cell suspension, trypan blue and DMEM at a 1:3:6 ratio, respectively. Viable and non-viable cells were counted using a phase contrast microscope.

% cell growth was also determined comparing the live cell population counted of the experimental group with those of the controls.

$$\% \text{ cell growth} = \frac{\text{No. of live cells}}{\text{Total No. of cells}} X100$$

2.5 ATP Concentration Analysis

The luminescent cell viability assay can be used to determine the number of viable cells in culture based on quantitation of the ATP present, which is indicative of the presence of metabolically active cells. The amount of ATP is directly proportional to the number of cells present in culture**.**

$2x10^3$ bEnd5 cells were seeded in 100µl supplemented DMEM culture medium per well in opaque-walled 96-well, white microtiter plates and incubated for 24hrs. subsequently the media was then removed and incubated with concentrations of 0.0001mM, 0.0001mM, 0.01mM, 0.1mM and 1mM of pure MA and street MA for 24, 48, 72 and 96hrs. Wells containing medium without cells were prepared in order to obtain a value for background luminescence, while control wells contained cells cultured in supplemented media only. Post incubation times, microtiter plates and its contents were allowed to equilibrate at RT for approximately 30min and a volume of reconstituted CellTiter-Glo Reagent (prepared as directed by the assay kit protocol) equal to the volume of cell culture medium was added to each well. The well contents were gently agitated for 2min on an orbital shaker to induce cell lysis. The microtiter plates were then incubated for an additional 10min at RT in order to stabilize luminescent signal and luminescence was recorded using the Glomax multiplate reader.

2.6 BrdU Proliferation Assay

The assay is based on the detection of BrdU incorporated into genomic DNA of proliferating cells. Cells grown in 96-well tissue-culture micro titter plates are labelled with BrdU. During this labelling period, BrdU is incorporated in place of thymidine into the DNA of cycling cells.

The stock of 1:100 aliquots were prepared and stored at -20ºC. For Anti-Pod and washing solution, the working solution of 1:100 (stock+ dilution solution) was prepared. $5x10^3$ bEnd5 cells were seeded in 100µl supplemented DMEM culture medium per well in black walled 96-well microtiter plates, (Biocam/Biotech S.A.) and

incubated for 24hrs. Media was then removed and cells were incubated with concentrations of 0.00001mM, 0.0001mM, 0.01mM, 0.1mM and 1mM of pure MA and street MA samples for 24, 48, 72 and 96hrs. Wells containing medium without cells were prepared in order to obtain a value for background luminescence, while control wells contained cells grown in supplemented media only. Post incubation times, 10µl of BrdU was added to all wells and the microtiter plate was re-incubated for 2hrs at 37ºC. Thereafter, the labelling medium was removed and 200µl FixDenat was added and fixation was allowed at RT for 30min. The FixDenat was removed after fixation and 100µl anti-BrdU-POD was added to each well and incubated for 90min at RT. After removal of the anti-Brdu-POD, the microtiter plate was washed with washing buffer three times (200µl). Subsequently 100µl of substrate was added to all well contents and gently shaken for 10min on an orbital shaker. The plate was read using luminescence Glomax multiplate reader.

2.7 Flow Cytometry

FACS (fluorescence activated cell sorter), is a type of flow cytometry that analyses internal structures of cells and separates them into different groups. In this application a cell suspension is forced through a tube in the form of droplets containing single cells.

Trypsinated cells were suspended in ice-cold 70% Ethanol (EtOH) to a final volume of 10ml and were placed at 20ºC for a minimum of 2hrs. Cells were centrifuged at 1000 rpm for 5min at room temperature (RT), the EtOH carefully removed and the loose pellet resuspended in 1ml ice-cold 70% EtOH. The resuspended pellet was transferred to an eppendorf and centrifuged at 1000 rpm with a bench top microfuge

for 1min to ensure pellet formation. The remaining EtOH was removed and the pellet was resuspended in 1ml (PBS) (White Sci. S.A.). RNase (20mg/ml) diluted in phosphate buffered saline PBS at a ratio 1:199 respectively was prepared and the required volume (50µl per 10^4 cells) added and incubated at RT for 1½hrs. The propidium iodide (PI) staining solution was prepared using 0.1% Triton-X100 (Cas No: 9002-93-1), 0.003M $MgCl_2$, 0.1M NaCl, 0.1Ml piperazine-N,N′-bis(2-ethanesulfonic acid) (PIPES) buffer (Sigma S.A.) pH6.8, 1mg/ml PI with the final volume made up with distilled water. Approximately 20min preceding flow cytometry analysis the required volume of PI staining solution was added to the cells (9X volume of RNase/PBS solution).

2.7.1 Cell Cycle Analysis

bEnd5 ($5x10^{5)}$ cells were seeded in supplemented DMEM in 25ml flasks. Individual samples were analysed using the Becton Dickinson FACSCalibur flowcytometer with a 488nm coherent laser. Each analysis was based on at least 10 000 events. The software used for acquisition of data, was Cellquest Pro version 5.2.1. The cell population was identified and gated (R1) on a forward scatter (FSC) vs. side scatter (SSC) dot plot in acquisition mode. Fluorescent Channel 2(FL2) at 575nm was used for propidium iodide detection. A dot plot of FL2A(area) vs FL2W(width) was used to identify single cells (R2) and thus eliminate doublets. A histogram plot of FL2A was used to enumerate G1/G0, S-phase and G2/M populations. The combined parameters of FSC, SSC, FL2A and FL2W displayed the results. A threshold of 52 on the FSC channel was set to remove sample debris. Nile Red fluorescent particles were

used for instrument standardization, stability and reproducibility. Analysis of the results were performed using Modfit version 2.0 software.

2.8 Statistical Analysis

Medcalc (version 11.5.1), using the Wilcoxon Rank Sum Test for not normally distributed, unpaired samples was employed for statistical analysis. All outliers were statistically identified by Box-and Whisker plot and removed before determining significance between the means, in which $P<0.05$ was designated as significantly different.

CHAPTER 3

3.1 Chemical analysis of street MA samples using GC-MS.

All samples were qualitatively analyzed for MA presence by gas-chromatography mass spectrometry (GC-MS). All data (Fig. 3.1-3.4) represent the presence of the MA. The presence of the MA was detected at elevation time of ranging between 8.5 to 8.9min.

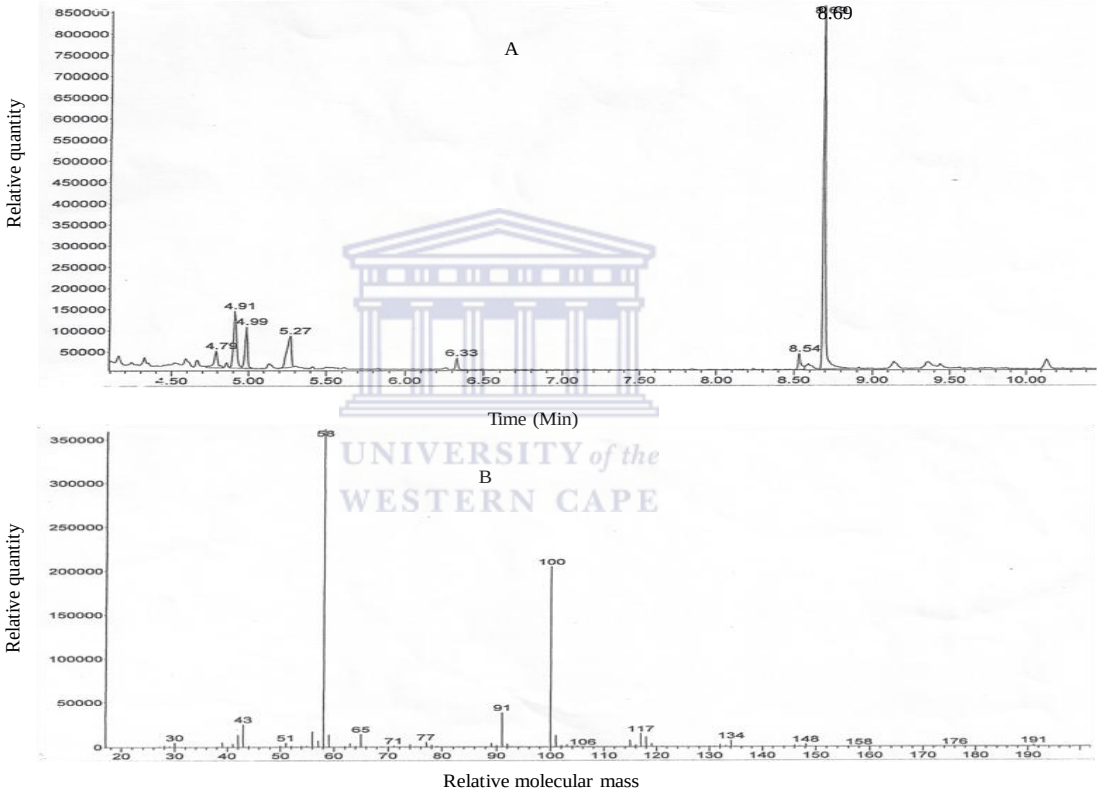

Figure 3.1. The above figure illustrates: A) methamphetamine analysed using GC elucidated at 8.69min. B) total ion chromatogram of methamphetamine analysed using MS for street MA sample 1 showing the chemical signature of MA.

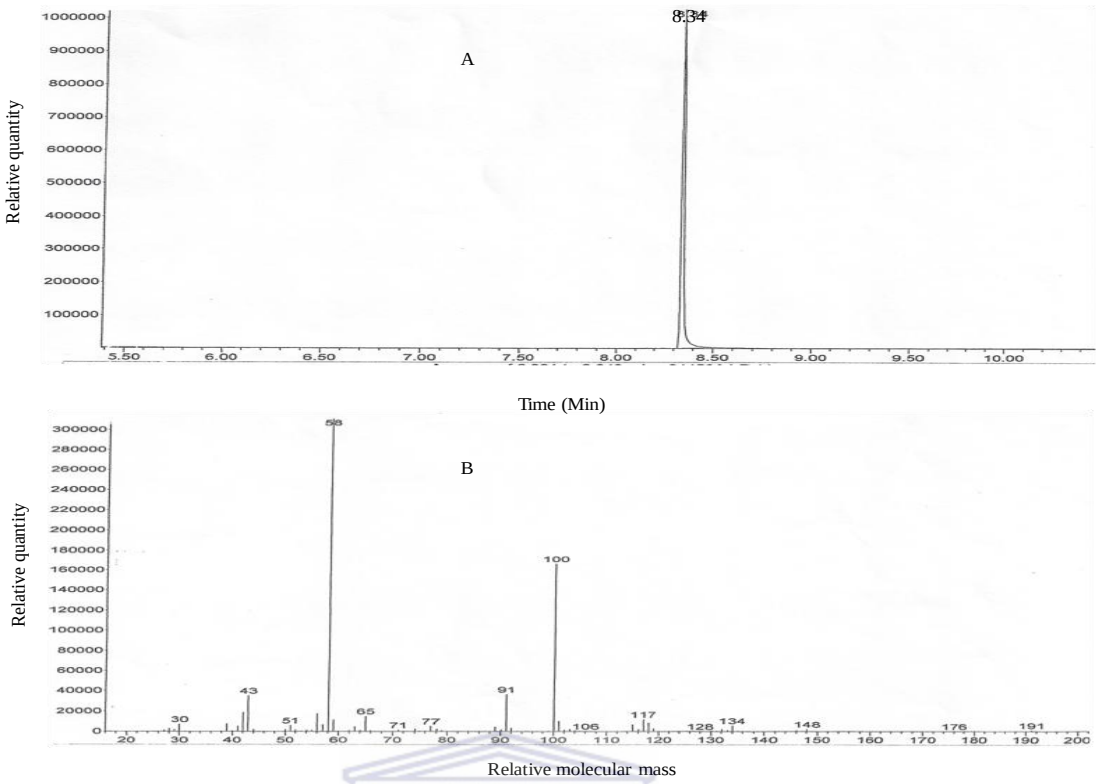

Figure 3.2. The above figure illustrates: A) methamphetamine analysed using GC elucidated at 8.34min. B) total ion chromatogram of methamphetamine analysed using MS for street MA sample 2 showing the chemical signature of MA.

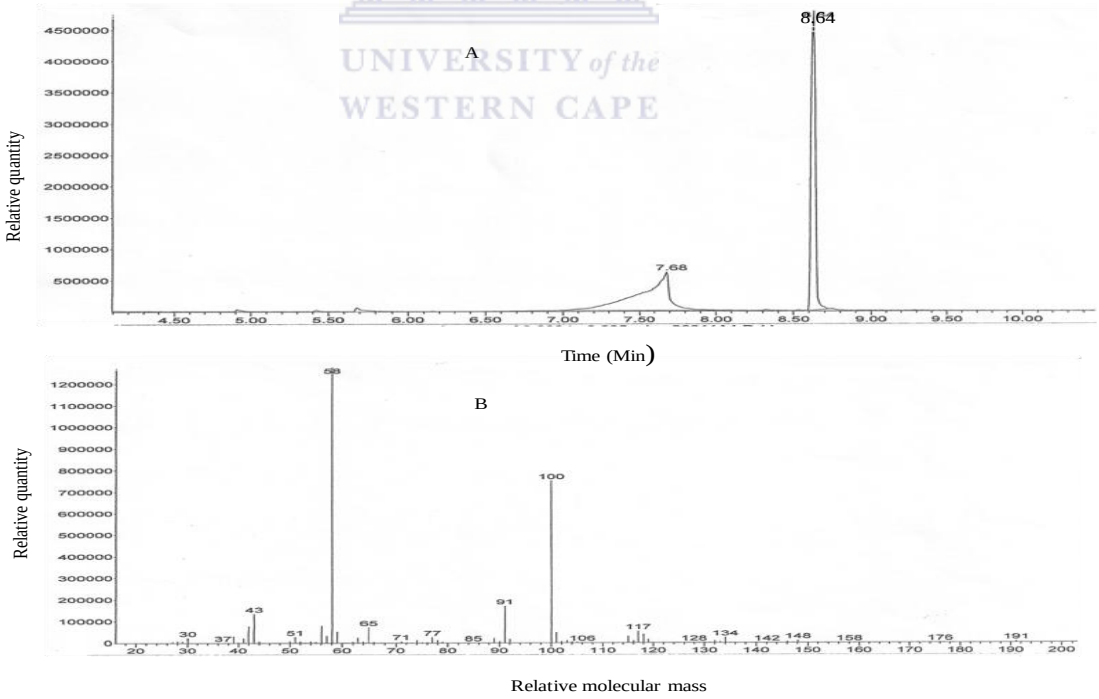

Figure 3.3. The above figure illustrates: A) methamphetamine analysed using GC elucidated at 8.64min. B) total ion chromatogram of methamphetamine analysed using MS for street MA sample 3 showing the chemical signature of MA.

.

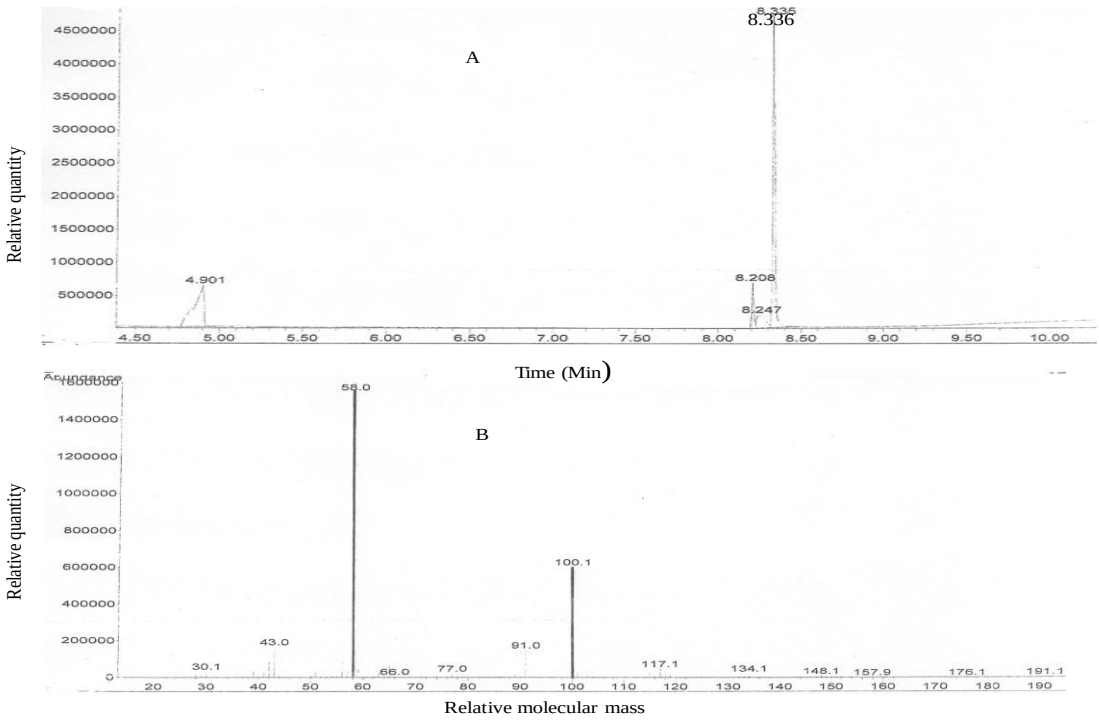

Figure 3.4. The above figure illustrates: A) methamphetamine analysed using GC elucidated at 8.34min. B) total ion chromatogram of methamphetamine analysed using MS for street MA sample 4 showing the chemical signature of MA.

3.2 The effect of pure and street MA on the viability of bEnd5 cells

Table 3.1 and figure 3.5 shows that no dead cells were observe at 24hrs except in the higher concentration (1mM). However, few dead cells were seen at 48, 72 and 96hrs of the experiment. Statistically, no significant difference ($P>0.05$) was observed in % cell viability between control and bEnd5 cells exposed to pure MA at all time intervals.

Table 3.1: The effect of selected concentrations of pure MA on % viability of bEnd5 cells at various time intervals (Mean ± SEM, n=6)

Compound	Pure MA			
Time	24 hr	48 hr	72 hr	96 hr
Control	93.89±4.52	98.97±2.83	99.78±0.14	98.99±0.87
0.0001mM	100.00±0.00	97.92±0.61	99.51±0.13	96.10±0.69
0.001mM	100.00±0.00	98.97±0.40	99.78±0.11	98.97±0.24
0.01mM	100.00±0.00	99.50±0.23	94.78±1.41	99.58±0.16
0.1mM	100.00±0.00	97.49±0.69	99.70±0.15	96.54±0.97
1mM	97.62±2.38	94.67±1.71	99.42±0.29	99.43±0.22

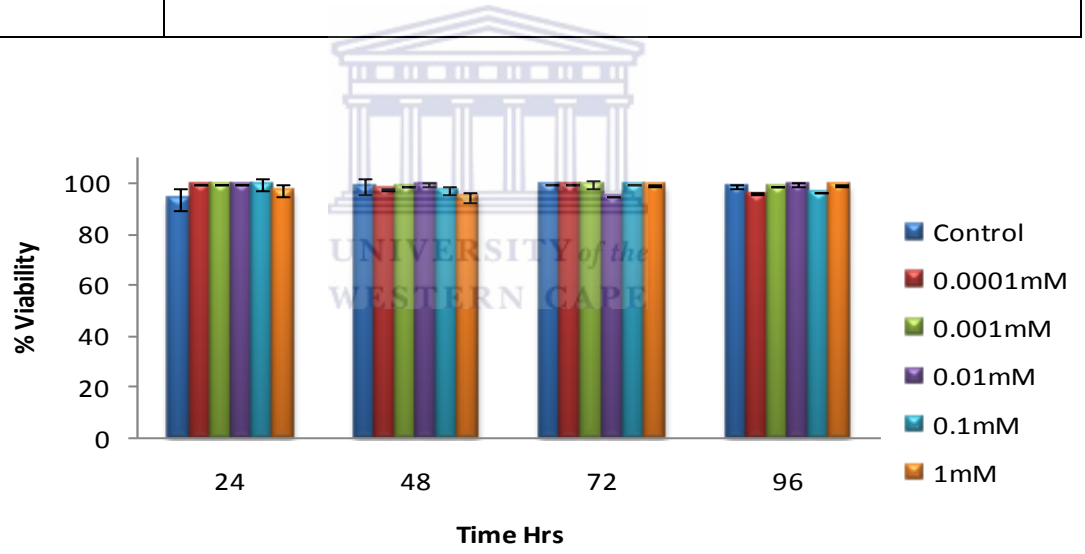

Figure 3.5. Effect of pure MA (mM) on viability of bEnd5 cells at selected concentrations between 24 and 96hrs. Results were displayed as mean ± SEM, (n=6).

Table 3.2 and figure 3.6 illustrate that during 24hrs of exposure of bEnd5 cells no dead cells were observed, while a few dead cells were observed at 48, 72 and 96hrs of the experiment. There was no statistical difference ($P>0.05$) between control values in % cell viability observed when bEnd5 cells were exposed to street MA sample 1.

Table 3.2: The effect of selected concentrations of street MA sample 1 on % viability of bEnd5 cells at various time intervals (Mean ± SEM, n=6)

Compound	Street MA sample 1			
Time	**24 hr**	**48 hr**	**72 hr**	**96 hr**
Control	92.67±4.52	96.31±23.83	97.58±00.18	92.13±1.47
0.0001mM	100.00±0.00	97.83±0.74	99.50±0.17	96.10±0.69
0.001mM	100.00±0.00	98.77±0.42	99.86±0.14	98.95±0.29
0.01mM	100.00±0.00	99.40±0.26	99.47±0.22	94.78±1.41
0.1mM	100.00±0.00	97.05±0.65	99.64±0.17	88.03±5.08
1mM	96.43±3.57	94.67±1.71	99.42±0.29	99.35±0.34

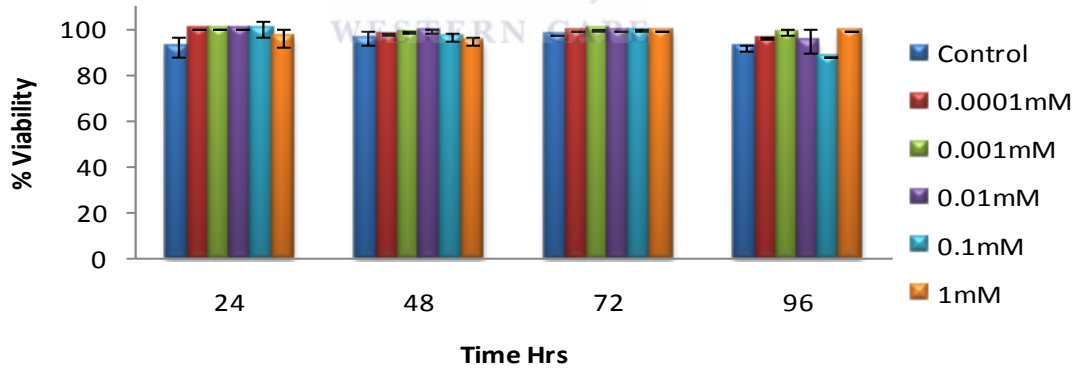

Figure 3.6. Effect of street MA 1 (mM) on viability of bEnd5 cells at selected concentrations between 24 and 96hrs. Results were displayed as mean ± SEM, (n=6).

Table 3.3 and figure 3.7 results indicate no significant difference in % cell viability ($P>0.05$) between control bEnd5 cells and those exposed to street MA sample 2 at all time intervals.

Table 3.3: The effect of selected concentrations of street MA sample 2 on % viability of bEnd5 cells at various time intervals (Mean ± SEM, n=6)

Compound	Street MA sample 2			
Time	24 hr	48 hr	72 hr	96 hr
Control	97.11±0.51	96.31±1.01	98.91±0.17	95.47±1.28
0.0001mM	97.67±0.31	95.92±0.79	98.90±0.08	97.52±0.26
0.001mM	98.09±0.31	97.47±0.34	98.82±0.06	96.79±0.44
0.01mM	97.05±0.34	98.02±0.33	98.93±0.21	97.29±0.28
0.1mM	97.08±0.33	97.65±0.28	98.88±0.20	95.80±0.36
1mM	96.75±0.31	96.13±0.32	98.08±0.26	95.84±0.64

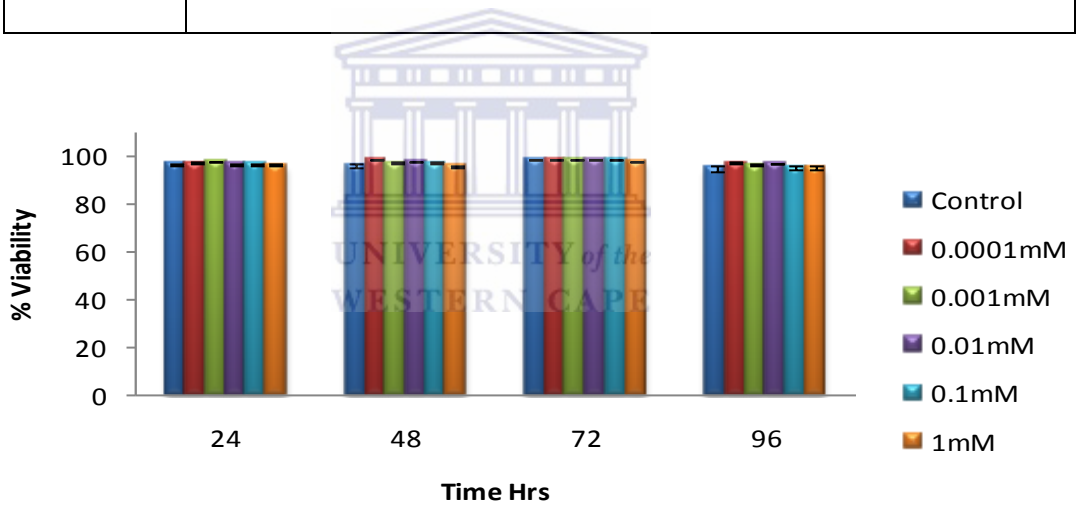

Figure 3.7. Effect of street MA 2 (mM) on viability of bEnd5 cells at selected concentrations between 24 and 96hrs. Results were displayed as mean ± SEM, (n=6).

Table 3.4 and figure 3.8 exhibits bEnd5 cell were exposed street MA sample 3, results showed that there were similar number of viable cells compared to that of controls however, no statistically significant difference between control and (P>0.05) in % cell viability in all time intervals was observed.

Table 3.4: The effect of selected concentrations of street MA sample 3 on % viability of bEnd5 cells at various time intervals (Mean ± SEM, n=6)

Compound	Street MA sample 3			
Time	**24 hr**	**48 hr**	**72 hr**	**96 hr**
Control	94.49±2.97	97.40±0.21	98.29±0.15	99.34±0.07
0.0001mM	79.42±1.47	97.91±0.15	98.00±0.22	99.24±0.10
0.001mM	88.88±0.85	97.64±0.24	95.95±2.06	98.47±0.14
0.01mM	89.92±0.82	97.40±0.14	97.95±0.21	97.95±0.21
0.1mM	73.75±1.79	95.39±0.92	96.16±0.70	98.96±0.09
1mM	81.40±2.46	95.61±0.51	96.64±0.39	98.43±0.18

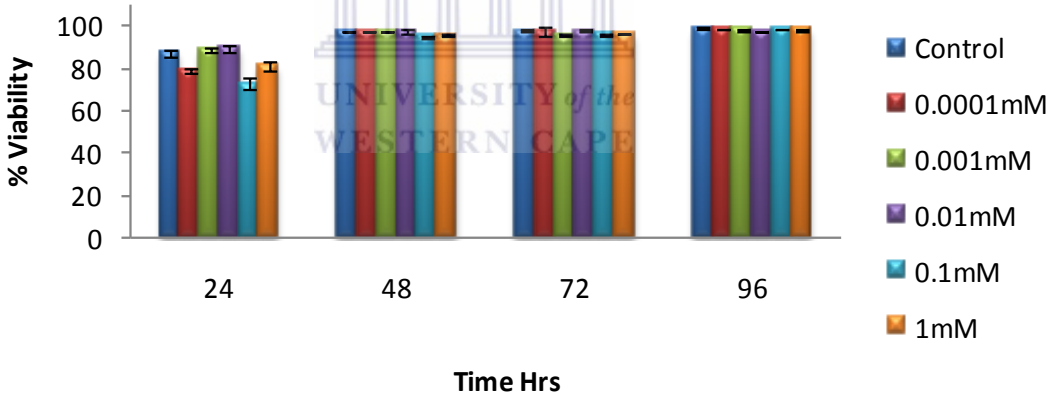

Figure 3.8. Effect of street MA 3 (mM) on viability of bEnd5 cells at selected concentrations between 24 and 96hrs. Results were displayed as mean ± SEM, (n=6).

Table 3.5 and figure 3.9 illustrates that cells exposed to street MA sample 4 indicated a similar % viability of cells compared to control data. At the concentrations used, data displayed no statistically significant differences between % cell viability and the control at all time intervals (P>0.05).

Table 3.5: The effect of selected concentrations of street MA sample 4 on % viability of bEnd5 cells at various time intervals (Mean ± SEM, n=6)

Compound / Time	Street MA sample 4			
	24 hr	**48 hr**	**72 hr**	**96 hr**
Control	94.49±1.21	98.65±0.26	98.26±0.27	96.32±1.94
0.0001mM	92.75±0.82	99.11±0.10	99.53±0.10	99.30±0.12
0.001mM	93.75±0.75	98.94±0.05	99.20±0.16	99.26±0.13
0.01mM	92.48±0.45	99.03±0.09	99.27±0.21	98.90±0.28
0.1mM	90.62±0.71	98.94±0.21	98.90±0.22	99.00±0.12
1mM	93.59±2.20	98.84±0.37	97.76±0.70	98.50±0.16

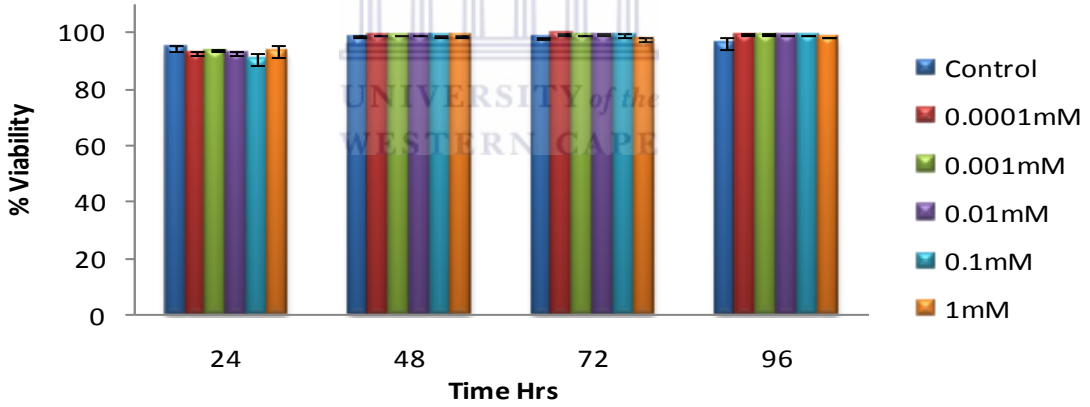

Figure 3.9. Effect of street MA 4 (mM) on viability of bEnd5 cells at selected concentrations between 24 and 96hrs. Results were displayed as mean ± SEM, (n=6).

3.3 The effect of selected concentrations of pure and street MA on the % cell growth of bEnd5 cells at various time intervals

The data for % cell growth was normalized against control groups, thus the control data is reflected at 100% in figures and tables (see materials and methods in chapter 2), and experimental data was expressed as percentage.

3.3.1 Effect of pure MA (Table 3.6 and Figure 3.10)

At the lower concentrations (0.0001-0.001mM) pure MA caused a decreased in % cell growth over the period of 24-96hrs (P=0.0105) by 4.35-fold relative to control. This decrease in trend was observed at 24 and 48hrs (P=0.0864). Relative to control, the lower concentrations showed to be suppressed by MA in cell growth. However, the % cell growth was not significantly different to the control (P≥0.05) at 72hrs.

The highest concentrations (0.01-1mM) initially displayed stimulation at 24 and 48hrs. This increase was significant (P=0.0433) for 0.1mM at 48hrs and 72hrs whereas at 96hrs pure MA caused a significant decrease (P=0.0275). This trend of decreased % cell growth was observed at 72 and 96hrs (P=0.0285) at 0.1mM.

Exposure at 24hrs: At 24hrs the effects of MA can be divided into two groups: lower concentrations and higher concentrations. The lower concentrations (0.0001-0.01mM) resulted in the significant stimulation (P<0.05) of cell growth compared to the control, where the higher concentrations showed a suppression in cell growth % which was statistically significant at P<0.05. A significant decrease in cell growth % was

observed (P= 0.0275) at 0.0001mM and 0.1mM and a 2.70-fold (P= 0.0209) decrease in % growth was observed at 0.0001mM and 1mM.

Exposure at 48hrs: % Cell growth exhibited a biphasic dose response type profile at 48hrs, then plateaued for all the concentrations used, except 1mM which showed non-significant suppression of cell growth %.

Exposure at 72hrs: At 72hrs, % cell growth showed to be approaching that of the control with the higher concentration (1mM) showing less % cell growth than that of controls. However, a statistically significant decrease (P=0.0143) was observed between the higher concentrations 0.01mM and 1mM.

Exposure at 96hrs: All bEnd5 cells exposed to pure MA illustrated % growth that was suppressed below that of controls. This suppression was found to be statistically significant (P<0.05) for all the concentrations

Table 3.6: The effect of selected concentrations of MA on the % cell growth of bEnd5 cells at the indicated time intervals (Mean ± SEM, n=6)

Compound	**Pure MA**			
Time	**24 hr**	**48 hr**	**72 hr**	**96 hr**
0.0001mM	319.74±66.796	163.43±31.26	122.88±28.06	73.48±6.63
0.001mM	305.26±46.78	211.55±22.60	158.00±34.52	57.04±3.86
0.01mM	192.63±39.12	257.76±27.73	172.27±18.38	76.795±3.39
0.1mM	98.69±14.95	253.32±52.28	130.24±17.66	89.63±4.79
1mM	118.43±10.19	190.98±27.40	89.26±6.92	65.45±6.69

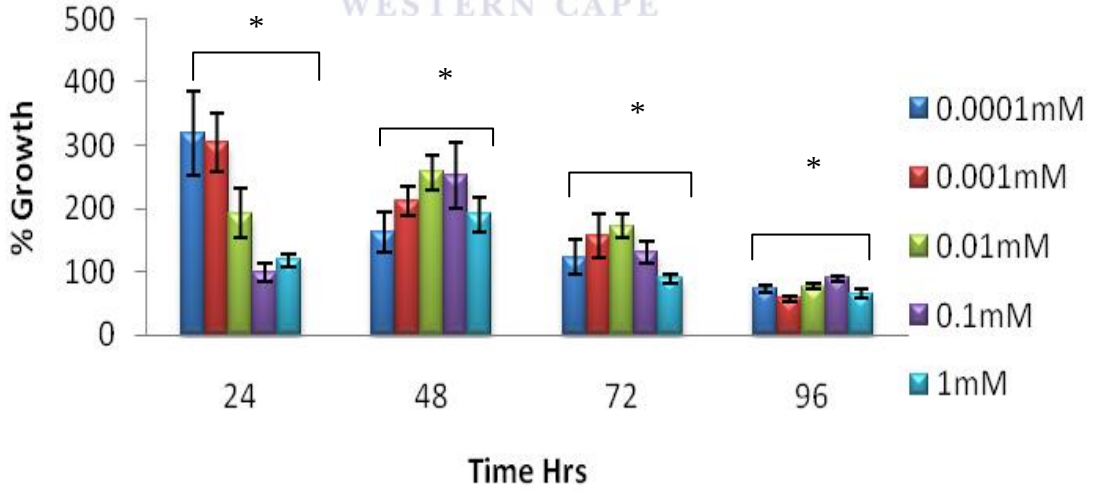

Figure 3.10. The above figure illustrate % cell growth when beEnd5 cell are exposed to pure MA at different time intervals. * indicates a significant difference P< 0.05 relative controls values. Results were displayed as mean ± SEM, (n=6).

3.3.2 Effect of street MA sample 1 (Table 3.7 and Figure 3.11)

The profiling in % cell growth for the selected street MA concentration mimicked the profiling of pure MA over the time between 24 and 96hrs (compare figure 3.6 and 3.7). For the lower concentrations (0.0001mM-0.001mM) % cell growth decreased by 5.18-fold at 96hrs (see fig. 3.7) relative to the control. Over the period 24 to 72hrs, all concentrations of street MA sample 1 exhibited enhanced cell growth. This enhanced cell growth was most noticeable in the lower concentrations (0.0001-0.001mM) at 24hrs. At the higher concentrations (0.1-1mM), enhanced cell growth was not as pronounced.

Between 48 and 72hrs, the enhanced cell growth was not as prolific as it was at 24hrs but was significant compared to the control ($P \leq 0.0275$). The exception to this trend was at a concentration of 1mM at 72hrs, which showed significant suppression of cell growth relative to control ($P < 0.05$).

At 96hrs, all concentrations, relative to the control, were significantly suppressed ($P \leq 0.02$).

Exposure at 24hrs: bEnd5 cells exposed to lower concentrations (0.0001-0.01mM) of street MA sample 1 exhibited stimulation in % cell growth, while, the two higher concentrations (0.1-1mM) showed suppression.

Exposure at 48hrs: Results displayed a biphasic effect in cell growth %: for the lower concentrations (0.0001-0.01mM), a dose response profile was observed, whereas for the higher concentrations (0.1-1mM), the dose profile in cell growth % was reversed compare to that of the control.

Exposure at 72hrs: At 72hrs, % cell growth was greater than the control except in the highest concentration (1mM).

Exposure at 96hrs: Results showed that cell growth % was significantly lower than that of controls, indicating MA sample suppression in cell growth.

Table: 3.7: The effect of selected concentrations of street MA sample 1 on the % cell growth of bEnd5 cells at the indicated time intervals (Mean ± SEM, n=6)

Compound	**Street MA sample 1**			
Time	**24 hr**	**48 hr**	**72 hr**	**96 hr**
0.0001mM	391.66±98.67	106.08±14.18	122.88±28.06	75.66±6.83
0.001mM	412.50±88.09	183.43±19.60	158.00±34.52	62.27±2.22
0.01mM	362.50±76.58	223.50±24.05	172.27±18.38	79.07±3.49
0.1mM	140.00± 24.49	192.73± 44.25	130.24± 17.66	86.29± 4.97
1mM	150.00± 27.00	150.82± 24.39	82.153± 9.08	66.26± 3.26

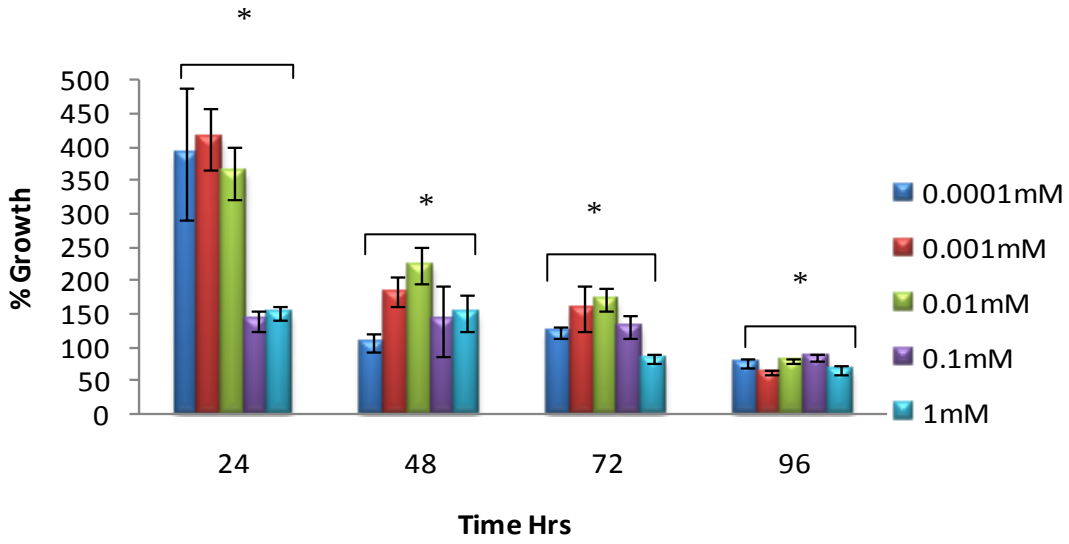

Figure 3.11. The above figure illustrate % cell growth when bEnd5 cell are exposed to Street MA 1 at different time intervals. * indicates a significant difference P< 0.05 to that of the controls. Results were displayed as mean ± SEM, (n=6).

3.3.3 Effect of street MA sample 2 (Table 3.8 and Figure 3.12)

At the lower concentrations (0.0001-0.001mM) street MA sample 2 induced a significant increase in % cell growth at 24 and 48hrs (P=0.0275).

At the higher concentrations (0.01-1mM), street MA sample 2 resulted in a significant suppression (P≤0.009) of % cell growth at 48 and 72hrs in.

Exposure at 24hrs: Results exhibited a dose response profile, with the higher concentrations (0.1-1mM) illustrating a significant decrease (P<0.05) compared to the control.

Exposure at 48hrs: Cell growth % exhibited significant stimulation (P<0.05) by MA compared to control. This increase was also observed when 0.01mM was compared with 0.1mM and 1mM during the sampling time of the experiment.

Exposure at 72hrs: The lower concentrations (0.0001-0.001mM) displayed a greater value in cell growth %, while the intermediate concentrations (0.01-0.1mM) showed results which are similar to each other. The highest concentration (1mM) displayed significant suppression ($P<0.02$) compared to control with $P<0.05$.

Exposure at 96hrs: The two higher concentrations (0.1-1mM) showed cell growth % that is lower than that of the lower concentrations (0.0001-0.01mM), with 1mM displaying cell growth that is less than that of the controls, indicating suppression ($P<0.05$).

Table: 3.8 The effect of selected concentrations of street MA sample 2 on the % cell growth of bEnd5 cells at the indicated time intervals (Mean ± SEM, n=6)

Compound	**Street MA sample 2**			
Time	**24 hr**	**48 hr**	**72 hr**	**96 hr**
0.0001mM	172.45±18.63	164.71±18.13	155.23±7.38	184.29±26.46
0.001mM	159.39±25.04	258.40±11.397	156.91±16.57	154.76±21.11
0.01mM	112.74±6.34	213.37±10.22	96.83±9.80	187.22±27.999
0.1mM	88.61±12.22	116.198±8.07	103.03±7.05	104.10±5.42
1mM	69.29±5.23	136.52±11.21	82.24±3.99	85.09±4.63

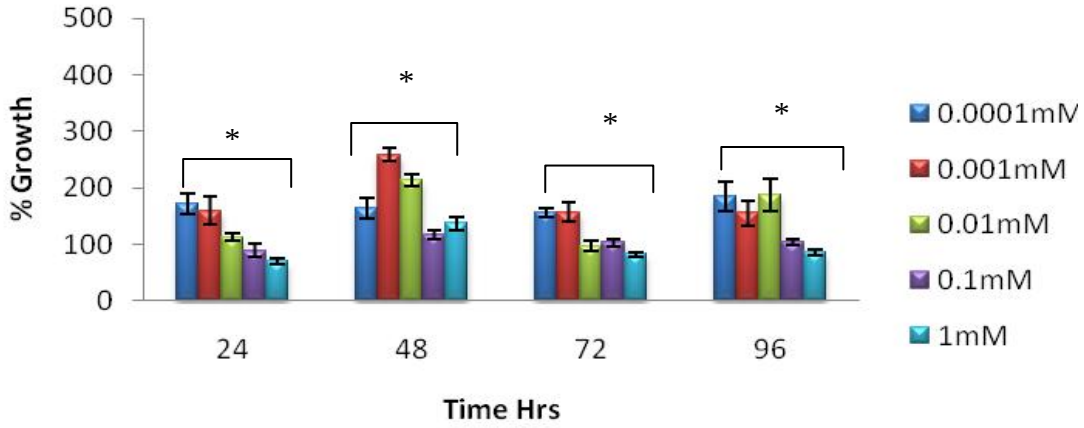

Figure 3.12. The above figure illustrate % cell growth when bEnd5 cell are exposed to Street MA 2 at different time intervals. * indicates a significant difference P< 0.05 to that of the controls. Results were displayed as mean ± SEM, (n=6).

3.3.4 Effect of street MA sample 3 (Table 3.9 and Figure 3.13)

Over the period of 24 to 96hrs, all the concentrations of street MA sample 3 induced MA suppression in % cell growth, with the exception of the lower concentration (0.001 and 0.01) which displayed similar results to the control.

Exposure at 24hrs: At 24hrs, cell growth % was suppressed at all the concentrations used, the exceptions were the intermediate concentrations (0.001-0.01mM) which illustrated similar results to that of the control.

Exposure at 48hrs: Cell growth % was suppressed at all the selected concentrations.

Exposure at 72hrs: At 72hrs, cell growth % was suppressed at all the selected concentrations with higher concentration (1mM) showing the most suppressed % cell growth.

Exposure at 96hrs: Cell growth % was suppressed through all of the selected concentrations, and was significantly lower than that of the control (P<0.05).

Table:3.9 The effect of selected concentrations of street MA sample 3 on the % cell growth of bEnd5 cells at the indicated time intervals (Mean ± SEM, n=6)

Compound	Street MA sample 3			
Time	24 hr	48 hr	72 hr	96 hr
0.0001mM	47.66±3.71	88.86±4.10	77.29±6.08	89.21±6.09
0.001mM	98.81±5.57	53.45±9.58	76.06±2.14	53.595±5.84
0.01mM	107.23±9.95	56.26±4.63	65.71±7.01	61.57±3.27
0.1mM	25.76±2.02	43.25±3.896	96.16±0.698	66.43±8.13
1mM	50.11±6.88	34.37±3.46	26.41±1.58	47.998±3.43

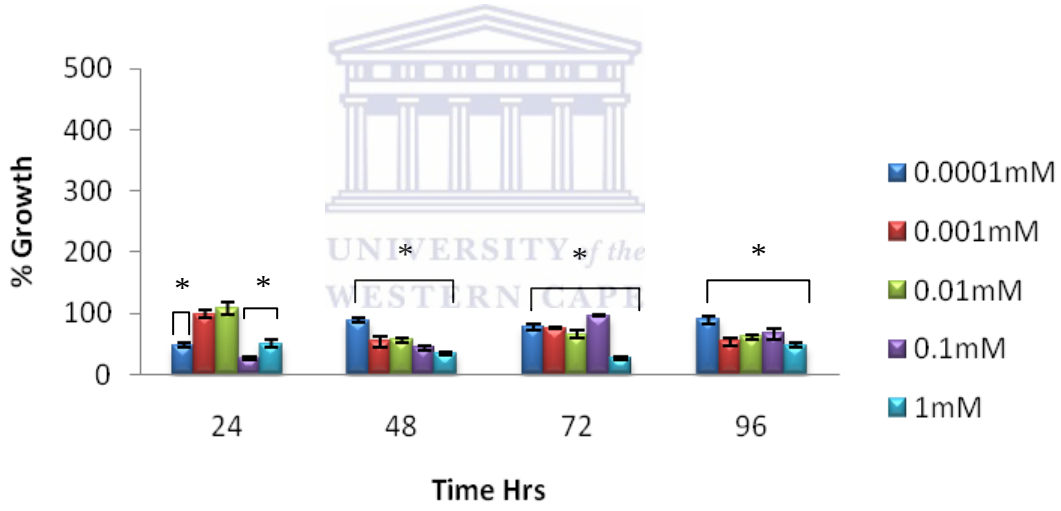

Figure 3.13. The above figure illustrate % cell growth when cell are exposed to Street MA 3 at different time intervals. * P< 0.05 indicate a significant difference from that of the controls. Results were displayed as mean ± SEM, (n=6).

3.3.5 Effect of street MA sample 4 (Table 3.10 and Figure 3.14)

At the lower concentrations (0.0001-0.001mM), it was observed that MA-induced stimulation of % cell growth for the time period 24, 48, 72 and 96hrs.

At higher concentrations (0.1-1mM), two trends were observed: at 0.1mM suppression (P=0.0090) of MA-induced cell growth % occurred between period of 24 to 72hrs. At 1mM, MA-induced stimulation of % cell growth occurred (P=0.0105) between 24 and 96hrs. This increase trend was extended to 48 and 72hrs.

Exposure at 24hrs: Results displayed suppression in % cell growth as the concentration of drug increased with the intermediate (0.001-0.01mM) concentrations showing similar results.

Exposure at 48hrs: All the concentrations used showed similar results indicating stimulation in cell growth %, with the exception of the highest concentration (1mM) displaying greater suppression.

Exposure at 72hrs: The highest concentration (1mM) showed suppression in % cell growth, whereas, the other concentrations displayed stimulation as compared to controls ($P<0.05$).

Exposure at 96hrs: Results demonstrated that the bEnd5 cells exposed to different concentrations shows similar stimulatory % cell growth with, 1mM being the only one showing results that are similar to that of the controls. Throughout the experiment at 96hrs, 1mM MA exposure showed a significant increase in % cell growth when compared to other selected concentrations ($P\leq0.0209$).

Table:3.10 The effect of selected concentrations of street MA sample 4 on the % cell growth of bEnd5 cells at the indicated time intervals (Mean ± SEM, n=6)

Compound	**Street MA sample 4**			
Time	**24 hr**	**48 hr**	**72 hr**	**96 hr**
0.0001mM	156.04±12.87	150.05±9.53	156.098±13.94	161.597±6.39
0.001mM	130.04±16.16	151.93±8.93	142.74±11.28	141.59±4.83
0.01mM	131.06±6.18	122.35±16.62	160.16±13.35	146.33±8.23
0.1mM	82.32±3.07	129.296±10.70	107.43±8.05	136.17±12.55
1mM	47.45±9.08	29.37±3.20	34.71±1.92	98.93±6.48

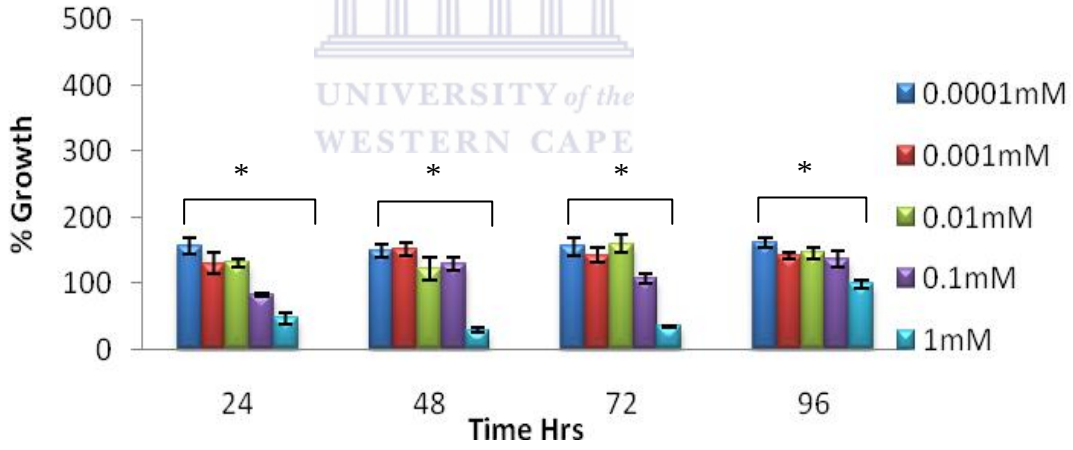

Figure 3.14 . The above figure illustrate % cell growth when bEnd5 cell are exposed to Street MA 4 at different time intervals. * indicates a significant difference P< 0.05 to that of the controls. Results were displayed as mean ± SEM, (n=6).

3.4 The effect of selected concentrations of pure and street MA on the % ATP production in bEnd5 cells at various time intervals

This ATP assay was used to determine the relative concentration of ATP in control compared to MA exposed cells. The assay determined cell viability via the detection of ATP activity which is indicative of the presence of metabolically active cells.

3.4.1 Effect of pure MA on ATP production (Table 3.11 and Figure 3.15)

At the lower concentrations (0.0001-0.001mM), pure MA caused dose-related increase in ATP production over time at 24 and 96hrs ($P<0.05$). Compared to the control, 0.001mM displayed a significant increase ($P\leq0.0209$) while, 0.0001mM showed results similar to that of the control ($P\geq0.05$). In of all the concentrations used, ATP production increased at 48hrs and decreased at 72hrs ($P\leq0.0209$), thereafter, followed by an increase at 96hrs ($P<0.05$) relative to controls (Table 3.11 and Figure 3.11).

Exposure at 24hrs: ATP produced by bEnd5 cells was slightly elevated yet statistically significant to that of controls, except at the lowest concentration (0.0001mM). bEnd5 treated with 0.0001mM displayed significant difference ($P\leq0.002$) of ATP production to all the concentrations of MA.

Exposure at 48hrs: ATP levels increased with an increase in MA concentration, with 0.001mM and 0.01mM showed similar response. Exposure of bEnd5 to 0.1mM MA showed a significant increase in ATP levels ($P=0.009$) relative to cells exposed to 0.0001mM, and 0.001mM.

Exposure at 72hrs: A dose related decrease in ATP production occurred at 72hrs where the lower concentrations of MA produced more ATP. All these concentration were significantly less than control values ($P<0.05$).

Exposure at 96hrs: With the exception of 0.0001mM, all doses of MA exhibited significantly greater ATP production relative to the control.

Table 3.11: The effect of selected concentrations of pure MA on % ATP of bEnd5 cells at various time intervals (Mean ± SEM, n=6)

Compound	**Pure MA**			
Time	**24 hr**	**48 hr**	**72 hr**	**96 hr**
0.0001mM	89.36±2.38	108.45±5.50	86.55±5.25	93.30±6.77
0.001mM	108.80±2.76	123.69±3.10	79.69±1.39	155.97±18.74
0.01mM	111.25±3.68	123.03±2.50	71.72±1.02	161.39±18.54
0.1mM	104.59±3.60	157.11±3.85	69.68±1.47	152.51±19.61
1mM	101.89±2.77	174.40±3.68	66.07±2.44	132.31±9.97

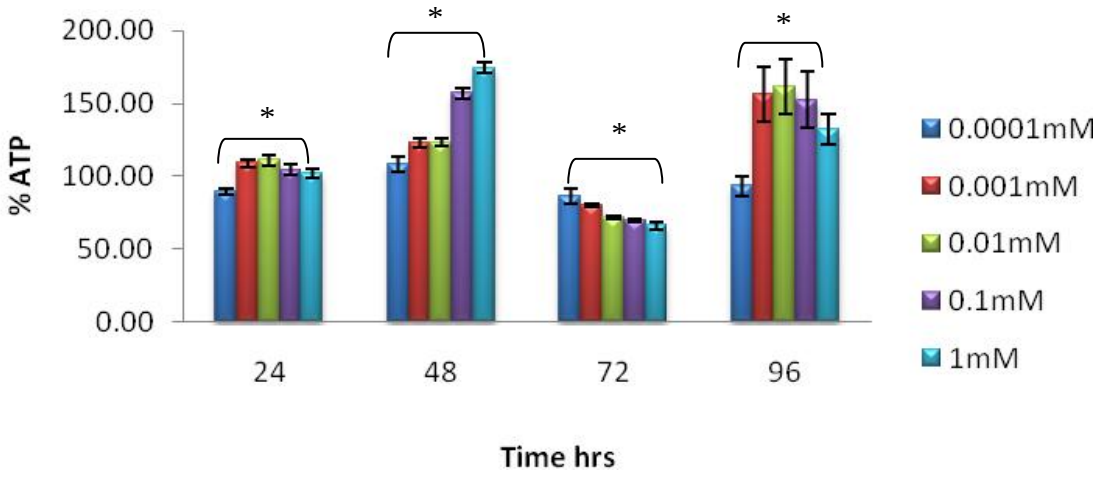

Figure 3.15. Effect on % ATP of cells exposed to pure MA. * indicates a significant difference $P< 0.05$ relative controls values. Results were displayed as mean ± SEM, (n=6).

3.4.2 Effect of street MA sample 1 on ATP production (Table 3.12 and Figure 3.16)

For all the selected concentrations used, street MA sample 1 caused an increase between 24 and 96hrs (P=0.0275). All concentrations displayed a significant increase (P≤0.0275) between 24 and 96hrs. Street MA sample 1 results displayed suppression in ATP production at 48hrs relative to control values which continued up till 72hrs (P<0.05) (table 3.12 and figure 3.12).

Exposure at 24hrs: With the exception of 0.0001mM, ATP production was significantly higher than that of control (P≤0.009).

Exposure at 48hrs: ATP production was significantly suppressed (P<0.05) by MA at all selected concentrations, with the exception of the intermediate concentration (0.01mM).

Exposure at 72hrs: This trend in decrease (P≤0.02) of ATP production relative to control continued at 72hrs. The higher concentration (1mM) showed a more acute suppression compare to other concentrations.

Exposure at 96hrs: The suppression of ATP production was reversed at all concentrations, with all bEnd5 cells exposed to MA sample 1 showing elevation of ATP production relative to control values.

Table 3.12: The effect of selected concentrations of street MA sample 1 on % ATP of bEnd5 cells at various time intervals (Mean ± SEM, n=6)

Compound	Street MA sample 1			
Time	**24 hr**	**48 hr**	**72 hr**	**96 hr**
0.0001mM	83.37±3.23	76.63±2.08	68.80±1.97	156.49±14.68
0.001mM	113.04±4.07	91.35±0.72	69.84±2.59	162.10±18.74
0.01mM	116.87±3.63	106.18±5.85	85.14±2.32	159.15±14.66
0.1mM	113.12±3.18	78.29±1.46	81.35±5.34	150.36±12.00
1mM	101.72±1.81	84.51±0.68	48.98±0.68	122.41±5.82

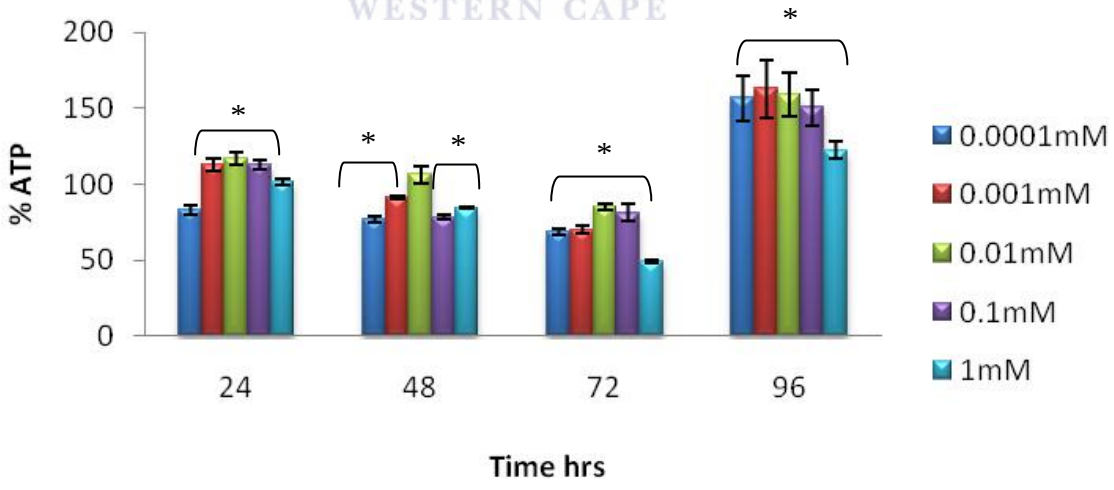

Figure 3.16. Effect on % ATP of cells exposed to street MA 1. * indicates a significant difference P< 0.05 relative controls values. Results were displayed as mean ± SEM, (n=6).

3.4.3 Effect of street MA sample 2 on ATP production (Table 3.13 and Figure 3.17)

Exposure of bEnd5 cells to both the lower and the higher concentrations results showed a significant increase between 24 and 96hrs ($P \leq 0.05$) with the exception of 0.01mM concentration. At 72hrs, all the concentrations used displayed a significant decrease ($P \leq 0.0209$) in ATP production compared to the control (Table 3.13 and Figure 3.13). This suppression was reversed at 96hrs with all cells exposed to MA displaying significant elevation of ATP production with the exception of 0.01mM.

Exposure at 24hrs: The higher concentrations (0.1-1mM) were significantly different to controls, with 0.01 and 0.1mM MA exposed cells elevating ATP production, while, 1mM MA suppressed ATP production ($P<0.05$).

Exposure at 48hrs: bEnd5 cells produced ATP that was not statistically different to that of the control ($P \geq 0.05$).

Exposure at 72hrs: ATP production was decreased when bEnd5 cells were exposed to the selected concentrations of MA.

Exposure at 96hrs: All selected concentrations of MA exhibited a significant increase in ATP production relative to that of the control ($P<0.05$), with the exception of 0.01mM MA exposed cells, which did not statistically differ from the control.

Table 3.13: The effect of selected concentrations of street MA sample 2 on % ATP of bEnd5 cells at various time intervals (Mean ± SEM, n=6)

Compound	**Street MA sample 2**			
Time	**24 hr**	**48 hr**	**72 hr**	**96 hr**
0.0001mM	94.39±4.47	91.13±5.76	85.11±4.73	124.12±9.14
0.001mM	100.25±2.73	101.24±1.29	86.02±2.59	141.83±12.49
0.01mM	109.60±3.36	99.63±3.93	87.30±1.47	98.11±7.88
0.1mM	111.75±3.18	107.01±4.12	75.72±5.34	145.34±10.63
1mM	75.12±1.418	96.08±3.17	75.14±2.32	134.43±3.03

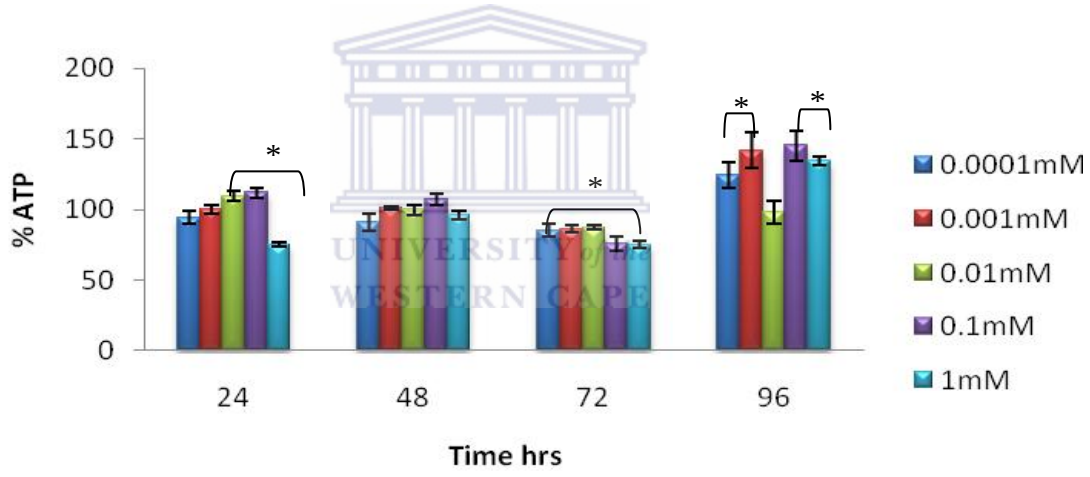

Figure 3.17. Effect on % ATP of cells are exposed to street MA sample 2. * indicates a significant difference P< 0.05 relative to controls values. Results were displayed as mean ± SEM, (n=6).

3.4.4 Effect of street MA sample 3 on ATP production (Table 3.14 and Figure 3.18)

A similar trend was observed when pure MA was exposed to bEnd5 cells: similar values to that of the control in ATP production was observed at 24hrs, slight elevation at 48hrs, acute suppression across all the concentrations at 72hrs, and at 96hrs

significant increased production of ATP. Specific variation will be described at the specific selected time frames.

Exposure at 24hrs: With the exception of 0.1mM, doses of MA exhibited similar results compared to the control ($P \geq 0.05$).

Exposure at 48hrs: ATP levels increased between (0.001-0.1mM) compared to the control. 0.0001mM and 1mM showed similar results to that of the control.

Exposure at 72hrs: All the selected concentrations of MA exhibited suppression in ATP production.

Exposure at 96hrs: ATP levels produced by bEnd5 cells exhibited a significant increase ($P \leq 0.0433$) to all other concentrations of MA with the exception of 1mM, which showed similar results to the control.

Table 3.14.The effect of selected concentrations of street MA sample 3 on % ATP of bEnd5 cells at various time intervals (Mean ± SEM), n=6

Compound	**Street MA sample 3**			
Time	**24 hr**	**48 hr**	**72 hr**	**96 hr**
0.0001mM	101.48±1.80	101.48±4.20	79.39±2.85	123.56±5.88
0.001mM	101.24±2.13	128.67±6.23	87.44±0.35	114.34±11.73
0.01mM	101.57±1.57	131.09±3.98	85.46±5.22	120.93±8.73
0.1mM	111.60±1.27	123.13±3.51	82.34±2.16	111.34±6.75
1mM	104.37±2.11	92.62±3.60	97.04±2.84	93.51±7.98

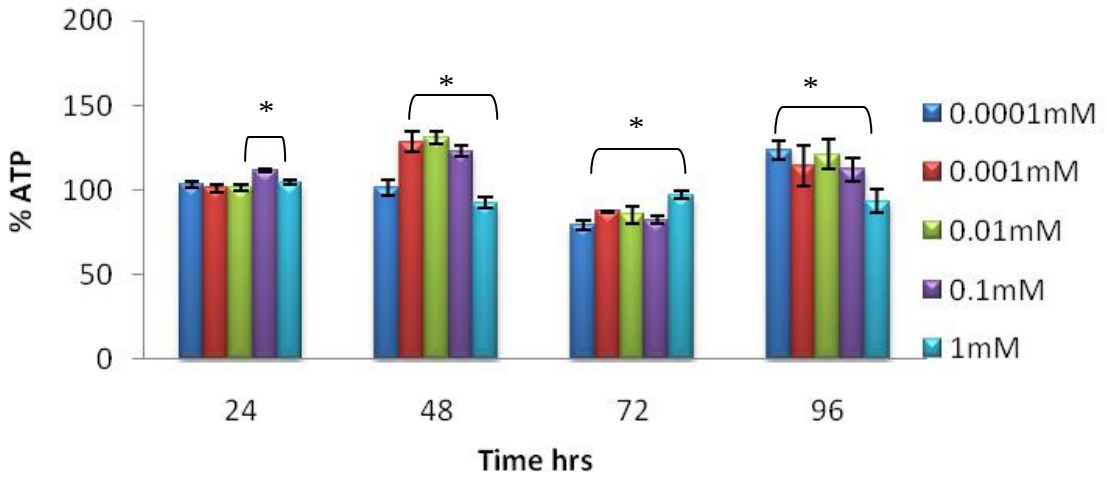

Figure 3.18. Effect on % ATP of cells are exposed to street MA sample 3. * indicates a significant difference P< 0.05 relative controls values. Results were displayed as mean ± SEM, (n=6).

3.4.5 Effect of street MA sample 4 on ATP production (Table 3.15 and Figure 3.19)

MA street MA samples differed most to that of the pure MA pattern. Lower concentrations (0.0001-0.001mM) showed a significant increase (P=0.0143) between 24 and 96hrs. The higher concentrations (0.1-1mM) showed no significant difference compared to the control (P≥0.05). A significant decrease (P<0.05) was observed at 48 and 72hrs for 0.0001mM and 1mM.

Exposure at 24hrs: bEnd5 cells treated with selected concentrations of MA displayed a significant increase (P≤0.0090) compare to the control with the exception of the lower concentration (0.0001mM).

Exposure at 48hrs: Intermediate concentrations (0.001-0.1mM) showed an increase in ATP production. Suppression of ATP production occurred at 1mM MA.

Exposure at 72hrs: The lower concentrations displayed less ATP production than the control ($P<0.0143$).

Exposure at 96hrs: The lower concentrations (0.0001-0.001mM) showed a suppression in ATP production, while the higher concentrations (0.1-1mM) showed results that were slightly ($P<0.05$) greater than that of the control.

Table 3.15: The effect of selected concentrations of street MA sample 4 on % ATP of bEnd5 cells at various time intervals (Mean ± SEM, n=6)

Compound	**Street MA sample 4**			
Time	**24 hr**	**48 hr**	**72 hr**	**96 hr**
0.0001mM	95.54±3.03	95.07±1.35	79.02±3.38	78.26±1.41
0.001mM	116.45±2.23	124.73±0.68	90.99±7.02	72.77±7.05
0.01mM	117.47±3.31	118.26±1.35	100.92±1.29	106.97±21.82
0.1mM	117.96±4.75	116.45±1.44	106.17±1.18	102.51±9.09
1mM	105.02±2.41	90.41±1.07	95.55±1.96	103.53±7.87

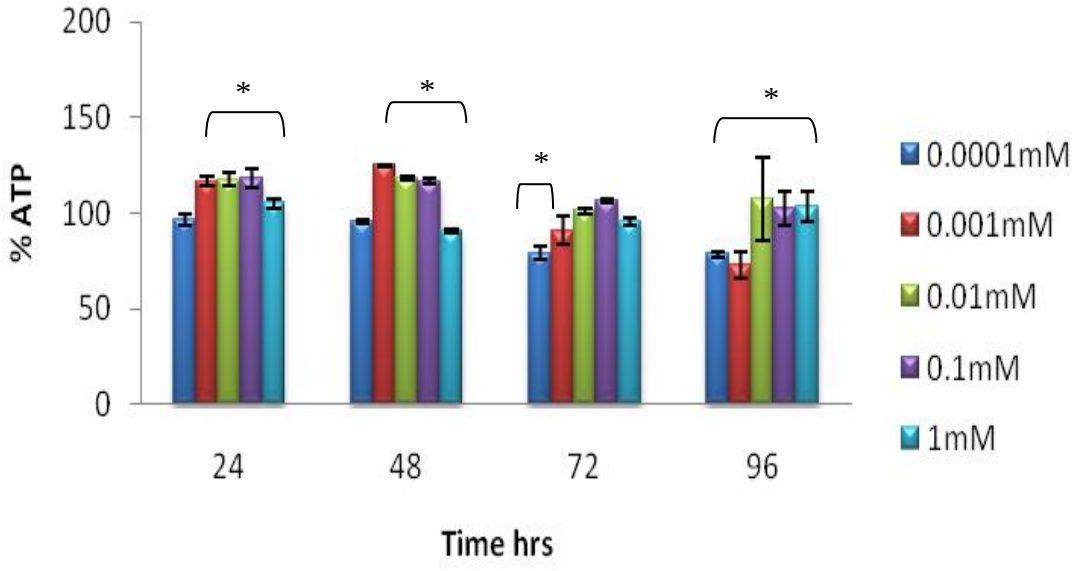

Figure 3.19. Effect on % ATP of cells are exposed to street MA sample 4. * indicates a significant difference P< 0.05 relative controls numbers. Results were displayed as mean ± SEM, (n=6).

3.5 The effect of selected concentrations of pure and street MA samples on DNA proliferation of bEnd5 cells at various time intervals

Cells assessed with the labeling medium containing BrdU. The BrdU is incorporated in place of thymidine during replication thus indicative of newly synthesized DNA of a proliferating cell.

3.5.1 Effect of pure MA on DNA proliferation (Table 3.16 and Figure 3.20)

The two lower concentrations (0.0001-0.001mM) MA caused a significant decrease in % DNA synthesis at 24 and 96hrs compared to controls ($P \leq 0.05$); this decrease trend continued at 48 and 72hrs. The higher concentrations (0.1-1mM) of MA induced suppression at 24 and 96hrs, while a significant decrease was observed when bEnd5 cells were exposed to 1mM ($P=0.0275$).

Exposure at 24hrs: The lower concentrations (0.0001-0.001mM) induced stimulation in DNA synthesis compared to the control, while the higher concentration displayed suppression of DNA.

Exposure at 48hrs: DNA synthesis levels differed at all the concentrations used: 0.001mM and 1mM MA stimulated DNA synthesis, while 0.0001mM and 0.1mM showed suppression of DNA synthesis compared to the control ($P<0.05$).

Exposure at 72hrs: DNA synthesis levels produced by bEnd5 cells was similar to that of the control at 72hrs ($P\geq0.05$).

Exposure at 96hrs: All concentrations of selected pure MA exhibited significant decrease of DNA synthesis relative to the control.

Table 3.16: The effect of selected concentrations of pure MA on DNA synthesis of bEnd5 cells at various time intervals (Mean ± SEM, n=6)

Compound	**Pure MA**			
Time	**24 hr**	**48 hr**	**72 hr**	**96 hr**
0.0001mM	143.64±8.32	92.12±1.18	97.90±4.90	66.39±6.15
0.001mM	138.13±13.74	146.24±12.04	99.07±6.53	91.21±9.77
0.01mM	58.27±4	102.03±8.97	90.31±7.38	56.83±11.58
0.1mM	94.94±14.20	62.02±4.20	101.73±10.53	87.38±9.39
1mM	86.31±13.42	117.87±5.07	101.73±10.53	72.11±10.49

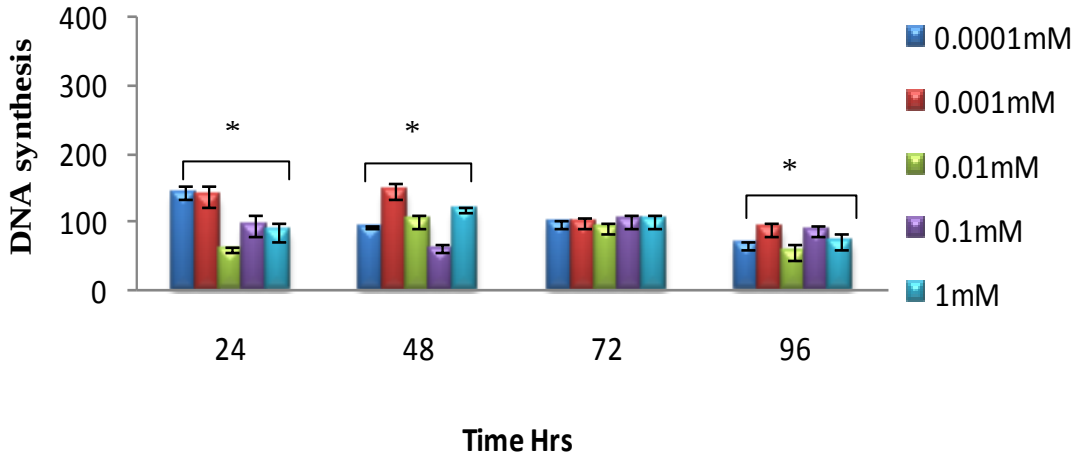

Figure 3.20. Effect of pure MA on % DNA synthesis. * P< 0.05 indicate a significant difference from that of the controls. Results were displayed as mean ± SEM.

3.5.2 Effect of street sample 1 MA on DNA proliferation (Table 3.17 and Figure 3.21)

No clear pattern was observed over the period 24 to 96hrs.

Exposure at 24hrs: Both the lower and the higher concentrations exhibited significant decrease in DNA synthesis relevant to the control (P≤0.0339).

Exposure at 48hrs: A decrease in DNA synthesis occurred at 48hrs with the exception of 0.001mM which was elevated significantly (P<0.0209) compared to the controls.

Exposure at 72hrs: At 72hrs, bEnd5 cells produced DNA replication that was less than that of the controls at the lower concentrations (0.0001-0.001mM), while the higher concentrations (0.1-1mM) showed elevation of DNA synthesis (P<0.05).

Exposure at 96hrs: 0.0001mM displayed supersession (P=0.0433), while 0.001mM showed elevated results to that of the control. The higher concentrations (0.1-1mM) displayed results that are similar to that of the control (P≥0.05).

Table 3.17: The effect of selected concentrations of street MA sample 1 on DNA synthesis of bEnd5 cells at various time intervals (Mean ± SEM, n=6)

Compound	**Street MA 1**			
Time	**24 hr**	**48 hr**	**72 hr**	**96 hr**
0.0001mM	85.43±2.97	54.12±4.52	17.82±4.74	79.85±5.06
0.001mM	95.59±3.65	127.30±3.99	49.99±2.15	105.50±6.87
0.01mM	67.70±8.38	104.98±3.89	194.79±51.94	93.75±12.73
0.1mM	86.35±6.51	84.00±19.62	112.86±16.98	106.20±20.30
1mM	71.68±16.23	55.20±12.71	105.47±6.23	93.50±14.15

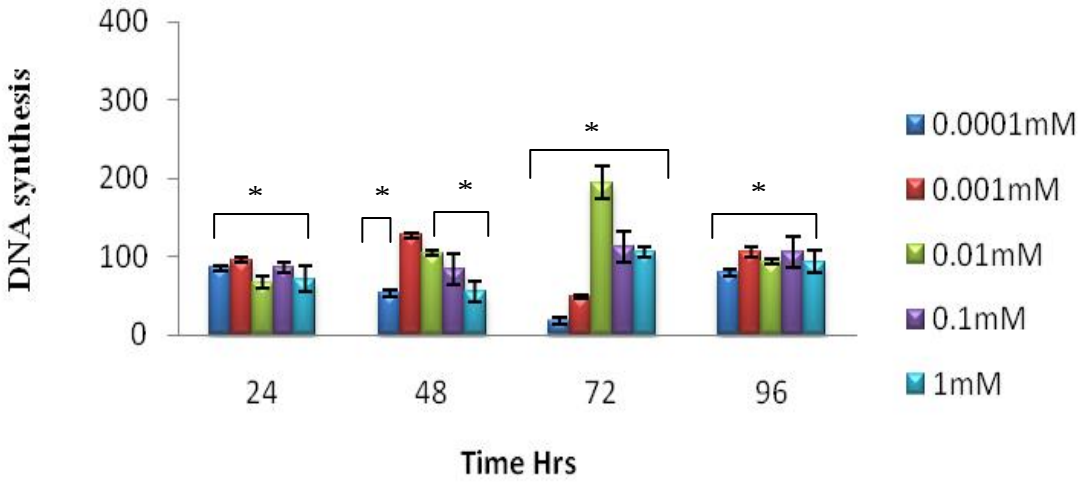

Figure 3.21. Effect of street MA sample 1 on % DNA synthesis. * P< 0.05 indicate a significant difference from that of the controls. Results were displayed as mean ± SEM.

3.5.3 Effect of street sample 2 MA on DNA proliferation (Table 3.18 and Figure 3.22)

No clear pattern was observed over the period 24 to 96hrs.

Exposure at 24hrs: All the concentrations produced elevated DNA synthesis with the exception of 0.001mM, which showed suppression of DNA synthesis (P=0.0339).

Exposure at 48hrs: Similar DNA synthesis was observed at 48hrs in all concentrations of selected MA except 1mM.

Exposure at 72hrs: At 72hrs, a biphasic response was observed which caused a dose-related elevation to MA samples at (0.0001-0.01mM), however, a dose related decrease was observed at (0.1-1mM).

Exposure at 96hrs: All the concentrations of MA showed significant increase in DNA synthesis relative to the control, with the exception of 0.0001mM.

Table 3.18:The effect of selected concentrations of street MA sample 2 on DNA synthesis of bEnd5 cells at various time intervals (Mean ± SEM, n=6)

Compound	**Street MA 2**			
Time	**24 hr**	**48 hr**	**72 hr**	**96 hr**
0.0001mM	58.63±8.85	101.93±2.16	94.50±27.23	70.81±10.60
0.001mM	115.22±7.22	119.01±9.38	150.27±10.77	130.09±8.54
0.01mM	110.98±11.11	114.58±1.33	194.79±51.94	93.75±12.73
0.1mM	125.00±3.09	104.93±4.65	135.67±9.86	121.88±12.60
1mM	115.21±6.49	81.48±5.05	97.90±7.03	205.43±5.50

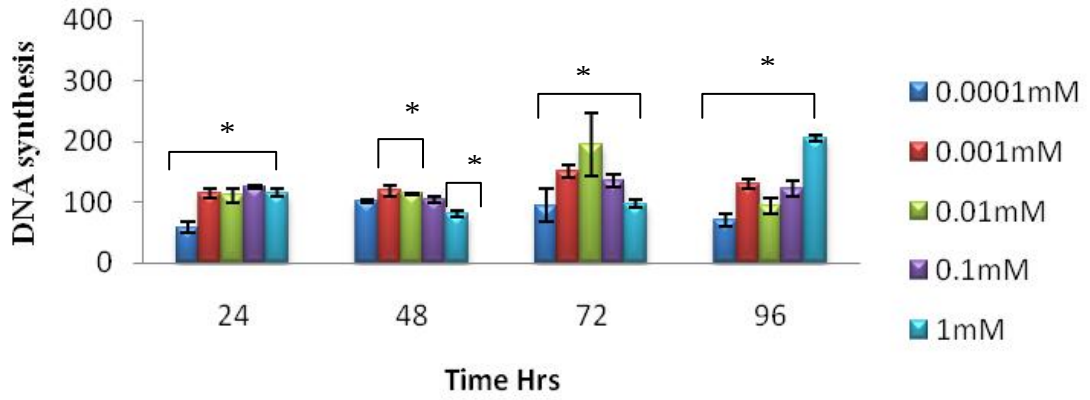

Figure 3.22. Effect of street MA sample 2 on % DNA synthesis. * P< 0.05 indicate a significant difference from that of the controls. Results were displayed as mean ± SEM.

3.5.4 Effect of street sample 3 MA on DNA proliferation (Table 3.19 and Figure 3.23)

At all the selected concentration used, DNA synthesis showed an increase between 24 and 96hrs (P≤0.0495). The same trend of increase of DNA synthesis was observed between 48 and 72hrs (P<0.025).

Exposure at 24hrs: The lowest concentration (0.0001 mM) showed suppression in DNA synthesis compared to the control, while higher concentrations (0.1-1mM) exhibited increase in DNA synthesis (P<0.05).

Exposure at 48hrs: Selected concentrations showed similar results to the control (P≥0.05) with the exception of (0.001-0.01mM).

Exposure at 72hrs: With the exception of 0.0001mM, all other selected concentrations exhibited a significant increase in DNA synthesis relative to the control.

Exposure at 96hrs: Dose related increase in DNA synthesis occurred at 96hrs where the higher concentration (1mM) produce the greater proliferation compare to control.

Table 3.19: The effect of selected concentrations of street MA sample 3 on DNA synthesis of bEnd5 cells at various time intervals (Mean ± SEM, n=6)

Compound	**Street MA 3**			
Time	**24 hr**	**48 hr**	**72 hr**	**96 hr**
0.0001mM	84.27±7.52	102.42±7.30	92.80±7.39	139.42±16.17
0.001mM	102.06±11.46	121.10±2.49	144.41±9.54	139.76±16.72
0.01mM	134.84±4.71	128.08±7.65	155.84±24.27	162.93±19.45
0.1mM	115.89±0.65	90.95±6.37	168.86±17.51	163.56±7.45
1mM	133.65±6.40	94.35±3.44	116.46±8.82	206.67±16.88

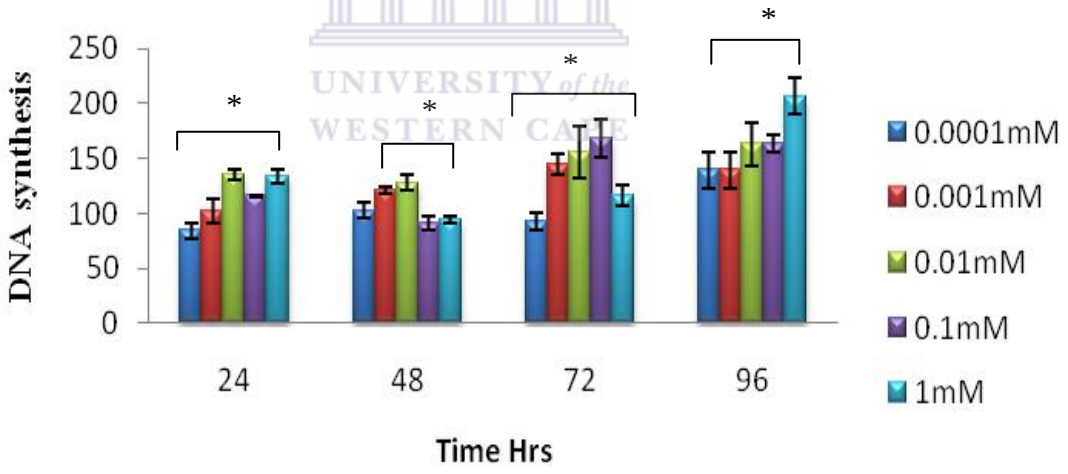

Figure 3.23. Effect of street MA sample 3 on % DNA synthesis. * P< 0.05 indicate a significant difference from that of the controls. Results were displayed as mean ± SEM.

3.5.5 Effect of street sample 4 MA on DNA proliferation (Table 3.20 and Figure 3.24)

Over the period of 24 to 96hrs, MA induced a significant suppression in % DNA synthesis ($P<0.05$) in contrast to the control.

Exposure at 24hrs: Significant decrease ($P\leq0.034$) in DNA synthesis was observed in all the selected concentrations.

Exposure at 48hrs: A significant decrease in DNA synthesis was also observed at 48hrs.

Exposure at 72hrs: Significant decrease in DNA synthesis was observed in all the selected concentrations.

Exposure at 96hrs: Dose response profile to the sequential increase in the concentrations of street MA sample 4 was observed.

Table 3.20: The effect of selected concentrations of street MA sample 4 on DNA synthesis of bEnd5 cells at various time intervals (Mean ± SEM, n=6)

Compound / Time	Street MA 4			
	24 hr	**48 hr**	**72 hr**	**96 hr**
0.0001mM	41.92±4.24	89.13±9.61	64.10±4.42	40.45±5.81
0.001mM	58.27±3.995	102.03±8.97	90.31±7.38	56.83±11.58
0.01mM	71.14±3.97	107.42±3.90	89.72±10.30	74.28±11.65
0.1mM	64.37±2.40	87.30±8.59	92.67±6.82	82.77±12.90
1mM	65.24±3.14	85.97±5.72	62.36±3.38	90.50±12.40

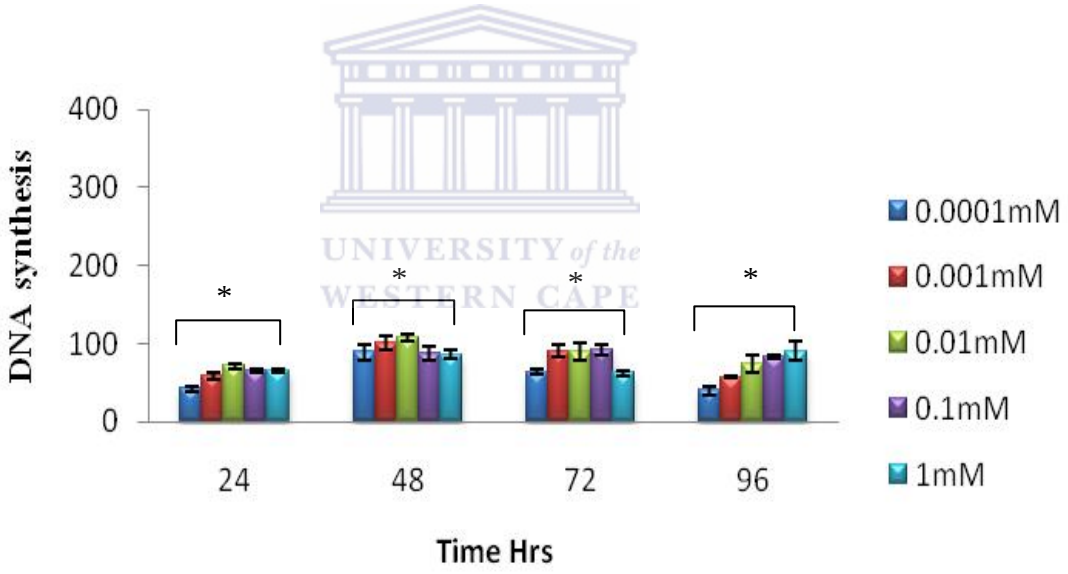

Figure 3.24. Effect of street MA sample 4 on % DNA synthesis. * P< 0.05 indicate a significant difference from that of the controls. Results were displayed as mean ± SEM.

3.6 Effect of selected concentrations of pure and street MA sample 1 on the cell cycles of bEnd5 cells

Flow cytometry is a technique used to measure the properties of individual cells. Flow cytometry was used to evaluate the effects of MA on the various stages of the bEnd5 cell cycle. Pure MA and street MA sample 1 were selected because of their experimental profile similarity. [Flow cytometry provides information as to the various stages of cells through the process of cell division, M, G1, S and G2 at selected time frames of 24, 48, 72, and 96hrs.]

Table 3.21. Effect of pure and street MA sample 1 on phases of the cell cycle at 24hrs (≥ 10000) events analysed)

	Cell Cycle phases					
Control	**G1**		**S**		**G2-M**	
	45.87		**40.39**		**13.45**	
	Pure	Street MA	Pure	Street MA	Pure	Street MA
0.1µM	42.96	37.99	51.20	52.37	5.84	9.64
1µM	41.85	45.84	39.49	36.73	18.66	17.43
0.01mM	42.99	46.61	39.89	39.58	17.12	13.61
0.1mM	41.59	44.00	39.77	36.64	18.64	19.36
1mM	46.40	49.86	40.56	32.30	13.04	17.84

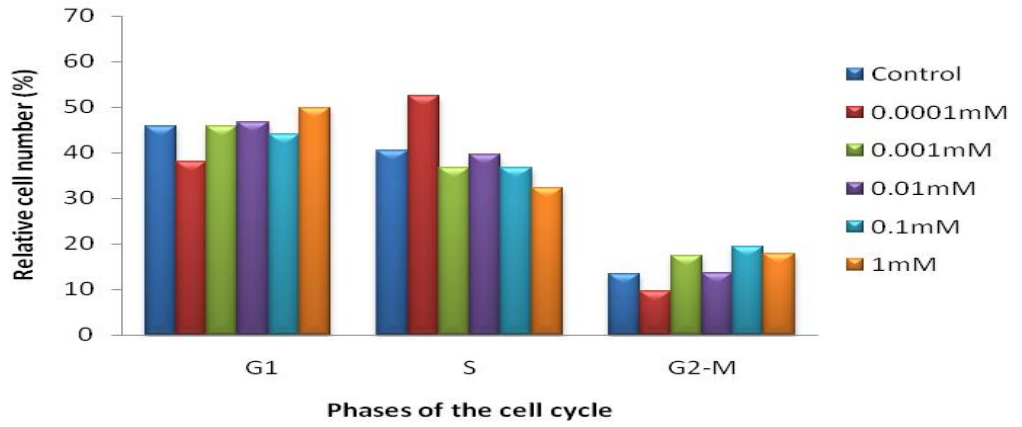

Figure 3.25. Relative cell numbers (%) at distinct phases of the cell cycle of bEnd cells exposed to pure MA at 24hrs (≥ 10000 events analysed).

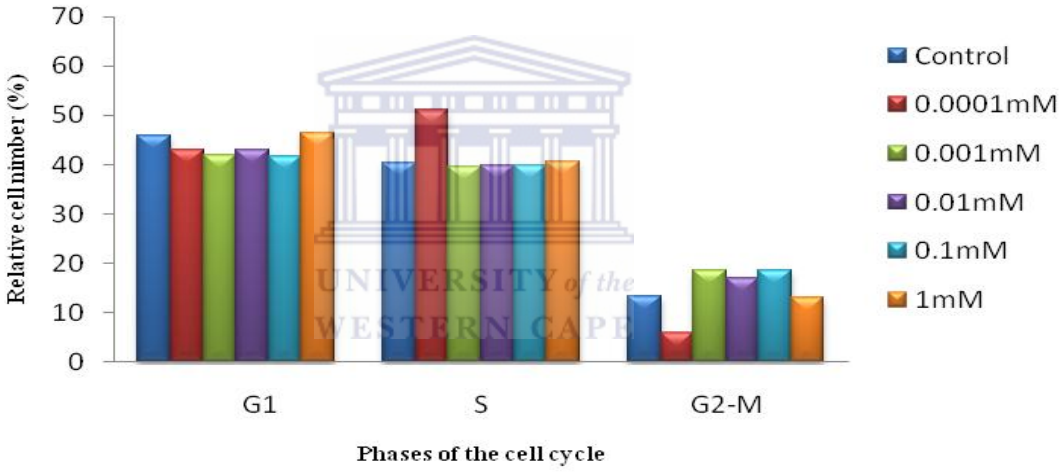

Figure 3.26 . Relative cell numbers (%) at distinct phases of the cell cycle of bEnd cells exposed to street MA 1 at 24hrs (≥ 10000 events analysed).

Table 3.2, Fig 3.25 and Fig. 3.26 showed that at 24hrs, the profiles of the cell cycle to pure and street MA sample 1 were remarkably similar. It is clear that for pure and street MA 1, the lowest concentration 0.0001mM caused less bEnd5 cells to enter into G2-M phase of the cell cycle, elevating cells in S-phase relative to the control. The other concentration did not appear to differ from controls.

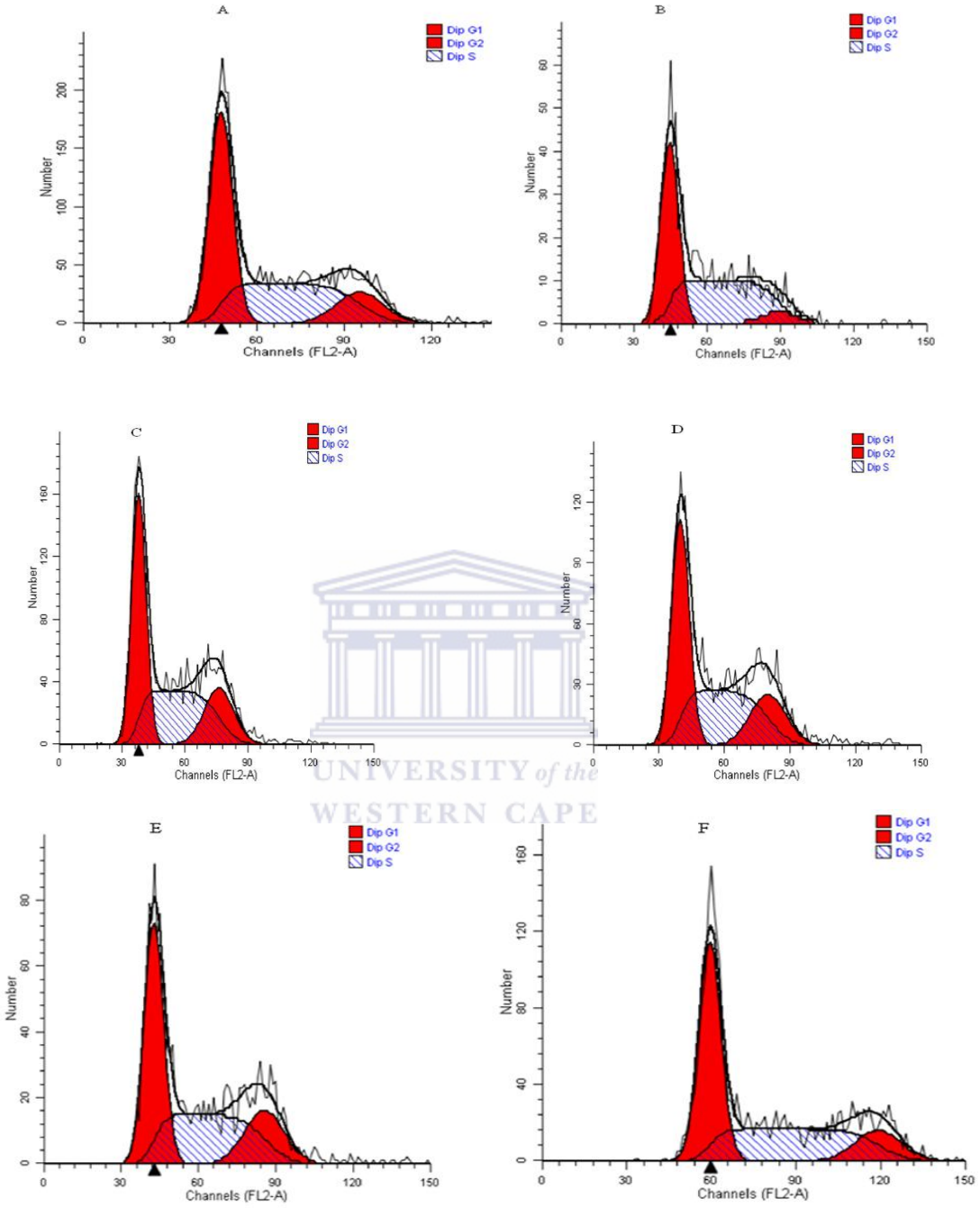

Figure 3.27. The above histograms were acquired using flow cytometry and A) represent results from control cells, while, bEnd5 cells treated with varying concentration of pure MA are represented by the following histogram after 24hrs: B) 0.0001mM, C) 0.001mM, D) 0.01mM, E) 0.1mM and F) 1mM after 24hrs (≥ 10 000 vents analysed). Note smaller quantity of G2-M cells in B) above.

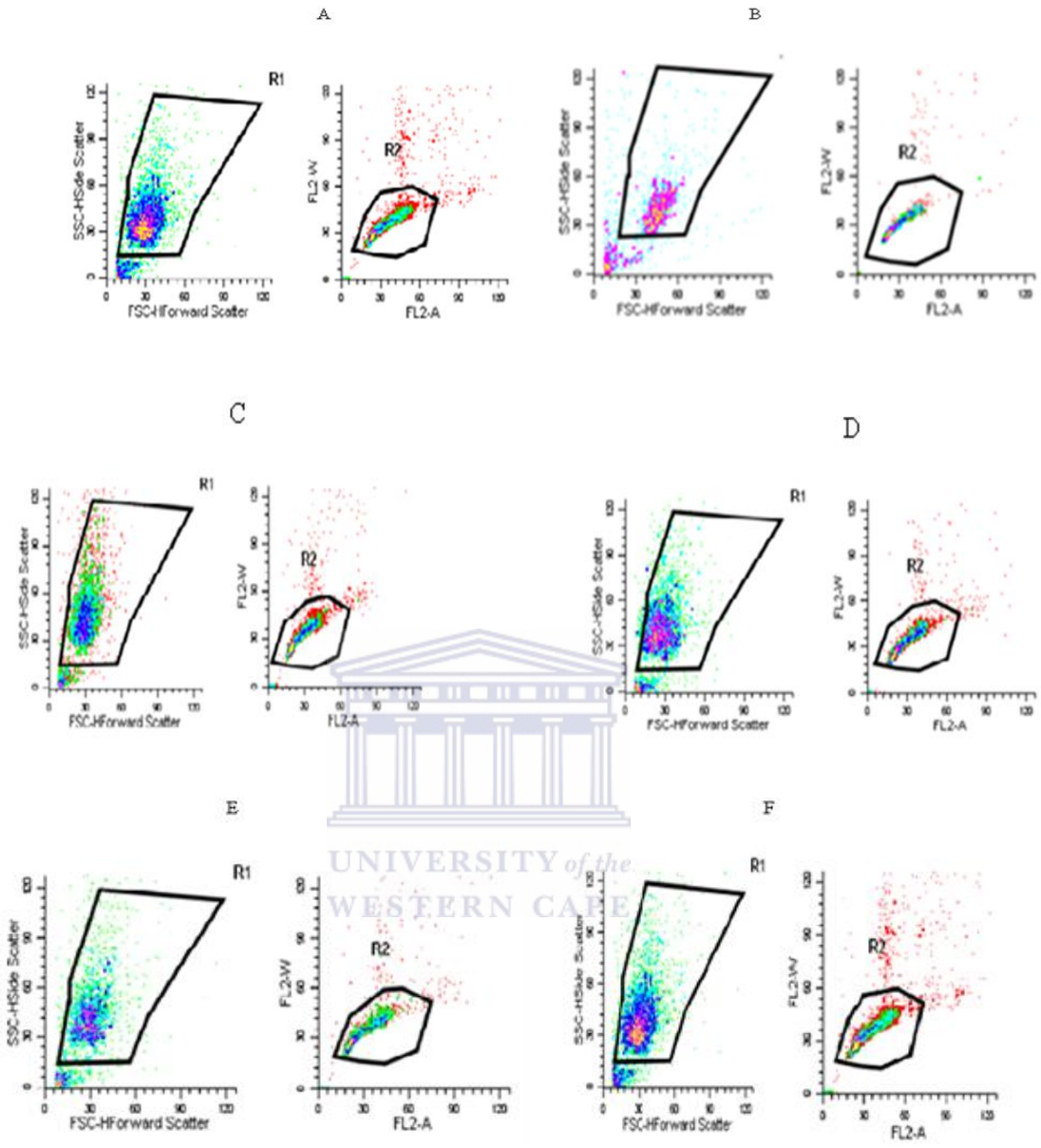

Figure 3.28. These Scatter plots display results obtained using flow cytometry where control cells represented by A) and bEnd5 cells exposed to B) 0.0001mM, C) 0.001mM, D) 0.01mM, E) 0.1mM and F) 1mM pure MA at 24hrs (≥ 10 000 events analysed). Scatter plots were used to generate histogram and the data was tabled and represented as bar graph. R1 representing the population and R2 represent single cells identified.

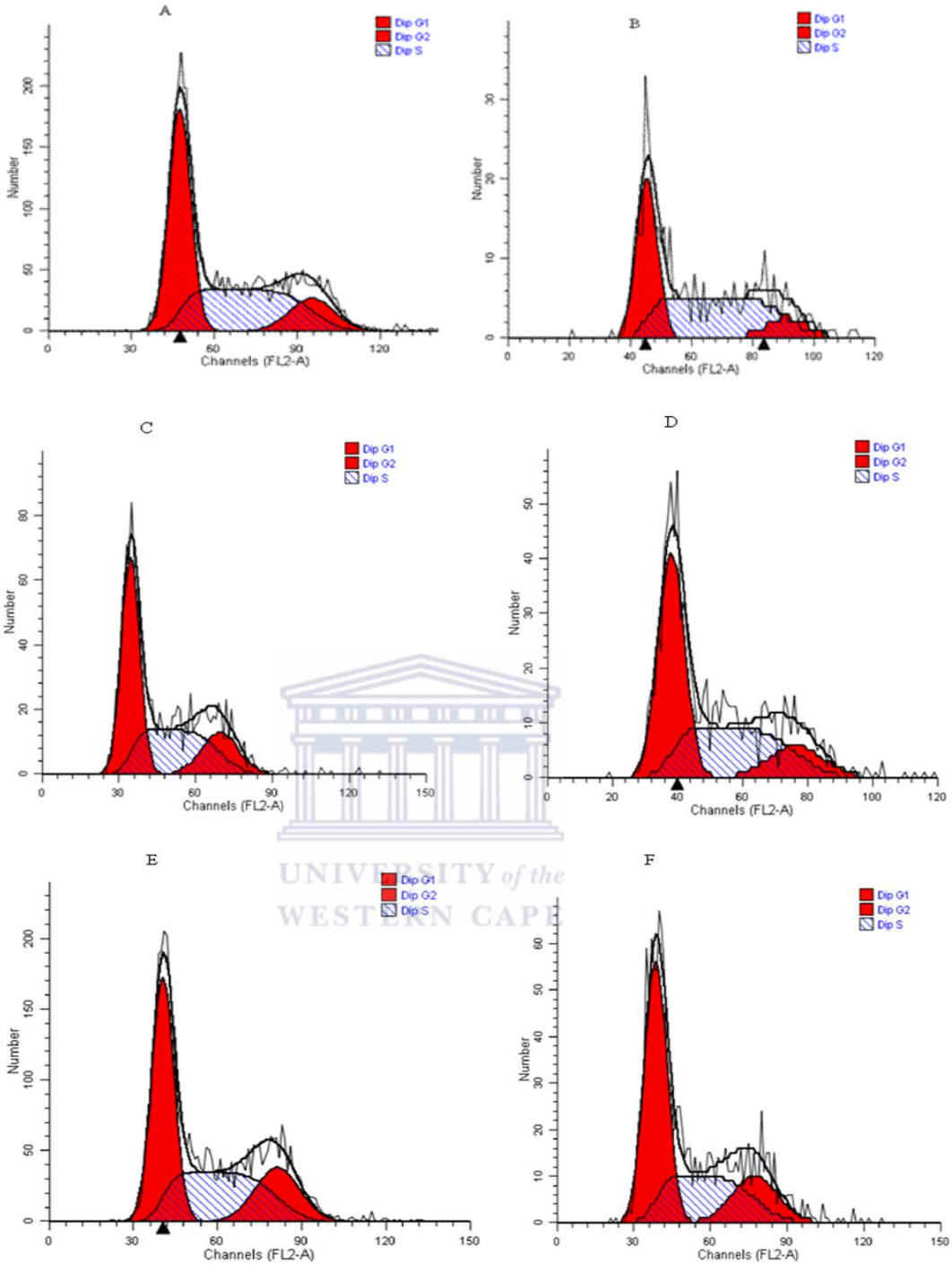

Figure 3.29. The above histograms were acquired using flow cytometry and A) represent results from control cells, while, bEnd5 cells treated with varying concentration of street MA sample 1 are represented by the following histogram after 24hrs: B) 0.0001mM, C) 0.001mM, D) 0.01mM, E) 0.1mM and F) 1mM after 24hrs (≥ 10000 vents analysed). Note the decrease G2-M number of bEnd5 cells in B) above.

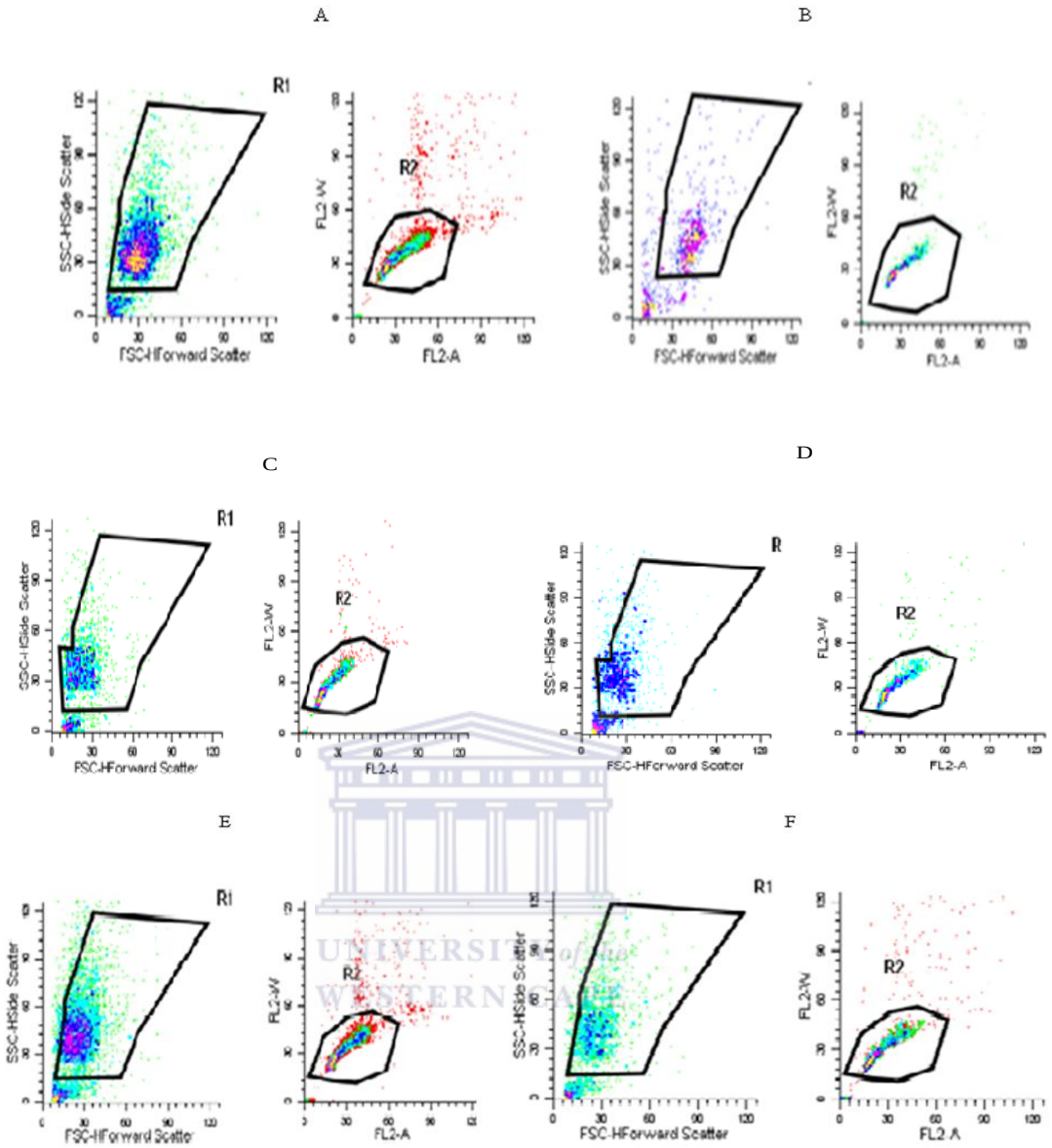

Figure 3.30. These Scatter plots display results obtained using flow cytometry where control cells represented by A) and bEnd5 cells exposed to B) 0.0001mM, C) 0.001mM, D) 0.01mM, E) 0.1mM and F) 1mM street MA sample 1 at 24hrs (≥ 10000 events analysed). Scatter plots were used to generate histogram and the data was tabled and represented as bar graph. R1 representing the population and R2 represent single cells identified.

Table 3.22. Effect of pure and street MA sample 1 on phases of the cell cycle at 48hrs (≥ 10000 events analysed)

	Cell cycle phases					
	G1		S		G2-M	
Control	**40.91**		**43.94**		**15.15**	
	Pure	Street MA	Pure	Street MA	Pure	Street MA
0.1µM	45.77	53.03	40.07	35.64	14.16	11.32
1µM	42.43	55.59	42.25	34.34	15.32	10.07
0.01mM	45.01	50.85	42.63	38.06	12.36	13.1
0.1mM	44.38	49.67	38.19	38.42	17.43	11.9
1mM	38.34	55.85	38.12	35.93	23.54	8.22

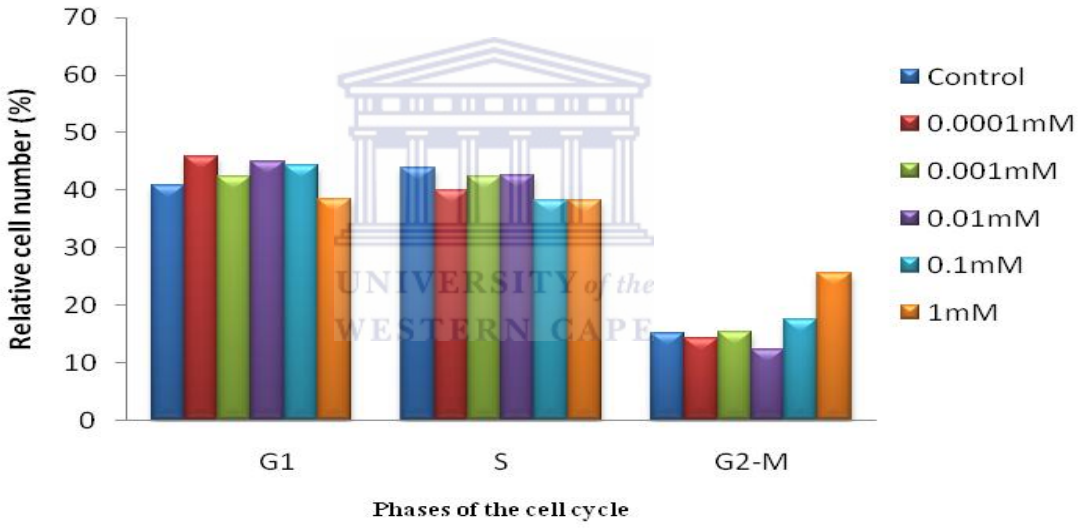

Figure 3.31. Relative cell numbers (%) at distinct phases of the cell cycle for pure MA at 48hrs of exposure.

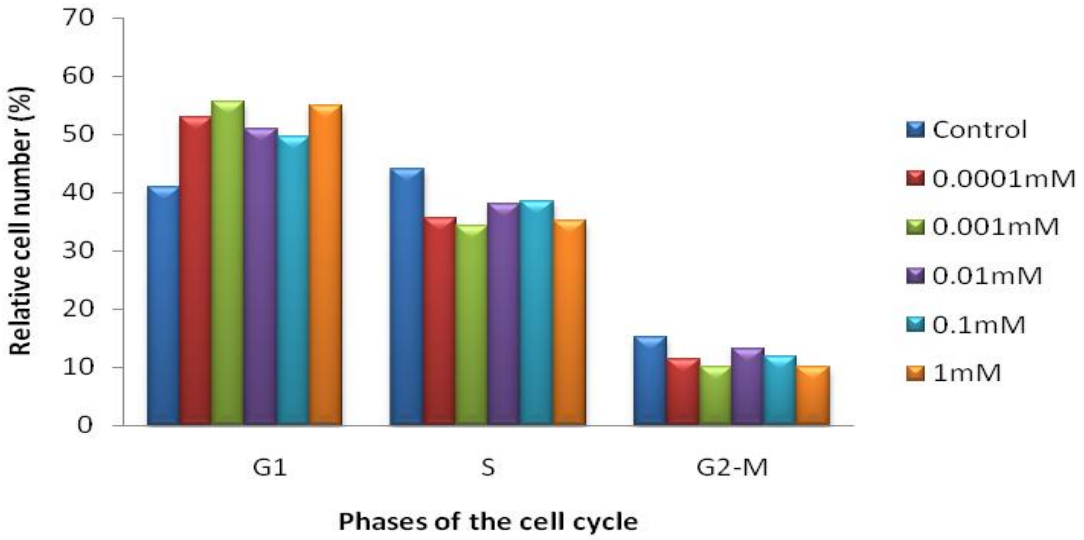

Figure 3.32. Relative cell numbers (%) at distinct phases of the cell cycle for street MA sample 1 at 48hrs of exposure. (See supporting histrogarms and scatter plots on appendix A-D).

Table 3.22, Fig.3.31 and Fig.3.32 demonstrated that after 48hrs, 0.1mM and 1mM concentrations of pure MA resulted in less cells occupying S phase, resulting in more cells entering the following stages (G2-M) at these concentrations. Street MA sample 1 displayed a difference to that of pure MA, here the G0-G1 phase was elevated relative to the control which indicated less cells entering into the S phase, which resulted in the decrease number of cells observed in G2-M phase.

Table 3.23. Effect of pure and street MA sample 1 on phases of the cell cycle at 72hrs (≥ 10000 events analysed).

	Cell cycle phases					
	G1		**S**		**G2-M**	
Control	**46.36**		**43.15**		**10.48**	
	Pure	Street MA	Pure	Street MA	Pure	Street MA
0.1µM	56.17	53.03	34.66	35.64	9.17	11.32
1µM	49.66	55.59	37.48	34.34	12.86	10.07
0.01mM	49.86	50.85	38.47	38.06	12.08	13.10
0.1mM	47.39	49.67	37.87	38.42	14.74	11.90
1mM	56.36	54.88	39.21	35.16	4.42	9.96

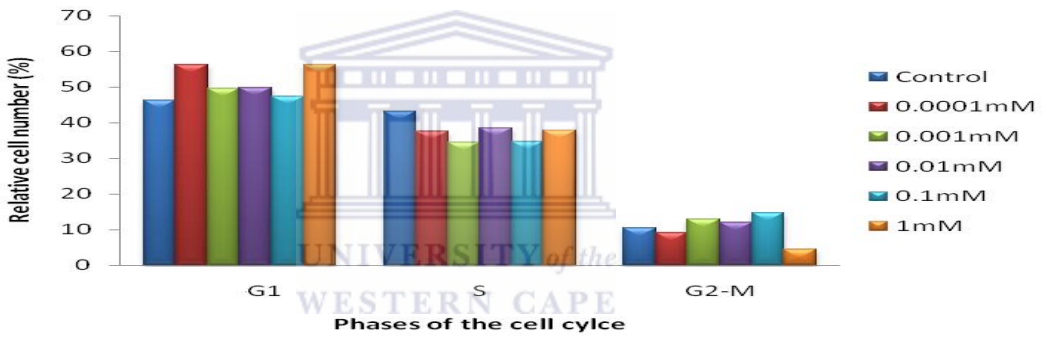

Figure 3.33. Relative cell numbers (%) at distinct phases of the cell cycle for pure MA at 72hrs of exposure.

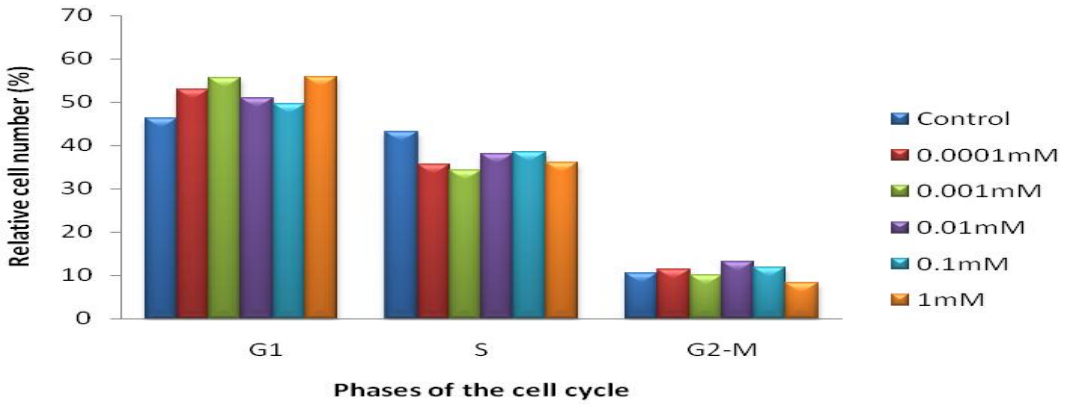

Figure 3.34. Relative cell numbers (%) at distinct phases of the cell cycle for street MA at 72hrs of exposure. (See supporting histrogarms and scatter plots on appendix E-H).

Table 3.2, Fig. 3.37 and Fig.3.38 shows that after 72hrs, profiles of the pure MA and street MA sample 1 were very similar: in both experiments MA caused increased numbers of cells to enter into G0-G1 phase of the cell cycle relative to the controls. This resulted in less cells entering into S phase and also acutely delayed entry of cells into the G2-M phase at the higher concentration of MA samples.

Table 3.24. Effect of pure and street MA sample 1 on phases of the cell cycle at 96hrs (≥ 10000 events analysed).

	Cell cycle phases					
	G1		S		G2-M	
Control	**36.75**		**63.25**		**0.00**	
	Pure	Street MA	Pure	Street MA	Pure	Street MA
0.1µM	57.02	63.86	36.38	28.20	6.38	7.94
1µM	58.45	64.86	37.50	26.49	4.05	8.65
0.01mM	33.66	44.94	66.34	55.06	0.00	0.00
0.1mM	58.55	39.48	30.44	60.52	11.02	0.00
1mM	59.37	57.52	40.63	25.59	0.00	16.89

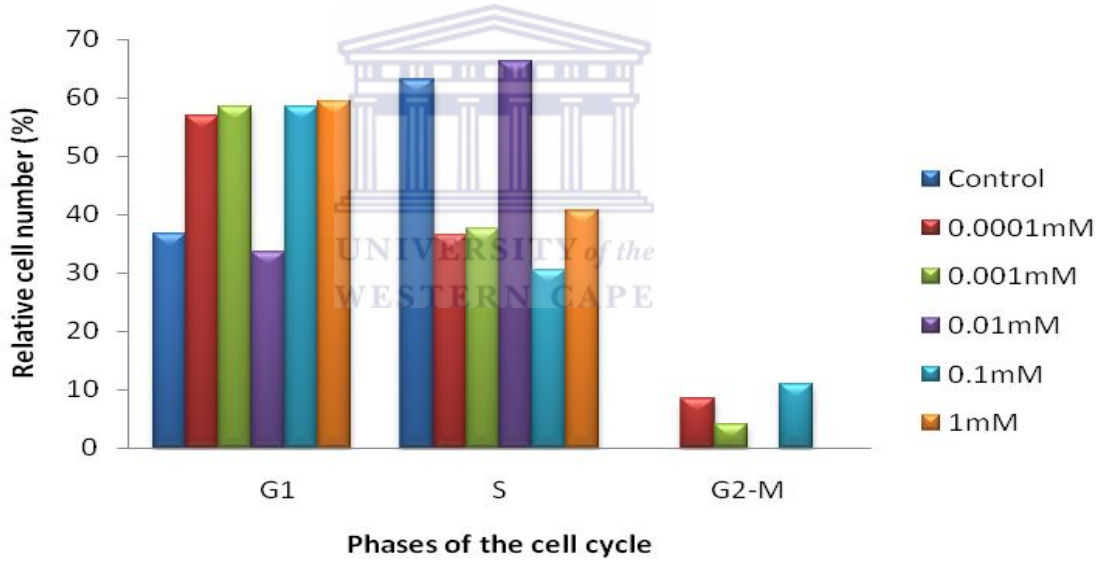

Figure 3.35. Relative cell numbers (%) at distinct phases of the cell cycle for pure MA at 96hrs of exposure.

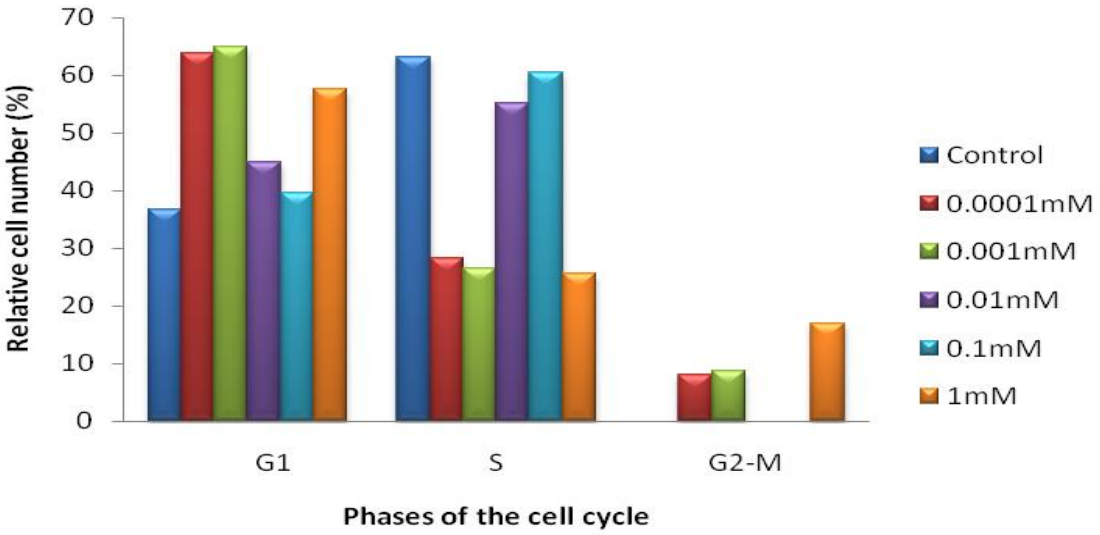

Figure 3.36. Relative cell numbers (%) at distinct phases of the cell cycle for street MA at 96hrs of exposure. (See supporting histrogarms and scatter plots on appendix I-L).

Table 3.24, Fig.3.43 and Fig.3.44 demonstrate that after 96hrs, profiles of pure and street MA sample 1 were very similar for the lowest concentrations. Compared to the control, bEnd5 cells were observed to be located in G0-G1 phase of the cell cycle compare to other phases of the cell cycle for both pure and street MA sample 1. Generally, street MA sample 1 had more cells in G0-G1 phase compared to pure MA. A small number of cells were obtained in G2-M phase.

CHAPTER 4

4.1 Discussion and Conclusion

The blood brain barrier (BBB) is an interface between the circulation and brain parenchyma, and is a very restrictive barrier (Shadi *et al.*, 2012). It has dual functions which includes the barrier function and regulated transport function (Imola *et al.*, 2011). The barrier function restricts the transport of potentially toxic or harmful substances from the intravascular compartment to the brain, while the regulated transport function is responsible for the transport of nutrients to the brain and removal of metabolites. The BBB therefore, functions in maintaining the homeostasis of the CNS to ensure proper brain function (Ijomone *at el.*, 2011). This barrier is composed of endothelial cells that are tightly stitched together by adhesion molecules, adherence and TJ proteins (Dietrich., 2009). TJs make up the primary anatomic component of the BBB, and acts as a physical barrier; forcing most molecular traffic to take a transcellular route, rather than moving paracellularly, as in most cases of endothelia (Imola *et al.*, 2011). In this study the effects on the bEnd5 immortalised brain endothelial cells from the balb/c mice was used to test the effects of MA and illicit MA, (derived from the streets of Cape Town) on their physiological function.

Blood concentration levels can generally be used to distinguish between therapeutic and recreational use. Normal concentration of MA in recreational use ranges between 0.01mg/L to 2.5mg/L in humans. Any concentration that is greater than this represents abuse, and could possibly results in toxicity. In this study, 0.0001-0.001mM which is

described as normal plasma ranges and 0.1-1mM which were higher than normal ranges, were used (Hart *et al*., 2008).

In general, results showed that MA did not affect the cell's viability at any of the concentrations used at any time intervals. Studies have reported on the neurotoxicity of MA (Dietrich., 2009) and it was, therefore expected that MA would decrease the bEnd5 cell's viability. However, in this study, the viability of MA exposed cells were found to be comparable to controls. Neurotoxicity as a result of MA leads to neuronal cell death in several brain areas, including the cortex, striatum, and hippocampus (Deng *et al*., 2001, Martins *et al.*, 2011). Studies have analyzed the effects of MA on the BBB *in vivo*, demonstrating that MA cause an effect on the BBB by increasing permeability correlated with the preceding temperature increase induced by MA (Martins *et al.*, 2011).

Cell growth % as a result of pure MA exposure decreased over time, with 96hrs showing a significant suppression in cell growth when compared to the control. At 48hrs, the intermediate concentrations (0.01mM and 0.1mM) of pure MA resulted in increased growth. Rizzo *at el.*, (2010) proposed that MA induced its effects by stimulating metabolic cell growth. Furthermore, it should be noted that physiological plasma levels of MA abuse ranges between 0.0001 and 0.01mM (Hart *at e*l., 2008). Data obtained from trypan blue assays showed that the bEnd5 cell numbers generally increased in the first 24hrs and then decreased over time with the exception of street MA sample 3 and 4. Street MA sample 3 data showed that bEnd5 cells growth was suppressed across all time intervals, while, street MA sample 4 demonstrated similar % cell growth over time compared to the control. This variation in sample effects could be due to impurities that may be found in the different street MA preparations,

(in the clandestine labs). During the manufacturing of illicit MA in various chemicals such as counterintuitive and prescription drugs (e.g. ephedrine) are used, which may have led to the different effects observed in the bEnd5 cells. Overall, the cell numbers decreased to increased MA doses over time, and displayed a dose-dependent effect (see chapter 3 fig 3.10-3.14). Street MA sample 1 also showed a significant elevation in % cell growth at 24, 48, and 72hrs followed by a decrease at 96hrs. Although MA was not quantified in this study, it can be suggested (based on the similar results between pure and street MA sample 1) that street MA sample 1 had comparable purity to the certified pure MA purchased from Sigma (Fig 3.10 and 3.11).

In contrast, 0.01mM and 0.1mM of street MA sample 2 resulted in suppression of % cell growth over 24hrs, and thereafter, the bEnd5 cells appeared to recover. Overall, % cell growth of street MA sample 4 was similar over time, with respect to the different concentrations. MA suppressed the growth of cells but it did not affect their viability compared to control. Studies by Bowyer *et al.*, (2006) showed the effect of MA on BBB functioning, in which leakage was observed across the barrier in the cerebral cortex of mice. This were also observed at high concentrations of MA causing disruption in the limbic system, and produced neuronal degeneration of mouse BBB (Bowyer *et al*, 2006). It can thus be inferred that MA interferes with the bEnd5 cell cycles since it interrupts these critical phases which could results in decrease cell division without affecting viability. It is clear from the results reported in this study that MA caused the suppression of cell growth, while not affecting their viability. These findings are supported by the work performed by Yuan *et al* (2011), who found that MA is, indeed, associated with a long-term exposure in BBB cells without specific modification in S-phase of the cell cycle.

Burrows *et al*. (2000) reported, that an increase in metabolic stress causes compromised energy production and has thus been thought to contribute to lasting changes in the neurotransmitter systems following high-doses of MA. Adenosine triphosphate (ATP) which is predominantly used by the cell for various functions is produced by the mitochondria (Riddle *et al*., 2008). In the current study cell viability did not show significant differences at selected MA concentration over the observed time intervals relative to the controls. Based on these findings the production of ATP by the bEnd5 cells was investigated to determine whether the division of endothelial cells were compromised by a lack of ATP production; metabolic status of a cell being crucial for cell division (Wallace., 2005). The ATP levels produced by bEnd5 cells treated with selected MA concentrations were similar to that of the control at 24hrs followed by a significant increase by 96hrs (chapter 3.3). The elevation of ATP level observed at 96hrs might be a mechanism by which bEnd5 cells are trying to compensate for the inhibited cell growth observed, thus, producing more ATP in preparation of the next phase which has been blocked by MA. Viable cells require energy to function and divide. The various concentrations of MA analysed showed no effect on the ATP levels at 24, 48 and 72hrs when compared to control.

Research performed on bEnd5 cells, investigating mitochondrial activity, showed that a mitochondrial checkpoint exists in late G1 phase, where low ATP prompts the activation of an AMPK–p53–cyclin E-dependent pathway (Marisa *et al.*, 2010). The low ATP may trigger a G1-S phase check point that involves the sequential activation of AMPK and p53, and ultimately the down-regulation of cyclin E levels. Activation of AMPK by impaired mitochondria activates p53 and leads to a decrease in cyciln E level, which could result in a block in the G1-S phases (Finke *et al.*, 2009). Triggering

of this pathway may possibly arrest metabolically impaired cells low ATP production instead of committing them to cell division. Mitochondria use energy pathways such as the citric acid cycle and electron transport chain (ETC), to produce ATP. Marisa *et al.*, (2010) showed that MA inhibits the ETC and up-regulates many ETC inhibitors such as complex IV via the activation of cytochrome oxidase. Consequently, these high doses of MA and activation of cytochrome oxidase increases reactive species, resulting in dopaminergic neurotoxicity (Burrowe *et al.*, 2000). ETC inhibitors are therefore strongly implicated in mitochondrial dysfunction and are thought to be linked in the mechanism of MA induced neurotoxicity. This premise is supported by studies which illustrate that energetic stress caused by administration of a citric acid cycle inhibitor, exacerbates the persistent dopaminergic deficits caused by MA (Riddle *et al.*, 2006).

In this study it was demonstrated that at 96hrs, cell numbers were significantly lower than that of controls. It was also noted that during this time interval, the ATP levels were significantly elevated compared to controls. This could be an indication that cells exposed to MA have sufficient ATP available for cell division, but their ability to use the energy source is blocked by an unknown mechanism. This predicts a possible connection between the decrease in cell growth and increase ATP levels at 96hrs. It can, therefore, be proposed that the increase in ATP is a mechanism by which bEnd5 cells attempt to compensate for the inhibited cell growth. This study's findings also suggest that the suppression in cell growth may be caused by the inability of bEnd5 cells to efficiently use ATP at 96hrs, and thus MA and/or its metabolites may be directly or indirectly impairing the cells ability to utilize ATP.

In order to investigate whether the suppression of bEnd5 cell numbers at 96hrs was due to changes in DNA production, DNA synthesis levels were analysed using BrdU incorporation. The selected concentrations used to determine DNA synthesis analysis was the same as those selected for the assays previously performed. The bEnd5 cells showed variation in their levels of BrdU incorporation, in which DNA synthesis was suppressed at 96hrs for pure and street MA sample 4 when compared to controls, while street MA sample 1 showed similar results to that of controls. Street MA sample 2 and 3 however, showed higher DNA synthesis than that of the control, with street MA sample 3 producing higher levels of DNA compared to all other MA samples. This distinct variation in which the different MA samples affect DNA levels might be due to the additional molecular components (Figure 3.1-3.4) found in the samples as a result of the illicit methods used to produce MA. This study showed that viability of bEnd5 cells exposed to MA were not affected, while cell growth was suppressed and accompanied by an increase in ATP at 96hrs. Overall DNA synthesis increased between 24 and 96hrs, however, the DNA levels for pure and street MA sample 4 did not exceed that of the controls. The increase in DNA levels observed compared to the decrease in cell numbers may be because the bEnd5 cells are able to generate enough DNA in preparation for division in the M phase, but are perhaps blocked at the G0-G1 stage of the cell cycle. This indicates that the suppression observed may be due to a mechanism that blocks the progression of cell division. To date, there are no reports investigating the effects of MA on the cell cycles of a monolayer of bEnd5 cells.

The results of this study suggest that MA slows down the proliferation of the bEnd5 cells by targeting a specific phase of the cell cycle. Normal cells undergo growth

phases in order to maintain survival in all living organisms. Cell growth and division is determined by a successful cell cycle which involves alterations within the cell in order to proliferate, repair or segregate the genome (Chaw *et al.*, 2010). The stages of the cell cycle are regulated by a control system that governs progression through the cell cycle (Bruce *et al.*, 2007).

As the cell cycle is an important component of viability (Del Bin *et al.*, 1991), we therefore looked at the effect of MA on the various stages (G1, G2, S and M phases). At 24 and 48hrs MA exposure showed no effect on the cell cycle phases when compared to the controls. This argument is supported by the study performed by Yuan *et al.*, (2011) which showed that MA had an effect only after an extended period (6hrs/day: 4-13days) of exposure without changing dynamics of the cell cycle stages. It is important to note that the significant changes in bEnd5 cell cycles were observed at 72 and 96hrs, which further aligns with the findings of Yuan *et al.*, (2011). MA exposure at 72 and 96hrs resulted in cell cycle arrest at G0-G1and G2-S phase (Fig: 3.33, 3.34, 3.35 and 3.36).

Using *in vitro* BrdU assays coupled to the analysis of cell cycle progression, this study illustrated that although MA affected the levels of DNA synthesis differently, it led to a specific G1-S phase arrest. Thus, long term exposure to MA impedes bEnd5 cell proliferation which could be detrimental to the integrity of the BBB and ultimately the homeostasis of the CNS.

The slight differences observed in the assays performed could be due to impurities used in the manufacturing of illicit MA and the quality of MA found in these samples.

In conclusion, it was surprising to observe that the viability of bEnd5 cells exposed to MA was unaffected and that MA did not appear to be toxic to the bEnd5 cells at the selected concentrations used. MA however, impeded cell growth over a period of 96hrs when compared to the controls, which may have resulted in an increase in ATP production. While DNA synthesis showed differences in their levels with respect to the various MA samples at 96hrs, cell cycle analysis demonstrated that the bEnd5 cells were arrested at the G1-S phase between 72 and 96hrs. The findings of this study therefore suggests that although the highly soluble compound MA permeates through all brain tissue leading to significant neurotoxicity, it surprisingly showed no toxic effects on the endothelial cells of the *in vitro* BBB. There seems to be yet undescribe mechanism whereby MA brings about its negative effects, not only in the endothelial cells but also in the neural of the brain (Yuan *et al.*, 2011*).*

CHAPTER 5

5.1 Future Perspectives

Future studies should attempt to elucidate the mechanism whereby MA affects the cell cycles, by specifically analysing cell cycle phase lengths and also identifying at which stage in these phases MA interferes. Moreover, it is acknowledged that cell cycle analysis in this study was not performed on a population of cells that were synchronized, and therefore this must also be included in the future approaches. Since it is evident that MA interferes with the energy metabolism of the cells, further investigations into the electron transport chain as well as the tricarboxy acid cycle are required.

Little is known about the effects of psychoactive drugs on the BBB structure and function, thus studies should also focus on the pathways involved in maintaining the physical integrity of the BBB by analysing the expression of important regulatory proteins such as the tight junction and adherens proteins.

Furthermore, understanding the bioavailability of MA in the bEnd5 cells may also shed light on the degree of interference MA may have on the cell cycles, since it seems that long-term exposure and presence of MA has greater adverse effects.

CHAPTER 6

6. References

Asanumaa, M., Miyazakia, I., Higashia, Y., Cadetb, L.J., Ogawa, N., (2002), Methamphetamine-induced increase in striatal p53 DNA-binding activity is attenuated in Cu,Zn-superoxide dismutase transgenic mice. *Neuroscience letters* 3, 325:191-194.

Bednarczyk, J., Lukasiuk, K., (2011), Tight junctions in neurological diseases. Acta *Neurobiologiae Experimentalis*, 71: 393–408.

Bloom, G.R., Suhail, F., Hopkins-Price, P., Sood, A., (2008), Acute anhydrous ammonia injury from accidents during illicit methamphetamine production. *Burns*, 34: 713-718.

Boveri, M., Kinsner, A., Berezowki, V., Lenfant, A.M., Dehouck, M. P., Hartung, T., Prieto, P., Bal-price, A., (2006), Highly purified lipoteichoic acid from Gram-positive bacteria induces in vitro-brain barrier disruption through glia activation: role of pro-inflammatory cytokines and nitric oxide. *Neuroscience* 4, 137: 1193–1209.

Bowyer, J.F., Ali, S., (2006), High doses of methamphetamine that cause disruption of the blood-brain barrier in limbic regions produce extensive neuronal degeneration in mouse hippocampus. *Synapse*, 60: 521-532.

Bruce, A., Alexender, J., Julian, L., Martin, R., Keith, R., Peter, W., (2002), Molecular biology of the cell. *4th Edition*. New York, Chapter 17, pp.

Burrows, K.B., Gudelsky, G., Yamamoto, B.K., (2000), Rapid and transient inhibition of mitochondrial function following methamphetamine or 3,4-methylenedioxymethamphetamine administration. *European Journal of Pharmacology*, 398: 11-18.

Caldwell, J., Dring, L.G., Williams, R,T., (1972), Metabolism of methamphetamine in man, the guinea pig and the rat. *Biochemical Journal*, 129: 11-22.

Chang, L., Daniel, A., Thomas, E., Volkow, N., (2007), Structural and metabolic brain changes in the striatum associated with methamphetamine abuse. *Addiction* 102, 1: 16–32.

Chi-Wei W., Yueh-Hsin P., Jiin-Cherng Y., Chia-Yu C., Sheng-Fan W., Chiao-Ling Y., Chin-Wen, C., Hsin-Chen, L., (2007), Enhanced oxidative stress and aberrant mitochondrial biogenesis in humanneuroblastoma SH-SY5Y cells during methamphetamine induced apoptosis. *Toxicology and Applied Pharmacology* 3, 220: 243–251.

Clara, J.Y., Jovy, M.D.Q., Airee, K., Sunmee, W., Chitra, D.M., (2011) Extended access methamphetamine decreases immature neurons in the hippocampus which results from loss and altered development of neural progenitors without altered

dynamics of the S-phase of the cell cycle. *Pharmacology, Biochemistry and Behavior*, PBB-71270.

Cody, J.T., (1993) Metabolic precursors to amphetamine and methamphetamine. *Forensic Science Review* 5: 109.

Colman, E., (2005) Anorectics on Trial: A Half Century of Federal Regulation of Prescription Appetite Suppressants. *Annals of Internal Medicine* 143:380-385.

Crossley, F., Moore, M., (1944), Studies on the leuckart reaction. *Journal organic Chemistry*: 529.

Davidson, C., Gow, A.J., Lee, T.H., Ellinwood, E.H., (2001), Methamphetamine neurotoxicity: necrotic and apoptotic mechanisms and relevance to human abuse and treatment. *Brain Research Reviews*, 36: 1–22.

Deng, X., Cadet, L.J., (2000), Methamphetamine-induced apoptosis is attenuated in the striata of copper–zinc superoxide dismutase transgenic mice. *Molecular Brain Research*, 83: 121-124.

Deng, X., Cain, N.S., McCoy, M.T., Chen, W., Trush, W.A., Cadet, J.L., (2002), Methamphetamine induces apoptosis in an immortalized rat striatal cell line by activating the mitochondrial cell death pathway. *Neurophamarcology*, 42: 837-845.

Deng, X., Wang, Y., Chou, J., Cadet, J.L., (2001), Methamphetamine causes widespread apoptosis in the mouse brain: evidence from using an improved TUNEL histochemical method. *Molecular brain research*, 93: 64-69.

Diamond, J., (1977), The epithelial tight junction: bridge, gate and fence. *Physiologist*, 20: 10-18.

Dietrich, J.B., (2009), Alteration of blood-brain barrier function by methamphetamine and cocaine. *Cell Tissue Research*, 336:385–392.

Dixon, M., Moody, M.D., (2006), The Blood-Brain Barrier and Blood–Cerebral Spinal Fluid Barrier. *Seminars in Cardiothoracic and Vascular Anesthesia*, 128-131.

Emad, H., (1929), Methamphetamine from ephedrine. *Helvetica Chimica*. *Ac*t 12: 365.

Engelhardt, B., (2003), Development of the blood-brain barrier: *Cell Tissue Research*, 314: 119–129.

Filipa, L.C., Dora, B., Maria, B., (2010), Looking at the blood–brain barrier: Molecular anatomy and possible investigation approaches. *Brain Research Reviews*. 64: 328 – 363.

Finkel, T., Hwang, P.M., (2009), The Krebs cycle meets the cell cycle: Mitochondria and the G1–S transition. *PNASE*, 29: 11825-11826.

Frosta, O.D., Cadet, J.L., (2000), Effects of methamphetamine-induced neurotoxicity on the development of neural circuitry: a hypothesis. *Brain research Reviews*, 34:103-118.

Gabrielle, E.D., Anne, C., Russell, D.F., Alan, R.H., (2010), Isotope fractionation during precipitation of methamphetamine HCl and discrimination of seized forensic samples. *Forensic Science International*, 200: 123–129.

Genca, K., Gencb, S., Kizildagb, S., Sonmezc, U., Yilmazd, O., Tugyan, K., Ergur, B., Sonmez, A., Buldan, Z, M., (2003), Methamphetamine induces oligodendroglial cell death in vitro. *Brain Research* 982, 1: 125-130.

Gerecht-Nir S., Osenberg S., Nevo O., Ziskind A., Coleman R., Itskovitz-Eldor J., (2004), Vascular development in early human embryos and in teratomas derived from human embryonic stem cells". Biology of reproduction,71: 2029-2036.

Gwënaël, P., Christophe, F., Roméo, C., Yannis, K., (2009), Understanding the blood–brain barrier using gene and protein expression profiling technologies. *Brain Research Reviews,* 62: 83-98.

Hart, C.L., Gunderson, E.W., Perez, A., Kirkpatrick, M.G., Thurmond, A., Comerm, S.D., Foltin, R.W., (2008), Acute Physiological and Behavioral Effects of Intranasal Methamphetamine in Human. *Neuropsychopharmacology*, 33: 1847-1855.

Hall, W., Hando, J., Darke, S., Ross, J., (1996), Psychological morbidity and route of administration among amphetamine users in Sydney, Australia. *Addiction*, 91: 81–87.

Hartsock, A., Nelson, W, J., (2008), Adherens and tight junctions: Structure, function and connections to the actin cytoskeleton. *Biochimica et Biophysica Acta*, 1778: 660–669.

Howard, P.H., William, C.H., McMillan, D.E., Michael, S.O., (2008), Bioavailability of (+)-methamphetamine in the pigeon following an intramuscular dose. *Pharmacology Biochemical Behav.*, 90, 3: 382–386.

Ijomone, O.M., Nwoha, P.U., Olaibi, O.K., Obi A.U., Alese. M.O., (2011), Effects of methamphetamine on the hippocampus of rats: Behavioural and morphological approach. *Journal of Neuroscience and Behavioural Health* 3, 8: 107-112.

Imam, S.Z., Itzhak, Y., Jean, L., Cadet, J.L., Islam, F., Slikker Jr., W., Alia, S.F., (2001), Methamphetamine-induced alteration in striatal p53 and bcl-2 expressions in mice. *Molecular Brain Research*, 91: 174-178.

Imola, W., Csilla, F., Istava, A.K., (2011), *In vitro* models of the blood-brain barrier, *Acta Neurobiologiae Experimentali*, 113-128.

Jae, S.L., Eun, Y.H., Soo, Y.L., Eun, M.K., Yong, H.P., Mi, A.L., Hee, S.C., Jeong, H.P., (2006), Analysis of the impurities in the methamphetamine synthesized

by three different methods from ephedrine and pseudoephedrine. *Forensic Science International*, 161: 209–215.

Jian, X.Z., Da, M.Z., Xu, G.H., (2008), Identification of impurities and statistical classification of methamphetamine hydrochloride drugs seized in China. *Forensic Science International*, 182:13–19.

Kanamoria, T., Tsujikawaa, K., Ohmaea, Y., Iwataa, Y.T., Inouea, H.T., Kishia, Nakahamab, T., Inouyeb, Y., (2005), A study of the metabolism of methamphetamine and 4-bromo-2,5-dimethoxyphenethylamine (2C-B) in isolated rat hepatocytes. *Forensic Science International*, 148: 131–137.

Krasnova, I.N., Cadet, J.L., (2009), Methamphetamine toxicity and messengers of death. *Brain Research*, 60: 379-407.

Kwang, S.K., (2006), Microbial translocation of the blood–brain barrier. *International Journal for Parasitology*, 36: 607–614.

Lamalice L., Le Beouf F., Huot J., (2007), Endothelial cell migration during angiogenesis, *Journal of the American Heart Association*, 100: 782-794.

Marcial M.A., Carlson, S.L., and Madara, J.L., (1984), Partitioning of paracellular conductance along the ileal crypt-villus axis: A hypothesis based on structural analysis with detailed consideration of tight junction structure–function relationship. *journal of Membrane Biology*, 80: 59–70.

Masato, A., Ikuko, M., Youichirou, H., Jean L.C., Norio, O., (2002), Methamphetamine-induced increase in striatal p53 DNA-binding activity is attenuated in Cu,Zn-superoxide dismutase transgenic mice. *Neuroscience Letters*, 325: 191-194.

Matthew, C., Gunter, K., Christina, Wei, M.K., (2009), Manufacturing by-products from, and stereochemical outcomes of the biotransformation of benzaldehyde used in the synthesis of methamphetamine. *Forensic Science International*, 189:60–67.

Maxime, C., Stefan, L., Dorothe´e, V., Ste´phane, N., Christophe, L., Yannick, D., Marie-Pierre, D., Vincent, B., Laurence, F., Rome´o, C., (2008), An *in vitro* blood-brain barrier model for high throughput (HTS) toxicological screening. *Toxicology in vitro*, 22: 799–811.

Nicolas, P., Salah, Y., Sylvie, C., Nathalie, C., Fanchon, B., Salvatore, C., Xavier, D., Satoko, H., Tetsuya, T., Maria, D.S., Jamal, T., Françoise, R., Pierre-Olivier, C., (2007), A functional *in vitro* model of rat blood–brain barrier for molecular analysis of efflux transporters. *Brain Research*, 1150: 1-13.

Nicolas, W., Florence, M., Sylvie, C., Pierre-Olivier, C., (2009), The blood-brain barrier in brain homeostasis and neurological diseases. *Biochimica et biophysica acta (BBA)-biomembranes*, 1788: 842–857.

Ogata, E., (1919), Chemistry. Abstract. *Journal of the Pharmaceutical Society of Japan*, 451, 752: 14-75.

Person, E.C., Meyer, J.A., Vyvyan, J.R., (2005), Structural determination of the principal by product of the lithium-Ammonia reduction method of methamphetamine manufacture. *Journal of Forensic Sciences*, 50: 87-95..

Plüddemann, A., Myers, B., Parry, C., (2000), Alcohol and Drug Abuse Research Unit, *Medical Research Council.*

Remberg, B., Stead, A.H., (1999), Drug characterization/impurity profiling, with special focus on methamphetamine: recent work of the United Nations International Drug Control Programme. *Bulletin On Narcotics*, Volume LI, Nos. 1 and 2.

Riddle, E.L., Fleckenstein, A.E, Hanson, G.R., (2006), Mechanisms of Methamphetamine-induced Dopaminergic Neurotoxicity. *The AAPS Journal*, 8(2) Article 48.

Schielke, G.P., Moises, H.C., Betz, A.L., (1990), Potassium activation of the Na,K-pump in isolated brain microvessels and synaptosomes. *Brain Research*, 524:291-296.

Schulze, C., Firth, J.A., (1993). Immunohistochemical localization of adherens junction components in blood-brain barrier microvessels of the rat. *Journal of Cell Science*, 104: 773–782.

Shadi, N.M., Susan, S., (2012), Core Concepts: Development of the Blood-Brain Barrier. *Neoreviews*, 13:241.

Sheng-He, H., Monique, F.S., Kwang, S.K., (2000), Bacterial penetration across the blood-brain barrier during the development of neonatal meningitis. *Microbes and Infection*, 2: 1237−1244.

Shinsuke, N., Ma´ria, A., Deli, H., Kawaguchi, Takeshi, S., Takanori, S., A´ gnes, K., Kunihiko, T., Masami, N., (2009), A new blood–brain barrier model using primary rat brain endothelial cells pericytes and astrocytes. *Neurochemistry International*, 54: 253–263.

Syed, Z, I., Yossef, I., Jean L, C., Fakhrul, I., William, S., Syed, F, A., (2001), Methamphetamine-induced alteration in striatal p53 and bcl-2 expressions in mice. *Molecular Brain Research*, 91: 174-178.

Thiriet, N., Jayanthi, S., McCoy, M., Ladenheim, B., Cadet, J.L., (2001), Methamphetamine increases expression of the apoptotic c-myc and L-myc genes in the mouse brain. *Molecular Brain Research*, 90: 202-204.

Tian, C., Murrin L.C., Zheng, J.C., (2009), Mitochondrial fragmentation is involved in methamphetamine-induced cell death in rat hippocampal neural progenitor cells. *PLoS ONE* 4, 5:5546.

Vermeulen, K., Berneman, N.Z., Van Bockstaele, D.R., (2003), Cell cycle and apoptosis. *Cell Proliferation* 36: 165–175.

Virgintino, D., Errede, M., Robertson, D., (2004), Immunolocalization of tight junction proteins in the adult and developing human brain. Histochem *Cell Biology,* 122, 1: 51–59.

Wallace, D.C., (2005), A mitochondrial paradigm of metabolic and degenerative diseases, aging, and cancer: A dawn for evolutionary medicine. *Annual. Reviews. Geneticist*, 39:359–407.

Watari, N., Sugiyyama, Y., Kananiwa, N., Hiura, M., (1988), Pharmacokinetics and biopharmaceutics. *International journal of pharmaceutics*, 16: 297-301.

Weksler B.B., Subileau E. A., Perrière N., Charneau P., Holloway K., Leveque. M., Tricoire-Leignel H., Nicotra A., et al., (2005), Blood-brain barrier-specific properties of a human adult brain endothelial cell line, *The FASEB journal*, 10:1096.

Wilson, J.M., Kalasinsky, K.S., Levey, A.I., Bergeron, C., Reiber, G., Anthony, R.M., Schmunk, G.A., Shannak, K., Haycock, J.W., Kish, S.J., (1996), Striatal dopamine nerve terminal markers in human, chronic methamphetamine users. *Nature Medicine 2*: 699–703.

Winfried, N., Regina, L., Silvester, O., Urs P.F., Gerhard, F., Ecker, C., Noea, R., (2006), A novel flow based hollow-fiber blood–brain barrier in vitro model with immortalised cell line PBMEC/C1–2. *Journal of biotechnology*, 126: 127–141.

Wolburg, H., Lippoldt, A., (2002), Tight junctions of the blood–brain barrier: Development, composition and regulation. *Vascular Pharmacology*, 38: 323– 337.

Xavier, N., Sandrine, B.E.E., Pierre-Olivier, C., (2005), How do extracellular pathogens cross the blood–brain barrier? *Trends in Microbiology*, 10: 277-232.

Yamamoto, B.K., Moszczynska, A., Gudelsky, G.A., (2010), Amphetamine toxicities: classical and emerging mechanisms. *Annals of the New York Academy of Sciences*, Review article. 1187:101-21.

Yamamoto, Y., Yamamoto, K., Hayase, T., Abiru, H., Shiota, K., Mori, C., (2002), Methamphetamine Induces Apoptosis in Seminiferous Tubules in Male Mice Testis. *Toxicology and Applied Pharmacology*, 178: 155-160.

Yan, C., Qing-Jun, Z., Jian, Y.Y., Xiao-Pei, W., (2009), A prediction model for blood–brain barrier permeation and analysis on its parameter biologically. *Computer methods and programs in Biomedicine*, 95: 280–287.

Yua, Q., Larsonb, D.F., Watson, R.R., (2003), Heart disease, methamphetamine and AIDS. *Life science*, 73: 129-140.

Zhoua, J., Jian-Hui Liang, J., Zheng, J., Li, C., (2004), A Nerve growth factor protects R2 cells against neurotoxicity induced by methamphetamine. *Toxicology Letter*, 150: 221-227.

APPENDIX A-L

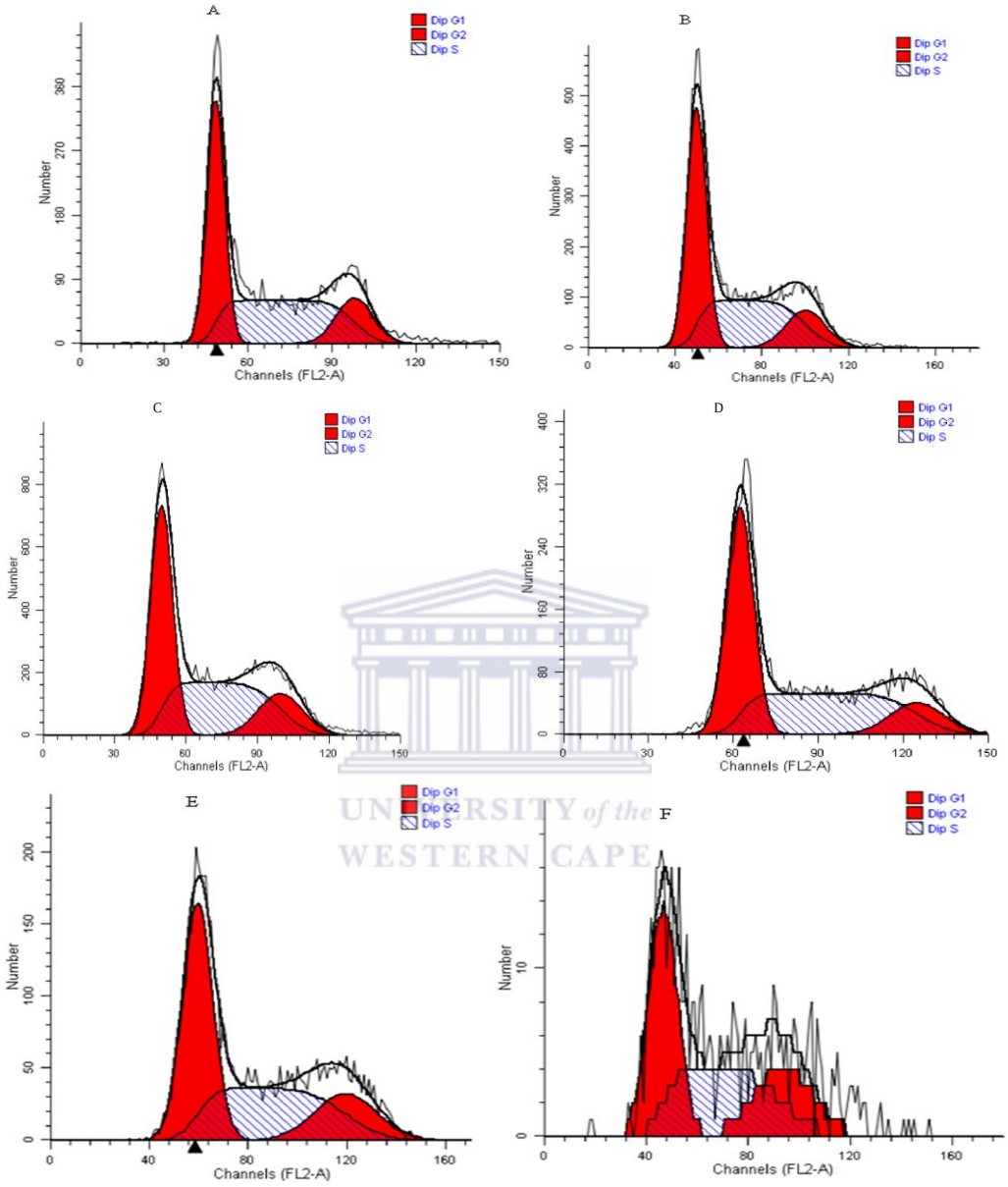

Appendix A. The above histograms were acquired using flow cytometry and A) represent results from control cells, while, bEnd5 cells treated with varying concentration of pure MA are represented by the following histogram after 48hrs: B) 0.0001mM, C) 0.001mM, D) 0.01mM, E) 0.1mM and F) 1mM after 48hrs (≥ 10000 vents analysed).

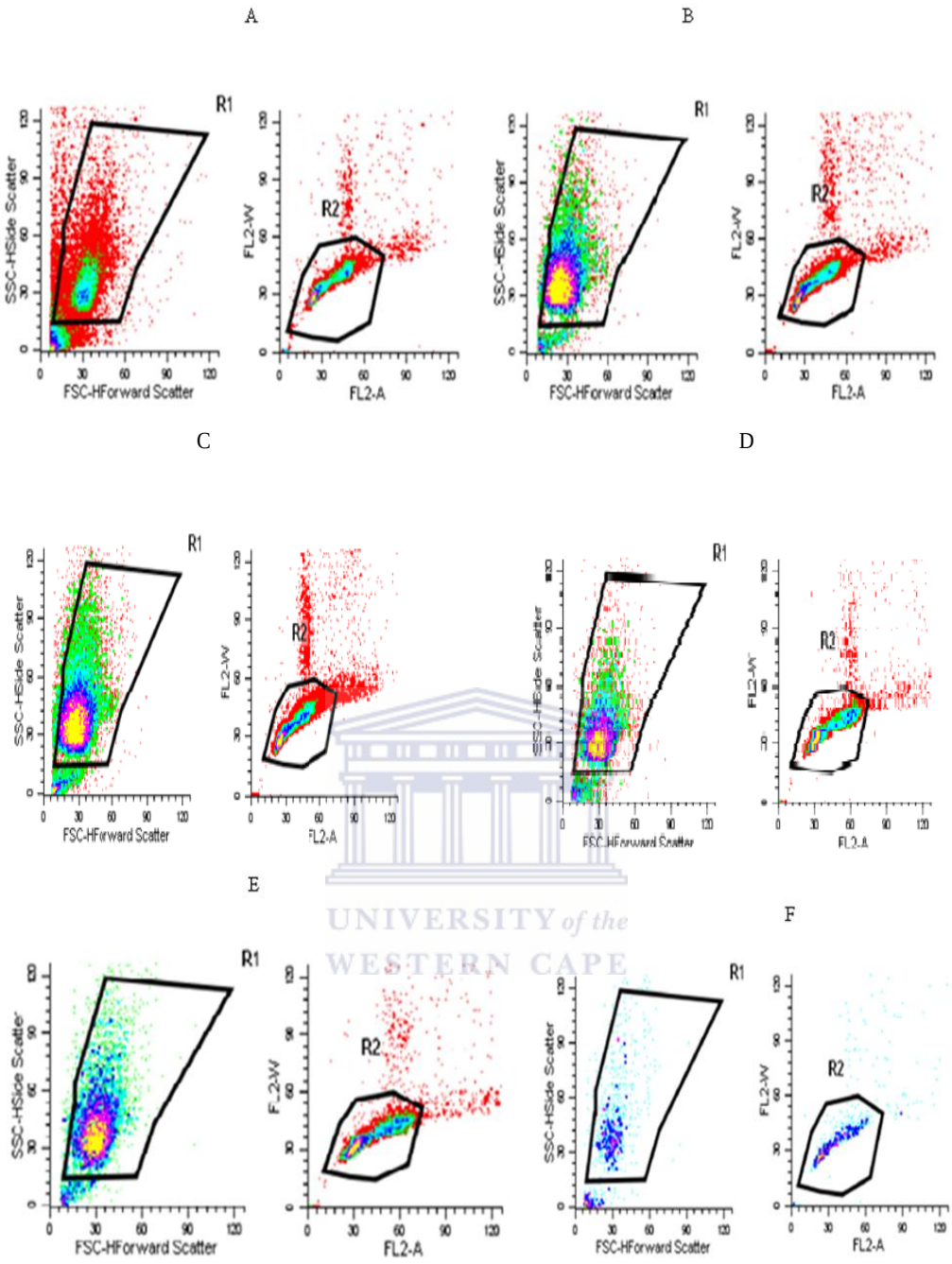

Appendix B. These Scatter plots display results obtained using flow cytometry where control cells represented by A) and bEnd5 cells exposed to B) 0.0001mM, C) 0.001mM, D) 0.01mM, E) 0.1mM and F) 1mM pure MA at 24hrs (≥ 10000 events analysed). Scatter plots were used to generate histogram and the data was tabled and represented as bar graph. R1 representing the population and R2 represent single cells identified.

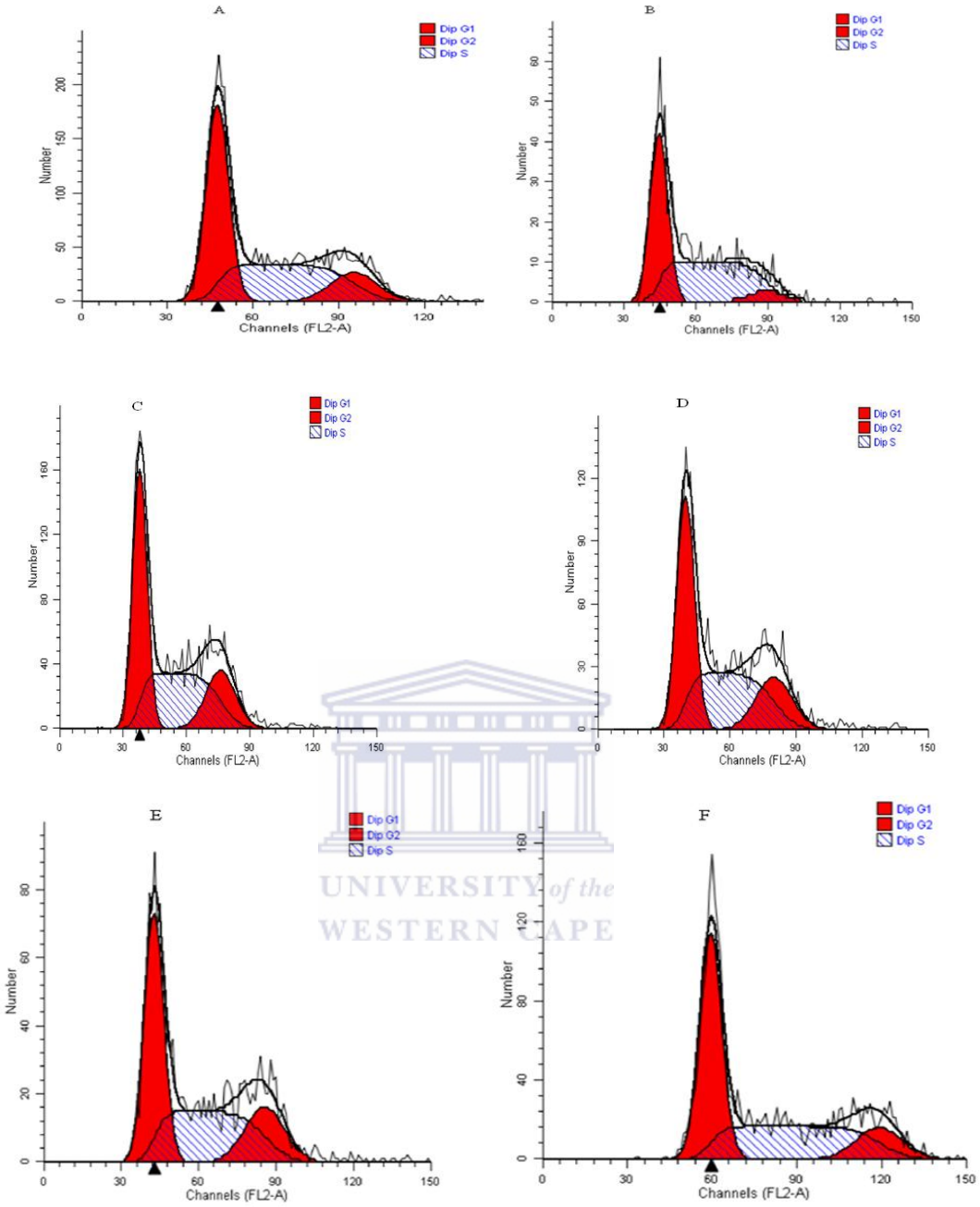

Appendix C. The above histograms were acquired using flow cytometry and A) represent results from control cells, while, bEnd5 cells treated with varying concentration of street MA sample 1are represented by the following histogram after 48hrs: B) 0.0001mM, C) 0.001mM, D) 0.01mM, E) 0.1mM and F) 1mM after 48hrs (≥ 10000 vents analysed

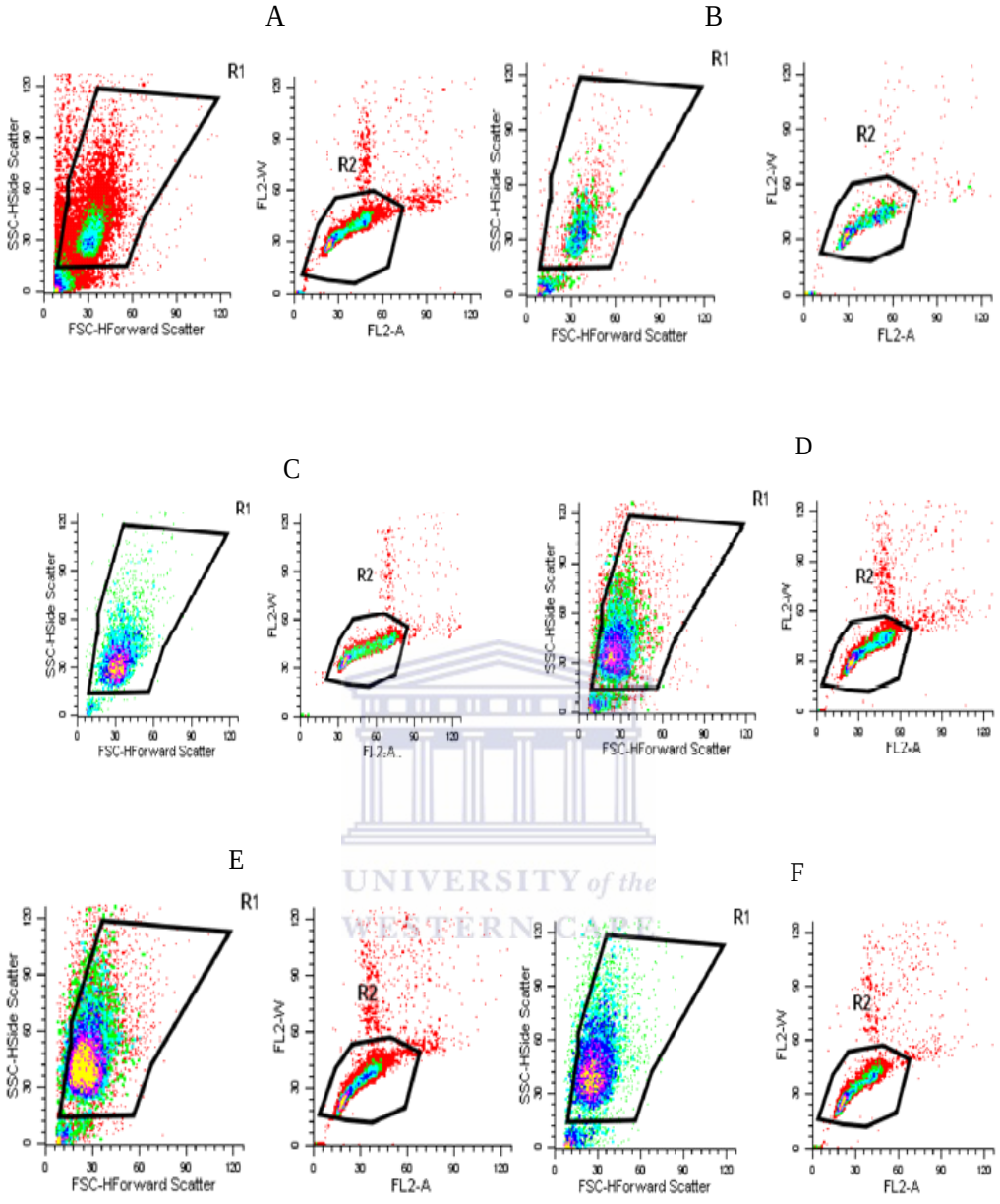

Appendix D. These Scatter plots display results obtained using flow cytometry where control cells represented by A) and bEnd5 cells exposed to B) 0.0001mM, C) 0.001mM, D) 0.01mM, E) 0.1mM and F) 1mM street MA sample 1 at 48hrs (≥ 10000 events analysed). Scatter plots were used to generate histogram and the data was tabled and represented as bar graph. R1 representing the population and R2 represent single cells identified

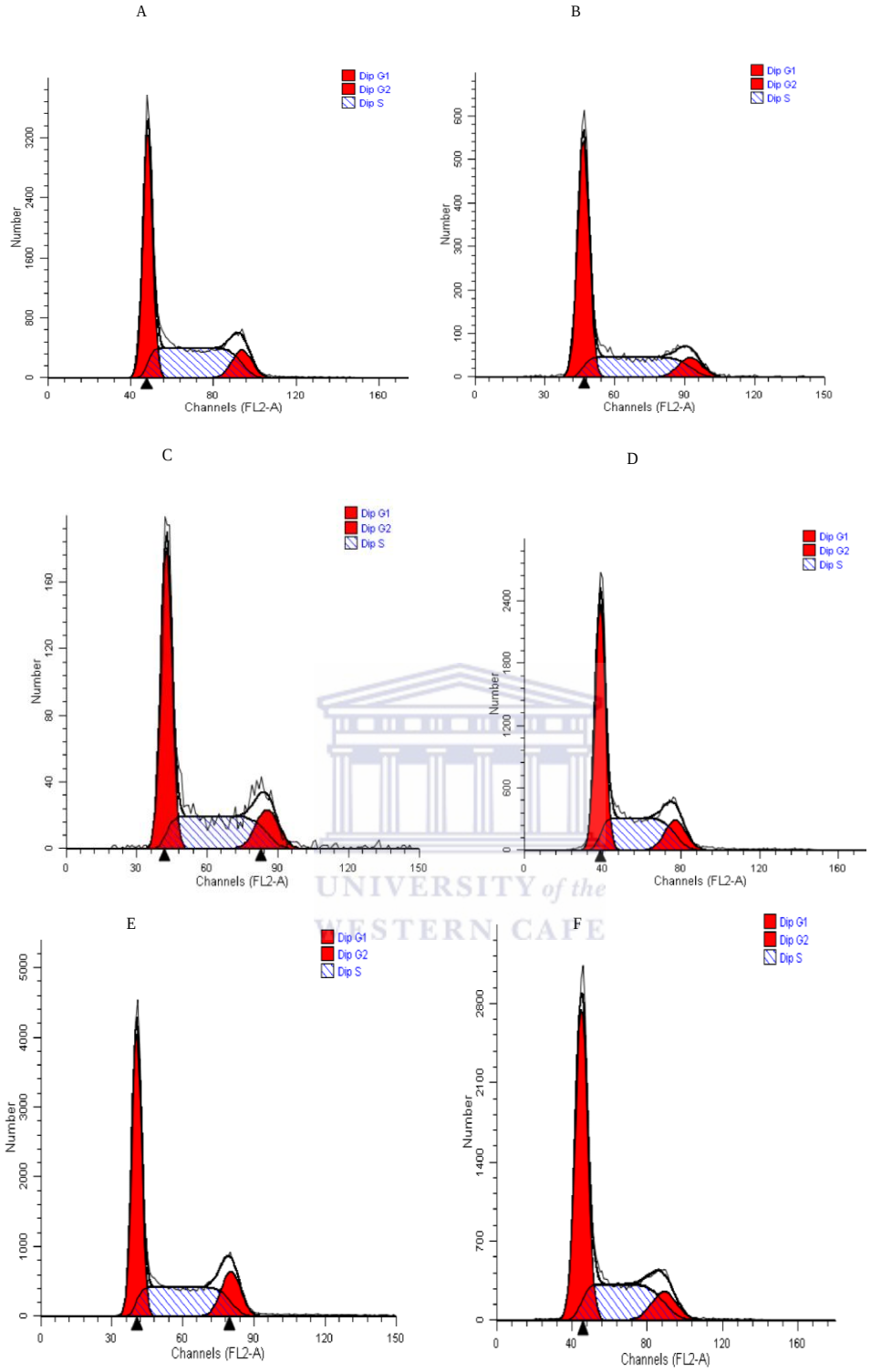

Appendix E. The above histograms were acquired using flow cytometry and A) represent results from control cells, while, bEnd5 cells treated with varying concentration pure MA are represented by the following histogram after 72hrs: B) 0.0001mM, C) 0.001mM, D) 0.01mM, E) 0.1mM and F) 1mM after 72hrs (≥ 10000 vents analysed).

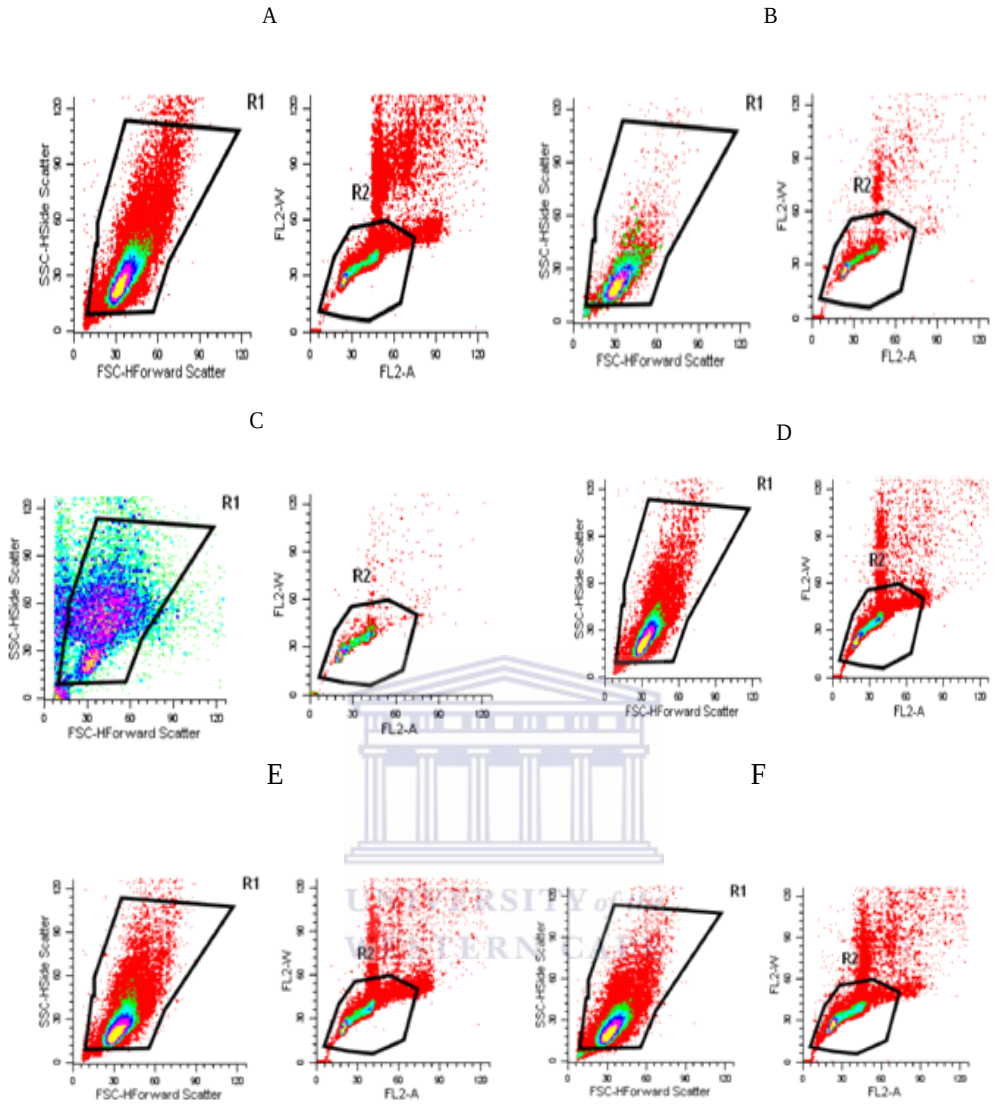

Appendix F. These Scatter plots display results obtained using flow cytometry where control cells represented by A) and bEnd5 cells exposed to B) 0.0001mM, C) 0.001mM, D) 0.01mM, E) 0.1mM and F) 1mM pure MA at 72hrs (≥ 10 000 events analysed). Scatter plots were used to generate histogram and the data was tabled and represented as bar graph. R1 representing the population and R2 represent single cells identified.

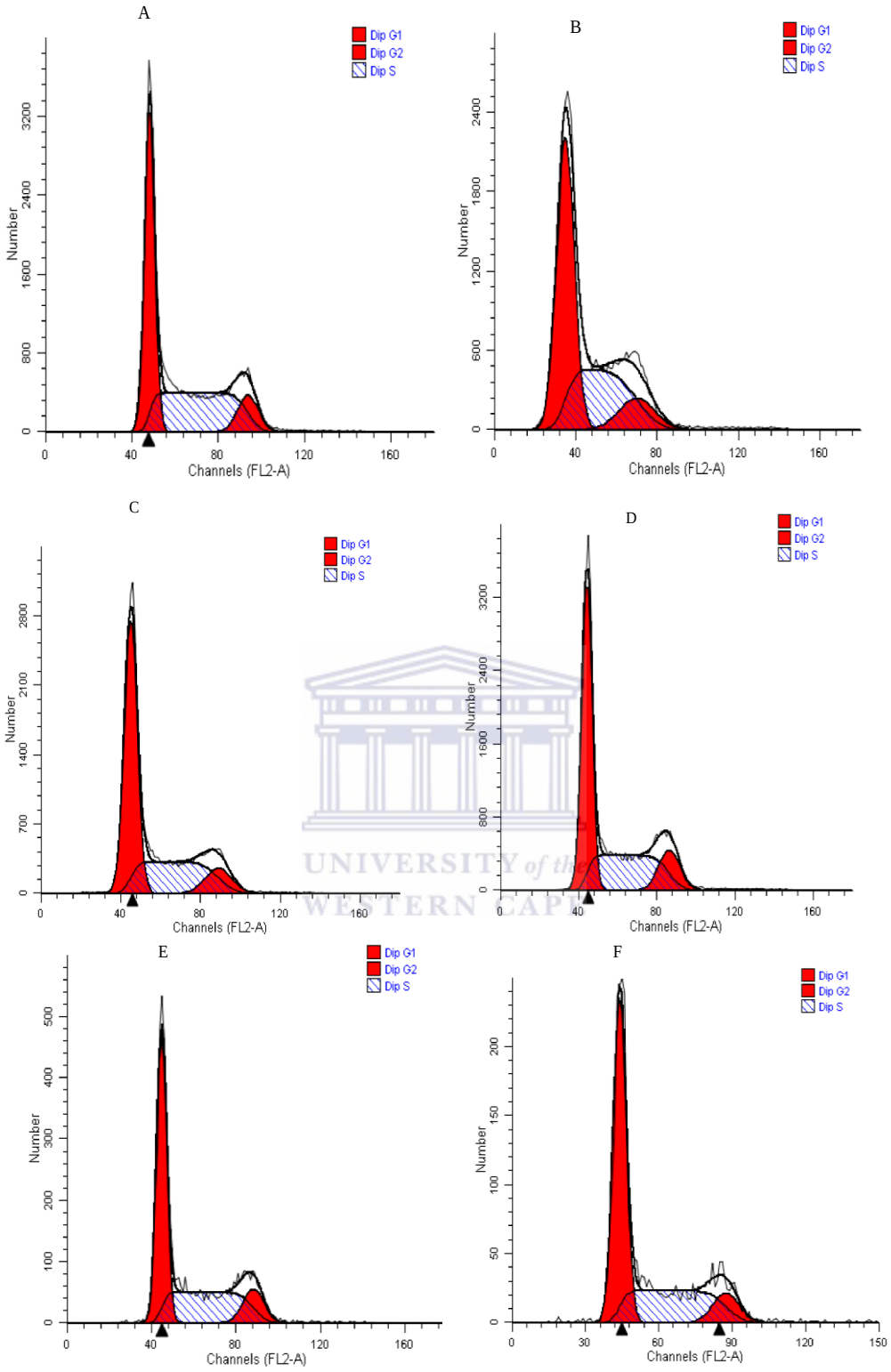

Appendix G. The above histograms were acquired using flow cytometry and A) represent results from control cells, while, bEnd5 cells treated with varying concentration of street MA sample 1 are represented by the following histogram after 72hrs: B) 0.0001mM, C) 0.001mM, D) 0.01mM, E) 0.1mM and F) 1mM after 72hrs (≥ 10000 events analysed).

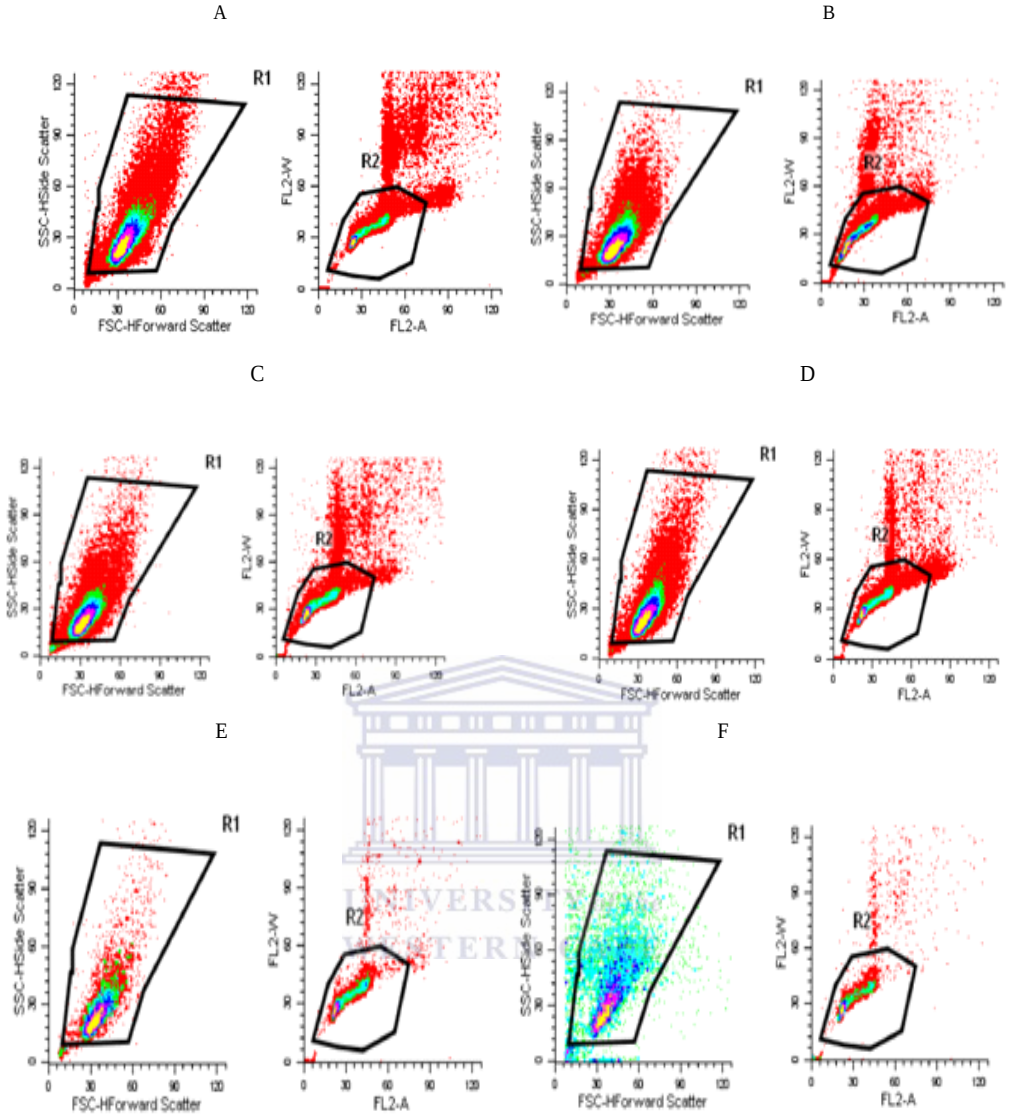

Appendix H. These Scatter plots display results obtained using flow cytometry where control cells represented by A) and bEnd5 cells exposed to B) 0.0001mM, C) 0.001mM, D) 0.01mM, E) 0.1mM and F) 1mM street MA sample 1 at 72hrs (≥ 10 000 events analysed). Scatter plots were used to generate histogram and the data was tabled and represented as bar graph. R1 representing the population and R2 represent single cells identified.

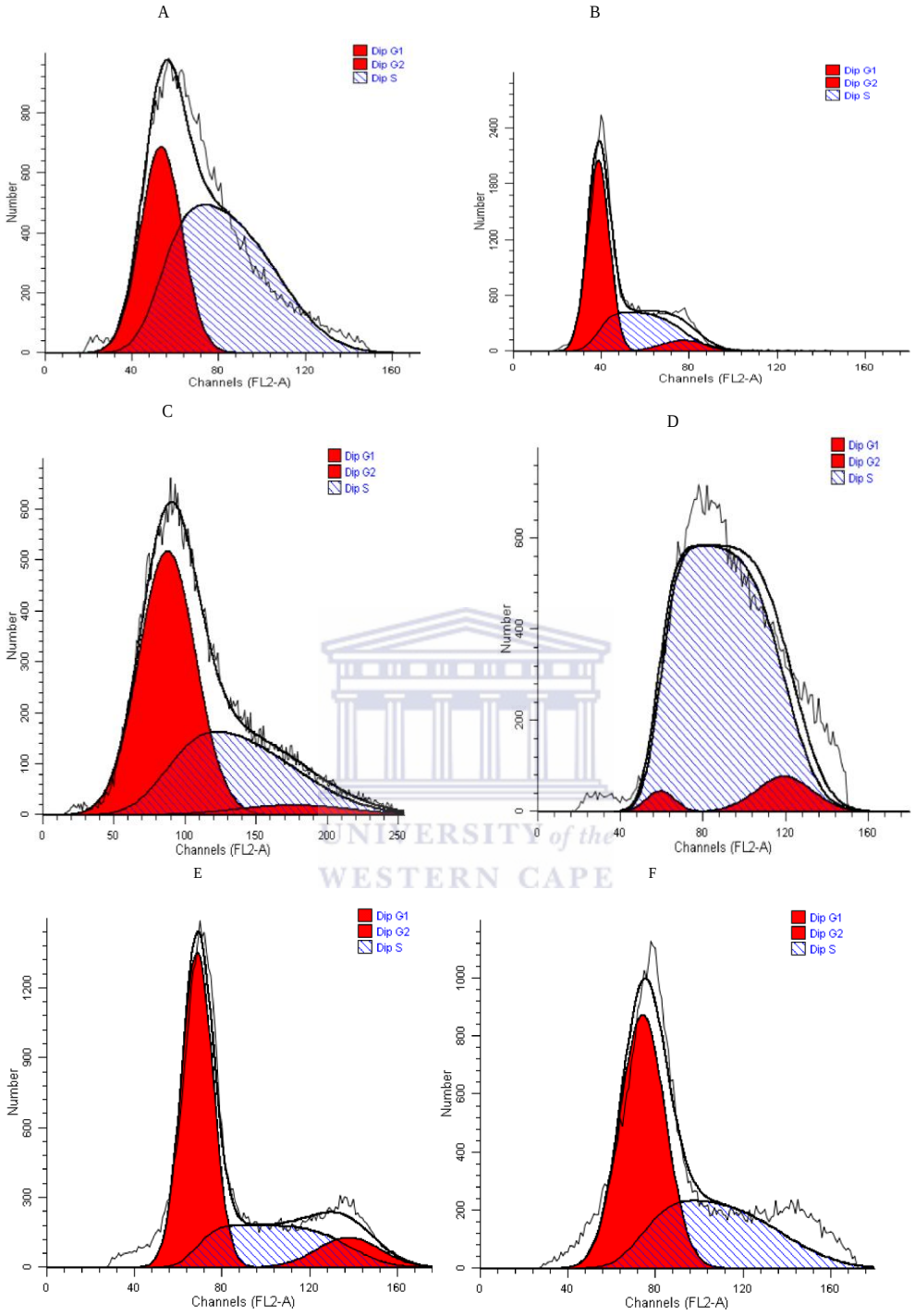

Appendix I. The above histograms were acquired using flow cytometry and A) represent results from control cells, while, bEnd5 cells treated with varying concentration of pure MA are represented by the following histogram after 96hrs: B) 0.0001mM, C) 0.001mM, D) 0.01mM, E) 0.1mM and F) 1mM after 96hrs (≥ 10000 vents analysed).

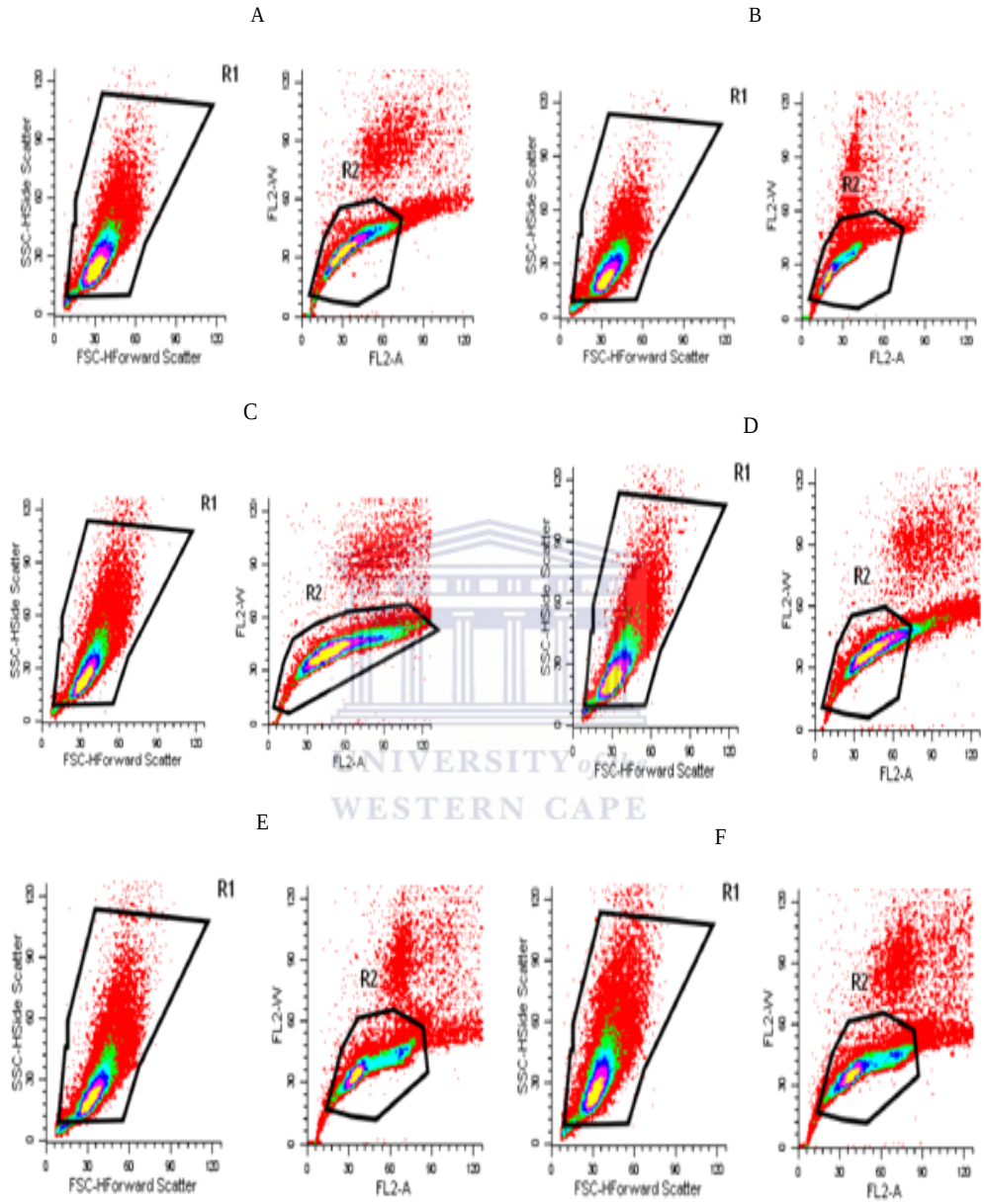

Appendix J. These Scatter plots display results obtained using flow cytometry where control cells represented by A) and bEnd5 cells exposed to B) 0.0001mM, C) 0.001mM, D) 0.01mM, E) 0.1mM and F) 1mM pure MA at 96hrs (≥ 10 000 events analysed). Scatter plots were used to generate histogram and the data was tabled and represented as bar graph. R1 representing the population and R2 represent single cells identified.

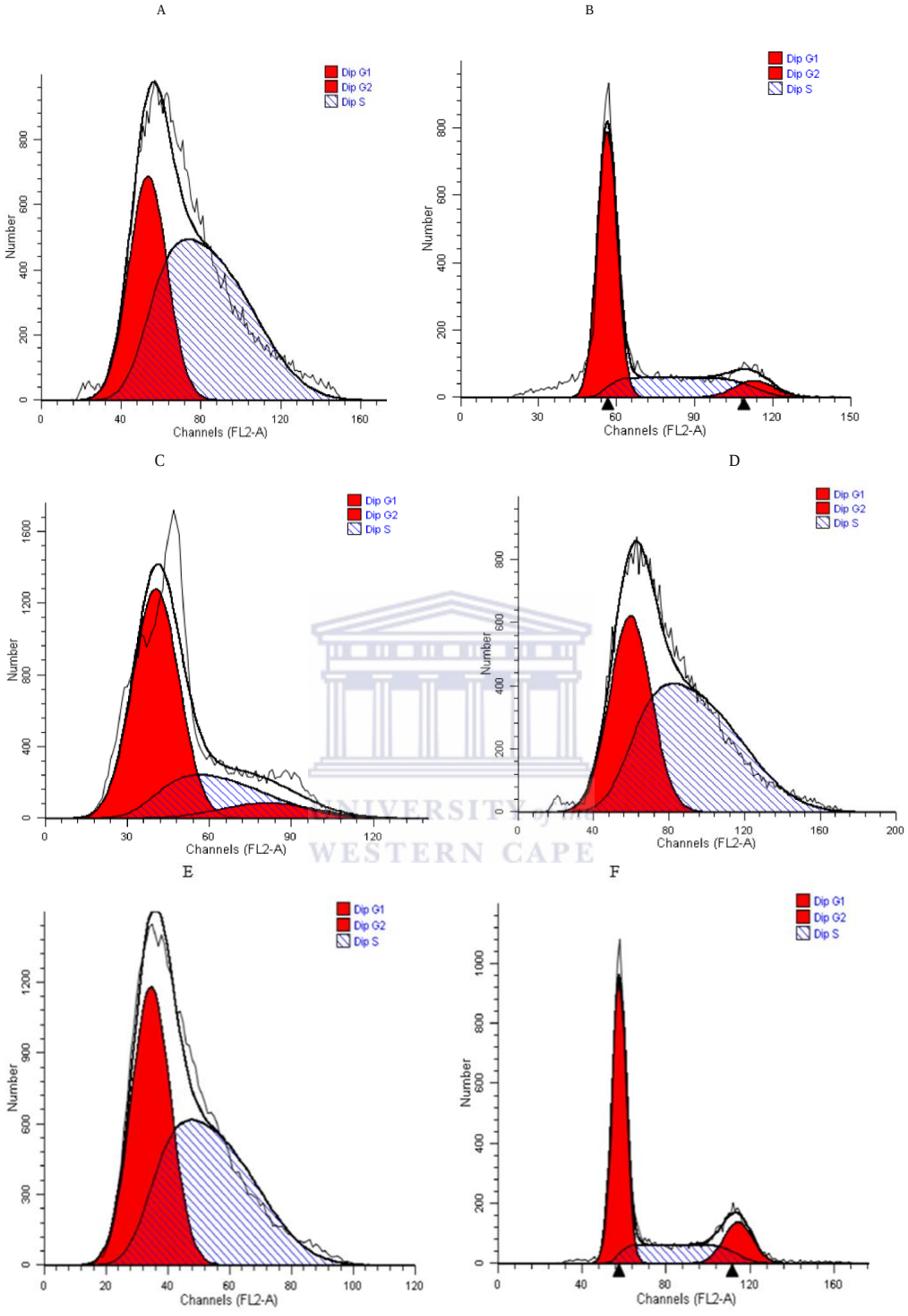

Appendix K. The above histograms were acquired using flow cytometry and A) represent results from control cells, while, bEnd5 cells treated with varying concentration of street MA sample 1 are represented by the following histogram after 96hrs: B) 0.0001mM, C) 0.001mM, D) 0.01mM, E) 0.1mM and F) 1mM after 96hrs (≥ 10000 vents analysed).

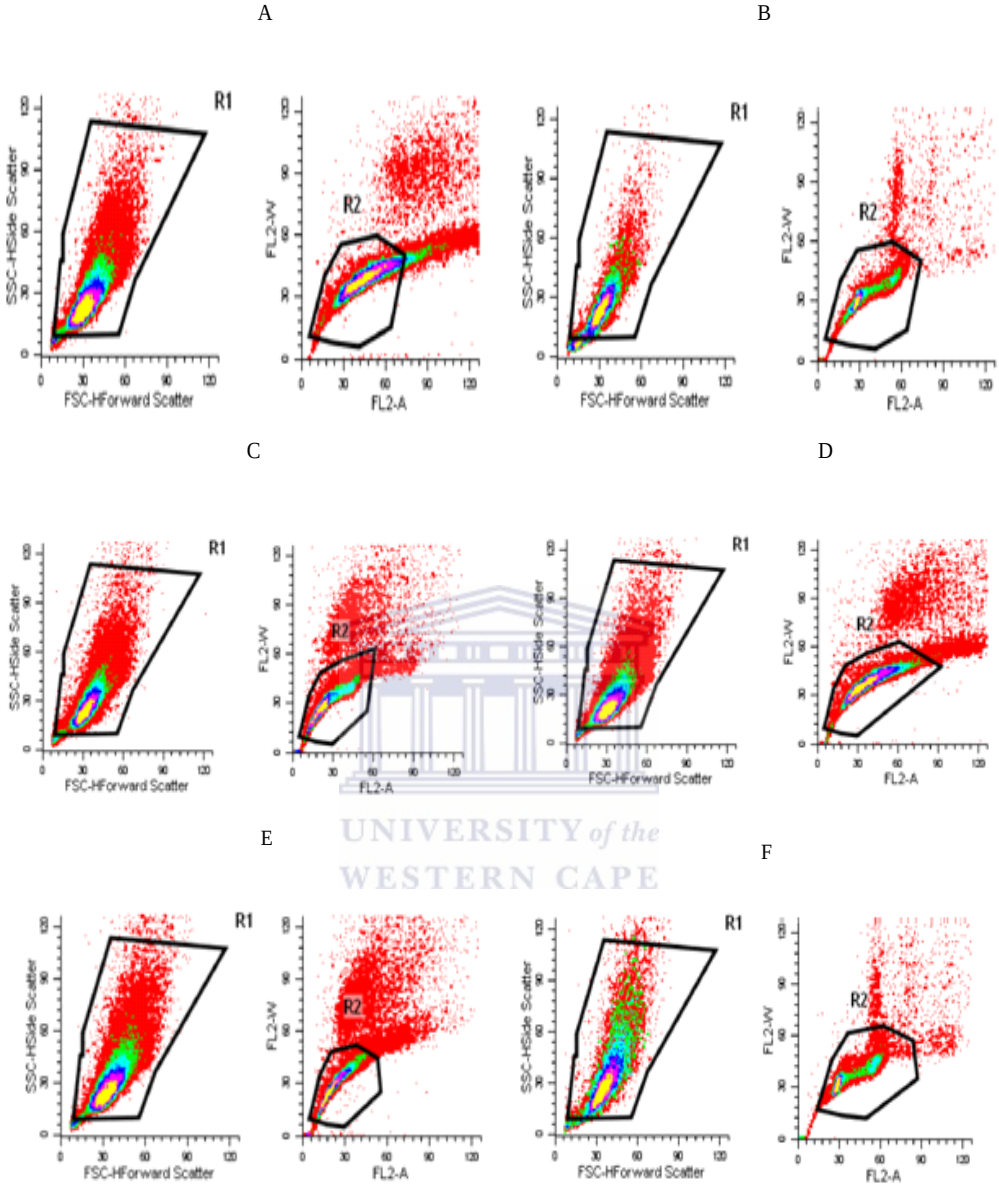

Appendix L. These Scatter plots display results obtained using flow cytometry where control cells represented by A) and bEnd5 cells exposed to B) 0.0001mM, C) 0.001mM, D) 0.01mM, E) 0.1mM and F) 1mM street MA sample 1 at 96hrs (≥ 10 000 events analysed). R1 representing the population and R2 represent single cells identified. Scatter plots were used to generate histogram and the data was tabled and represented as bar graph. R1 representing the population and R2 represent single cells identified.